Vickers

Feasibility Study on Submerged Oscillating Water Column Wave Energy Devices

PROGRESS REPORT

1st July 1979 to 31st May 1980

Vickers Limited
Design and Projects Division

K11/30012 June 1980

Vickers

Feasibility Study on Submerged Oscillating Water Column Wave Energy Devices

PROGRESS REPORT

1st July 1979 to 31st May 1980

Vickers Limited
Design and Projects Division
Wessex House
Market Street
Eastleigh, SO5 4FD
Hampshire
England

Telephone 0703 619722
Telex 477313 VICDPS-G

LIST OF CONTENTS

LIST OF CONTENTS (CONTINUED)

1.0 EXECUTIVE SUMMARY

The period covered by this report (July 1979 to May 1980) has seen the emergence of two new devices, the Submerged Wave Chamber and the Twin Oscillating Water Column. Both these concepts are logical extensions of the original Vickers device which suffered from a bulky air volume resulting in large construction costs. The new devices, working on a similar principle but without the large air volume, have proved to be cost effective, although their roles are expected to be different. The Wave Chamber is an attenuator, designed to be moored submerged on tension leg moorings in deep water. The Twin Oscillating Water Column, which does not require wave spanning capability for its operation is envisaged as an inshore submerged device, piled into the sea bed.

The devices were first tested experimentally in November 1979, and the results were very encouraging.

Further tests were made with a Twin Oscillating Water Column point absorber (a modification of the original Vickers device model) and a modified Wave Chamber, in February 1980. The results of both the November and February experiments are presented in this report.

We have been able to make extensive use of the Edingburgh Tank Facility. It has enabled us to do in months what would have taken years previously, and we were fortunate in being the first team to use the full facility. The findings of the experiments are voluminous and have led to a much better understanding of the devices and water columns in general.

1.0 EXECUTIVE SUMMARY (CONTINUED)

The results have been extrapolated to suggest that both the Wave Chamber and the Twin Oscillating Water Column could produce electricity from a 2 GW station for approximately 6p/kW hr, but it is difficult to put confidence limits on this figure until full scale design studies have been made.

It has been our policy to commit resources to detailed drawings of full scale structures only when the concept has been thoroughly explored. A full scale design study has therefore been made of the original Vickers concept, but the Twin Oscillating Water Column and the Wave Chamber, need further experimental work to optimise dimensional parameters and detailed shapes before they reach this stage, hopefully early in 1981.

Meanwhile methodology for full scale design is being developed along with the devices and we are building up our relationships with civil engineering designers and contractors to provide skills which we do not ourselves possess. The chapters of this report which relate to scale, computer simulation of forces and the discussion on moorings and anchorages describe the progress made. This should enable us to produce costs for the devices with tight confidence limits by the middle of 1981, and full scale working drawings by the end of that year.

1.0 EXECUTIVE SUMMARY (CONTINUED)

The most important development in the period under review has been the clarification of our development objectives. It is now apparent that the point absorber concept, which initially appeared attractive from the aspects of structural shape and high theoretical capture width, has inherent disadvantages in gross sensitivity to depth and sensitivity to the disposition of the bottom duct. This results in a lower capture width per unit volume relative to the terminator mode. It is unlikely that further changes in design of the point absorber could achieve more than a 20% improvement while modifications to the terminator could result in a much larger improvement.

Future work will concentrate on the design of a Twin Oscillating Water Column terminator and development of the design of the Wave Chamber. There is also work common to both devices which is needed, including dynamic modelling. In particular this relates to a chamber shape which would limit oscillations within the device in storm conditions, and an automatic latching system.

2.0 ACKNOWLEDGMENTS

We wish to acknowledge our indebtedness to :

Sir James Lighthill for his two-dimensional analysis that has greatly aided our understanding of Oscillating Water Columns.

Michael Simon for his work on three-dimensional analysis that has been of further help in our understanding, particularly of point absorbers.

Stephen Salter, who gave us complete freedom in his wide tank for a period of six weeks, and to his team, every one of whom gave us great support. Particular thanks go to Ian Young, who was adept at diagnosing bugs in computer programs over the telephone at 2 o'clock in the morning, when a night's programme of testing was threatened!

Professor Michael French and his colleagues who made us so welcome at Lancaster University, and provided a most stimulating environment in the earlier stages.

3.0 NOMENCLATURE

3.1 Symbols Used

a	Width of device
b	Height of device
c	Cost
C_d	Drag coefficient
C_m	Mass coefficient
C_w	Capture width
d	Diameter of device(2r)
De	Energy extraction damping coefficient
Dr	Radiation damping coefficient
F_H	Horizontal force
F_V	Vertical force
g	Gravitational acceleration
h	Wave height (peak to trough)
H	Water depth
K	Wave number ($2\pi / \lambda$)
l	Length of device
l_t	Length of tether
L	Water column length
M	Mass of device
M_w	Mass of water displaced by device
n	Index (cost = scale^n)
Q	Flow rate in duct
s	Scale
T	Wave period
T_e	Energy period
u	Horizontal water particle velocity
u	Horizontal water particle acceleration
v	Vertical water particle velocity
v	Vertical water particle acceleration
w	Wave frequency
x	Horizontal displacement
z	Height below mean sea level
γ	Weight of water per unit volume
σ	$(gK \tanh KH)^{1/2} = W$ for large H/λ
λ	Wave length
ρ	Water density
μ	Dimensionless ratio ($\pi d/\lambda$)

3.2 Abbreviations Used in Text

FFT	Fast Fourier Transform
PM	Pierson Moskowitz
SEV	Special Emplacement Vessel
SWC	Submerged Wave Chamber
TOWC	Twin Oscillating Water Column

4.0 EXPERIMENTAL RESULTS OF MODEL TESTS

Introduction

This chapter describes tests made in the Edinburgh Wide Tank in November 1979 and February 1980. Three devices were tested:

(1) The Twin Oscillating Water Column Terminator

(2) The Twin Oscillating Water Column Point Absorber

(3) The Submerged Wave Chamber

4.1 MODEL TESTS ON THE TWIN OSCILLATING WATER COLUMN TERMINATOR

4.1.1 Description of the Twin Oscillating Water Column Principle

The twin oscillating water column is an underwater device designed to work in a similar way to the original Vickers device, but using two water columns acting on a common air space. One column is in the shape of a 'U' with an upwards-facing mouth while the other column is straight with a downwards-facing mouth. The upwards-facing mouth is subject to the large wave-induced pressure variations close to the surface of the sea, while the downwards-facing mouth is subject to small pressure variations close to the sea-bed. The air spaces above each column are interconnected by a duct containing a bi-directional turbine, possibly a Wells turbine.

As the crest of a wave passes over the device the increased pressure in the upwards-facing duct forces the air/water interface of its column upwards, thus displacing the air/water interface of the downwards-facing column. By this means air is pumped back and forth through the turbine.

The device can take various forms. It could be a circular device acting as a point absorber, or it could be designed as a long narrow device in either terminator or attenuator modes. It is too early to state which would be the most cost-effective, but the first prototype model was designed as a terminator, which, due to its small size relative to a wavelength could be rotated through 90°, whereupon it would act as an attenuator.

4.1.2 Description of Model

Figure 1.1 shows a cross-section of the model in a plane parallel to the direction of the waves.

A represents the upward-facing mouth, B the downward-facing mouth. D and C show the relative positions of the air water interfaces of the downward and upward-facing columns respectively at a typical point in the cycle. E shows the airspace which is effectively incompressible and F the method of power extraction which in the model consists of a variable throttle.

The model is symmetrical about the $\underline{\ell}$ and the variable sections, G and H are duplicated on the right hand side. The dotted positions of both G and H represent the three positions in which each section can be fixed.

The model was attached to a base frame which was in turn attached to the bottom of the wave tank.

Tests on the Twin Oscillating Water Column Terminator

4.1.3 Aim

The aim of the experimental programme was to study the effect of various parameters and changes in configuration listed below, on the power output and bandwidth of the model:

1. Damping
2. Depth
3. Waveheight
4. Column Geometry
5. Placing a Reflector immediately behind the Model
6. Placing the Model in Attenuator Mode
7. Surge forces in Storm Waves

4.1.3 Aim (Continued)

These are the most important features of the device for initial testing. Data on the effect on the model of waveheight, mixed seas, and depth is essential for computing the cost effectiveness of the device. The other variables, for instance column geometry and reflector tests are useful for optimising the mode of operation of the device with a view to the design of future models.

4.1.4 Monochromatic and Mixed Sea Selection and Measurement

We decided it was necessary to test the device with monochromatic seas to fully appreciate the effect of any variable on bandwidth and peak power and also with P.M. seas to study the power response of the model to a random sea state. For the monochromatic tests we used a 20 frequency mixed sea which we "brewed" on the Edinburgh Wave-maker Computer. This sea spectrum was designed so that no second harmonics coincided with first harmonics, and the amplitude of the sea was specifically chosen to avoid wave interaction. The response of the model was Fourier analysed and it was found that not only was the second harmonic content extremely small (about 1% of the first harmonic in power terms), but that there was very little power at frequencies adjacent to the first harmonics. It was therefore possible to compute capture width at each frequency by dividing the power output of the model at that frequency by the power in the wave. This would have been difficult if there had been frequency spreading or second harmonics.

4.1.4 Monochromatic and Mixed Sea Selection and Measurement (Continued)

Each variable was tested in this monochromatic sea and in P.M. seas as in Figure 1.2. We stored four P.M. spectra with Mitsuyasu spreading, defined by different energy periods of .7, .8, .9 and 1.0 second. Initially each one of these P.M. seas was run for each variable but this was time consuming and it was found that the P.M. that produced most power could be found by inspecting the monochromatic sea response.

We found that there was inevitable wave interaction and some reflection which meant that the best way to measure the wave at the model was not to monitor probes in front of the model but to monitor a single probe in the exact position that the model was to be put. The power in the monochromatic and the P.M. seas was stored in the computer. This was found to be very repeatable as is shown in Figures 1.3 and 1.4.

4.1.5 Data Logging and Processing

We used the Edinburgh Wavepower PDP11/60 for this task. Data was put onto floppy disc and then processed using 'Prodat' a computer programme developed by Edinburgh specifically for wave energy device data.

4.1.5.1 Data Processing Programme for Twin Oscillating Water Column Terminator

A typical output from this programme is shown in Figure 1.5. The level information shows the level of one of the water columns in the Twin Oscillating Water Column Termintor. The level could fluctuate from a maximum of 30mm (where it touched the top) to a minimum of 0mm (where the model might lose air). It was also important that the mean did not change to any degree between experiments especially where taper or antitaper was being used.

Then follows the pressure generated by the left hand column across the throttle (measured by the micro-manometer) together with its accompanying flow (measured by differentiating wave probe data in the downward-facing column). In fact the flow measurement was duplicated. The probe in the upward-facing column was also monitored and the data differentiated to give flow. These two values were then compared (see position 10 to give the per cent flow error (left hand).

This was repeated for the right hand probes to give per cent flow error (right hand) (see position 11). An error of $^{+8}_{-0}$% was found on average. This was explained by the fact that the upward-facing columns had a choppy surface due to the greater forcing pressure. This gave it, on average, a higher value. The smooth surface of the downward-facing column was used as control and these easily repeatable values were used to calculate power.

4.1.5.1 Data Processing Programme for Twin Oscillating Column Terminator (Continued)

Position 6 shows the total power from both the left hand and the right hand side while position 7 shows the capture width values in mm. These were deduced by dividing all power by the power in the wave (recalled from computer memory). These channels were stored in F.F.T. form and Figure 1.6 shows channel 604 plotted on the graph plotter.

Position 12 shows the per cent power error. This takes the power from the left hand and compares it with the power in the right hand part of the Twin Oscillating water column. This error was always small but was a further check on the measurement system. If, as happened on occasions, this error jumped to a large value there was a good reason. It was generally due to water entering the tubes of the manometer. Positions 10, 11 and 12 were a very powerful check on the measurement system, were checked for every reading and subsequently gave us great confidence in our results.

Position 8 shows the power that existed outside the 20 frequencies. If there had been some stray harmonics, for instance a spurious resonance in the tank, it could have appeared as a large maximum value. In fact this maximum value was always very small.

Position 13 indicates the sum of the power output from the device, this value being used mainly for P.M. sea analysis.

4.1.6 Twin Oscillating Water Column Terminator Device Experiments and Analysis

Test 1 - Damping

This test involved adjustments of the throttle setting to achieve optimum power. The optimum P.M. (.8 second Te) was used with the model at a depth of 5cm. Figure 1.7 shows the effect of damping, and gives the optimum damping figure as 10mm/LS^{-1}. This gives an interesting non-dimensional figure for optimum performance of the Twin Oscillating water column: The damping should be such that the pressure drop across the turbine is approximately equal to .5 waveheight. At full scale this implies that a wave with an H_{rms} of 1 metre would produce an R.M.S. pressure drop of .5 metre of water. This is a useful figure for turbine designers.

Another non-dimensional figure, useful for modelling power take-off, is that the optimal X sectional area of orifice is $\frac{1}{150}$ th the size of the X sectional area of the upwards facing column.

Figure 1.8 shows the effect of damping on the response of the device, using monochromatic waves. The top curve shows the damping at near optimum. The other two represent underdamping and overdamping. The import feature to note is that there is no frequency shift, and therefore no benefit, to be gained by either over or underdamping.

Test 1 - Damping (Continued)

It was with some reluctance that we used orifice damping rather than linear damping. We tried a large selection of different materials ranging from Hairlok to foam rubber but had problems with their characteristics changing as their dampness changed, quite apart from the difficulty of designing an adjustable linear absorber which is by no means easy. However, efficiency is not first order dependent on damping. Capture width is a function of $\frac{4De\ Dr}{(De+Dr)^2}$ which is equal to 1 at resonance, i.e. (De = Dr). If the radiation damping Dr is constant and the internal damping (De) is varied the effect on capture width is not great: if De ranges between 1/3 and 3, a change of 900% the efficiency varies from .75 to 1.0, a change of only 33%.

This theoretical curve is plotted in Figure 1.7 - with the assumption that De = Dr at the optimum value. It is surprising that the correlation is so good, considering the wave used was not monochromatic and the damping values are r.m.s. values of non-linear damping. It suggests that non-linear compared with linear damping does not have a serious effect on efficiency. For instance, in the worst case the damping of the turbine could be non-linear (i.e. similar to orifice damping). For waves that vary in power from 4kW/m to 80kW/m, the full working range of the device, the effect of non-linear damping will cause the impedance value P/Q to vary from 8 through to 10 at 10kW/metre to 16 at 80kW/metre (see Figure 1.9). This will cause a loss of efficiency, due to non-linear damping, of 12% at either end of the range.

Test 1 - Damping (Continued)

This will result in an average loss of efficiency, due to the distribution of energy in the sea, of about 4%, if the device is in shallow water. If the device is in deeper water, however, and limited to say 80kW/m there will be a large percentage of the total power, approximately 40%, at the cut-off point of 80kW/m. This clearly increases the range of the wave heights over which the device is designed to work and hence means that a turbine with fixed orifice type damping might be unsuitable.

Test 2 - Depth

Once the damping characteristics of the model had been optimised the next most important feature to study was the effect of depth.

In Figure 1.10 the graph marked ◘ shows the capture width obtained with the resonant frequency of the device, while that marked ▽ represents the capture width with the optimal P.M. sea (T_e = .8s).

The P.M. sea data shows the device producing peak power at 3cms depth (3 metres full scale). This power drops off sharply at shallower depths and more slowly at greater depths. It can also be seen that the capture width in a P.M. sea is about half of that in a resonant monochromatic sea.

Also shown is the effect of placing a reflector immediately behind the mouth of the model. This shows that the optimum depth of the front panel of the model is 4cms and that the power is greatly increased. The reflector, however, would penetrate the surface with all the resultant penalties of so doing. It would be necessary to do tests with strain gauges to ascertain the cost of the reflector in structural terms.

Test 2 - Depth (Continued)

Figure 1.11 shows the effect of depth on the response of the model to monochromatic seas. It is interesting to note that there is a significant frequency shift. The shift is to higher frequency with increasing depth. Also it is worth noting that the effect that is predicted from theory - that the peak power remains relatively unaffected by depth while the bandwidth is greatly affected - is not evident. The peak power steadily decreases with the bandwidth.

Test 3 - Waveheight

Figure 1.12 is a plot of capture width against waveheight using a .8 second P.M. sea. The maximum wave used represents a full scale power of 60kW/m, the minimum 2kW/m. As the device would be designed at full scale with a safety chamber that limits the oscillations at values greater than 80kW/m, this graph covers almost the entire range we are interested in. It was thought possible that the effective change in damping due to the non-linearity of the orifice could be causing attenuation at low and high amplitudes. Unfortunately it was not possible to optimise the damping at these extremes. However, it was possible to compensate for loss of efficiency due to mismatching the damping by using the r.m.s. damping figures measured in each test. (See Figure 1.9). This certainly accounts for some of the attenuation at small wave heights, but not at the large wave heights which still show attenuation of about 20%. Without more detailed knowledge of turbine impedance, in particular the impedance of the Wells turbine, it would be prudent to take the original curves, representing non-linear damping, as the most pessimistic case and the modified curves, representing linear damping, as the most optimistic.

Test 4 - Internal Geometry

Theory suggests that if the area of either or both columns at the air water interface is increased there is a corresponding decrease in natural frequency.

To test this the model was designed so that the upward-facing sections could be changed (see Figure 1.1). If the top flaps are cranked inwards the area at the air water interface is increased while if cranked outwards the area is decreased. This is a particularly interesting design because the overall size of the model is unaffected. In other words the aim of this test is: Given a basic structure of given outside dimensions how should the internal geometry be designed to optimise the power and frequency response?

Figure 1.13 shows a plot of capture width versus frequency. The effect of the variable geometry can be clearly seen. With the flaps swung inwards (i.e. large A_2) the peak power is increased and the frequency lowered, both highly desirable features. The bandwidth is, however, marginally reduced. Conversely, with the flaps swung outwards (small A_2) the peak power is reduced, the frequency raised and the bandwidth marginally increased. It was important to gain insight into the potential of such geometric variations for reducing costs.

P.M. seas were run with the three configurations. The large A_2 position allowed the model to operate best with a .9 second sea. The parallel position a .8 and the small A_2 a .7 second sea. To evaluate the cost effectiveness of the model in these different seas it is necessary to establish a basis of calculation.

Test 4 - Internal Geometry (Continued)

Case 1

$$C_{F1} = C_{M1} \times \left(\frac{T_F}{T_{M1}}\right)^2$$

Case 2

$$C_{F2} = C_{M2} \times \left(\frac{T_F}{T_{M2}}\right)^2$$

i.e.

$$\frac{C_{F1}}{C_{F2}} = \frac{C_{M1}}{C_{M2}} \times \left(\frac{T_{M2}}{T_{M1}}\right)^2 = \text{Ratio of full scale capture widths}$$

Where C_F = Capture width (full scale)
C_M = Capture width (model scale)
T_F = Energy Period (full scale)
T_M = Energy Period (model scale)

Case 1

$$V_{F1} = V_{M1} \times \left(\frac{T_F}{T_{M1}}\right)^6$$

Test 4 - Internal Geometry (Continued)

Case 2

$$V_{F2} = V_{M1} \times \left(\frac{T_F}{T_{M2}}\right)^6$$

i.e. $$\frac{V_{F1}}{V_{F2}} = \frac{V_{M1}}{V_{M2}} \left(\frac{T_{M2}}{T_{M1}}\right)^6 =$$ Ratio of full scale volumes

Where V_F = Volume (full scale)

V_M = Volume (model scale)

Now Cost Effectivensss = $\frac{\text{CAPTURE WIDTH}}{\text{VOLUME}} = C_E$

So cost effectiveness ratio, $\frac{\text{Case 1}}{\text{Case 2}}$

$$\frac{C_{E1}}{C_{E2}} = \frac{C_{M1}}{C_{M2}} \left(\frac{T_{M1}}{T_{M2}}\right)^4 \frac{V_{M2}}{V_{M1}}$$

$$\frac{C_{E1}}{C_{E2}} = \frac{C_{M1}}{C_{M2}} \frac{V_{M2}}{V_{M1}} \left(\frac{T_{M1}}{T_{M2}}\right)^4$$

or cost effectiveness of any particular arrangement

$$= C_E = KC_M T_M^4/V_M$$

To assess the cost effectiveness of the different geometries refer to the table overleaf.

Test 4 - Internal Geometry (Continued)

Geometry	P.M.	Capture Width	Model Volume	Cost Effectiveness $KC_MT_M^4/V_M$	Scale ANNUAL AV Te=8s	Scale ANNUAL AV Te=10s
Large A_2	.9	75.4	V	K. 49.42	1/79	1/123
Large A_2	.8	74.8	V	K. 30.6	1/100	1 156
Parallel	.9	73.0	V	K. 47.89	1/79	1/123
Parallel	.8	80.3	V	K. 32.89	1/100	1/156
Small A_2	.8	67.7	V	K. 27.7	1/100	1/156
Small A_2	.7	72.0	V	K. 17.3	1/130	1/204

The table shows that the most cost effective design is the geometry which has a large air/water interface (Antitaper). It further shows that this geometry implies a small scale device which is an advantage from a construction point of view.

Test 5 - Bottom Duct Geometry

Figure 1.1 shows the different positions that the bottom doors, H, can assume. Tests were done with the bottom doors in three different positions relating to .66A, A, 1.67A, where A is the width of the duct at position D.

The graphs in Figure 1.14 show the effects of these three different configurations compared with the parallel position. The closed position .66A shows a decrease in frequency with accompanying decrease in peak power and bandwidth. The wide open position, however, shows very little difference in peak power, bandwidth or frequency. In fact the results from the P.M. suggest very little improvement.

Position	P_M/Te	Capture Width	Volume	Cost Effectiveness
	.9	64.2	.96V	43.8K
	.9	73.0	V	47.8K
	.8	80.3	V	32.9K
	.8	81.8	1.08V	31.0K
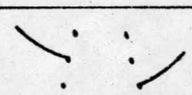	.8	83.0	1.04V	32.7K
	.8	83.0	1.04V	32.7K

Test 5 - Bottom Duct Geometry (Continued)

The table shows all the configurations of the bottom door positions that were tried. Two more positions apart from the ones previously mentioned were also tried. These are shown in the table along with an arrow that indicates the direction of the wave. It is interesting to note that the capture width is the same for both these positions which suggests that directionality is not important in the bottom duct, although actual position may be. This will be tested in a later model.

The optimum geometry appears to be the parallel section.

As the cost effectiveness improves dramatically with lower frequencies it can be seen that a frequency that gives optimum capture width does not necessarily give optimum cost effectiveness.

To study this effect further it will be necessary to run the model in seas of 1.0, 1.1, and possibly even 1.2 seconds period. It should be borne in mind, however, that this cost effectiveness formula is of necessity crude. Rigorous cost optimisation would require analysis of the effectiveness of large numbers of small devices where the total resource may not be efficiently utilised. Such factors will weigh against the surprising result that the most cost effective device is apparently one that resonates at a much higher frequency than the frequency of the wave. The implications of scale are discussed more fully in this report in section 4.3.

Test 6 - Attenuator Mode

Only one test was done with the device in this mode. The monochromatic frequency response is very similar to that of the model in terminator mode in that the resonant frequency and bandwidth are about the same. Nevertheless, peak power is reduced. A P.M. sea of .8 second produced 87% of the power obtained with the model in terminator mode.

It is impossible to draw any conclusions from this test. A model of an attenuator is invalid unless it is about 1 wavelength long, when it becomes directional otherwise it acts more like a point absorber. Even with a model one wavelength long it is difficult to predict the behaviour effect of a device two or three wavelengths long. Figure 1.15 is by courtesy of N.E.L. It shows the complex effect of length on efficiency. The only effective way of testing the Twin Oscillating Water Column in attenuator mode would be to make similar tests with a series of models bolted together.

Test 7 - Surge Forces

The yoke on which the device was mounted was modified to incorporate strain gauges. A window was machined in one of the vertical supports, leaving 1mm thickness of aluminium, approximately 20mm long, on either side. These strips were strain gauged at their points of maximum bending using four gauges which were wired to form a full wheatstone bridge. This was repeated on the other arm of the yoke, and both arms were calibrated using dead-weights. The yoke was thus instrumented to measure surge and yaw.

Test 7 - Surge Forces (Continued)

As the yaw component in a monochromatic long crested sea should be negligible the yoke effectively had a dual surge measurement system - in keeping with the philosophy used on the rest of the model. As it turned out one system became unreliable on immersion and was therefore not used, while the other worked well, except that it had a signal to noise ratio of only 3:1. This was greatly improved with a low pass filter which gave a 20:1 signal to noise ratio.

Three different seas were "brewed". They were all equivalent to 16 second waves but of height (peak to trough) 6.7m, 14m and 16.5m. It was intended to use an 18m wave, the one in a hundred year wave expected at the inshore location. Unfortunately the Edinburgh tank was not designed to handle this height of wave. Figure 1.16 shows the results achieved compared with theoretical computer simulation using D.D. Lappo's equations modified for a horizontal cylinder (See section of this report on Wave Loadings). It is interesting to note that at depths below the r.m.s. waveheight the agreement between theory and practice is extremely good. As the device reaches the surface the measured forces exceed the theoretical predictions, reaching a peak for the largest wave of about 3m. The reasons for this are not yet clear, but it is significant that using Lappo's equations (which are based on Morrison's equation, the basic tool for calculating surge forces) could result in an estimation of surge that is only 55% of that which actually occurs. It appears, therefore that a horziontal cylindrical device at 4m depth (i.e. the Twin Oscillating Water Column Terminator) experiences surge forces in a 16.5m wave that are 80% of those that a surface device, for instance a duck, might experience.

Test 7 - Surge Forces (Continued)

No tests have been made on local slamming forces on submerged versus surface devices, but further tests with a fully strain gauged model will be made. It is expected that these local forces will be considerably greater in the case of surface devices.

4.1.7 The Twin Oscillating Water Column Terminator: Summary

Compared with original Vickers device, the Twin Oscillating water column not only shows improved capture width per unit volume, it also shows that this improvement is available at low frequencies which implies that the cost effectiveness could be greater than the 2:1 improvement that the graph in Figure 1.17 implies. The addition of a reflector makes a further enormous improvement, and this effect warrants further study.

This series of experiments on the Twin Oscillating Water Column Terminator has been very informative, and our main findings are :

(A) Experimental

(1) Waves interact when their steepness ratio becomes greater than 1/25 causing errors in wave measurement unless the measurement is made at the position the model is tested.

(2) There is very little evidence of any device power in either the second or third harmonics, even though the device uses a non-linear power take off.

(3) It is valid to use the movement of the surface of a water column as a flow measurement, although the surface may have some standing wave on it. However, an accuracy of $^{+10}_{-0}\%$ only can be expected. This statement can be made as the Twin Oscillating Water Column incorporates a downwards-facing column which is not subject to standing waves or hash as it is only subject to the greatly decayed forcing pressure well below the sea surface.

4.1.7 The Twin Oscillating Water Column Terminator : Summary (Continued)

(A) Experimental (Continued)

(3) continued

We used this smooth surfaced column to measure air flow, but it also enabled us to study the effects mentioned above in the upwards-facing column.

(4) Duplication of results coupled with constant comparison shows errors quickly, thereby saving time and giving greater confidence in results.

(B) Device

(1) Damping

The device is sensitive to damping, but this is not critical. No benefit is obtained by either overdamping or underdamping as the bandwidth is reduced while the natural frequency remains unaffected. By effectively reducing oscillations, however, overdamping could be advantageous to reduce the chance of internal slamming or air loss. A non-linear power take off (with orifice damping characteristics) results in approximately 4% power loss in shallow water.

4.1.7 The Twin Oscillating Water Column Terminator: Summary (Continued)

(B) Device (continued)

(2) Depth of Submergence

It appears that the hopes of last year - that good efficiencies could be obtained at depths of 20 metres are not to be realised.

The model worked best at 3cm (which implies a full scale depth of 3m). Not only was the peak power greatest at this depth, the frequency was lowest at this depth. Greater depths imply a less cost effective device. There is less peak power, similar bandwidth and an increase in the resonant frequency. The design depth of the device is 5m: this takes into account tidal variations.

(3) Waveheight

The device is waveheight dependent and does not give a linear increase in power with the square of the waveheight. The power drops off at waveheights higher or lower than the waveheight of a 30kW/m sea at full scale. This means that the device is not greatly affected by waveheight for the expected wave spectra.

4.1.7 The Twin Oscillating Water Column Terminator: Summary (Continued)

(B) Device (continued)

(4) Internal Geometry

A large air/water interface gives a large peak power at lower frequency. This is beneficial in itself but it appears that if the outside dimensions are limited it is worth adding to the air/water interface at the expense of reducing the cross-sectional area of some other part of the column. How far this trading can be taken will be studied in a further model.

(5) Duct Geometry

It appears that throttling the bottom duct to try to lower the frequency of the device is not cost effective, but the effect is not so detrimental that it may not be worth doing if by doing it some other benefit, not just reduction in volume, accrues.

(6) Attenuator Mode

More model tests are required, the data acquired with a single short device is not sufficient.

4.1.7 The Twin Oscillating Water Column Terminator: Summary (Continued)

(B) Device (continued)

(7) Reflector

A reflector behind the device created more power and improved the bandwidth. A model will be built to further test this. In particular, however, tests will be made to measure the forces on this surface piercing device. It will then be possible to study its effect on survivability and cost of structure and fixing.

(8) Surge Forces

Tests on the Twin Oscillating Water Column Terminator at different depths show that Morrison's equations give good correlation with model tests at depths greater than the r.m.s. waveheight. When the device breaks the surface the theory predicts forces which are, in the worst case, only 55% of the measured forces. Surge forces on the Twin Oscillating Water Column terminator are only approximately 80% of those experienced by a similar sized duck in a 16.5m wave.

4.1.7 The Twin Oscillating Water Column Terminator: Summary (Continued)

(C) General

The device, from this initial series of tests, has proved to be more cost effective than the original Vickers device. Initial indications are that it could be twice as cost effective although this needs to be confirmed from cost estimates based on a full scale design study.

Apart from reduced costs the device also has the attraction of not requiring a large air volume. This implies that, at full scale, the device need not operate in an Atlantic swell to be cost effective - it could operate efficiently in the relatively small swell off Aberdeen without incurring a costly air volume penalty.

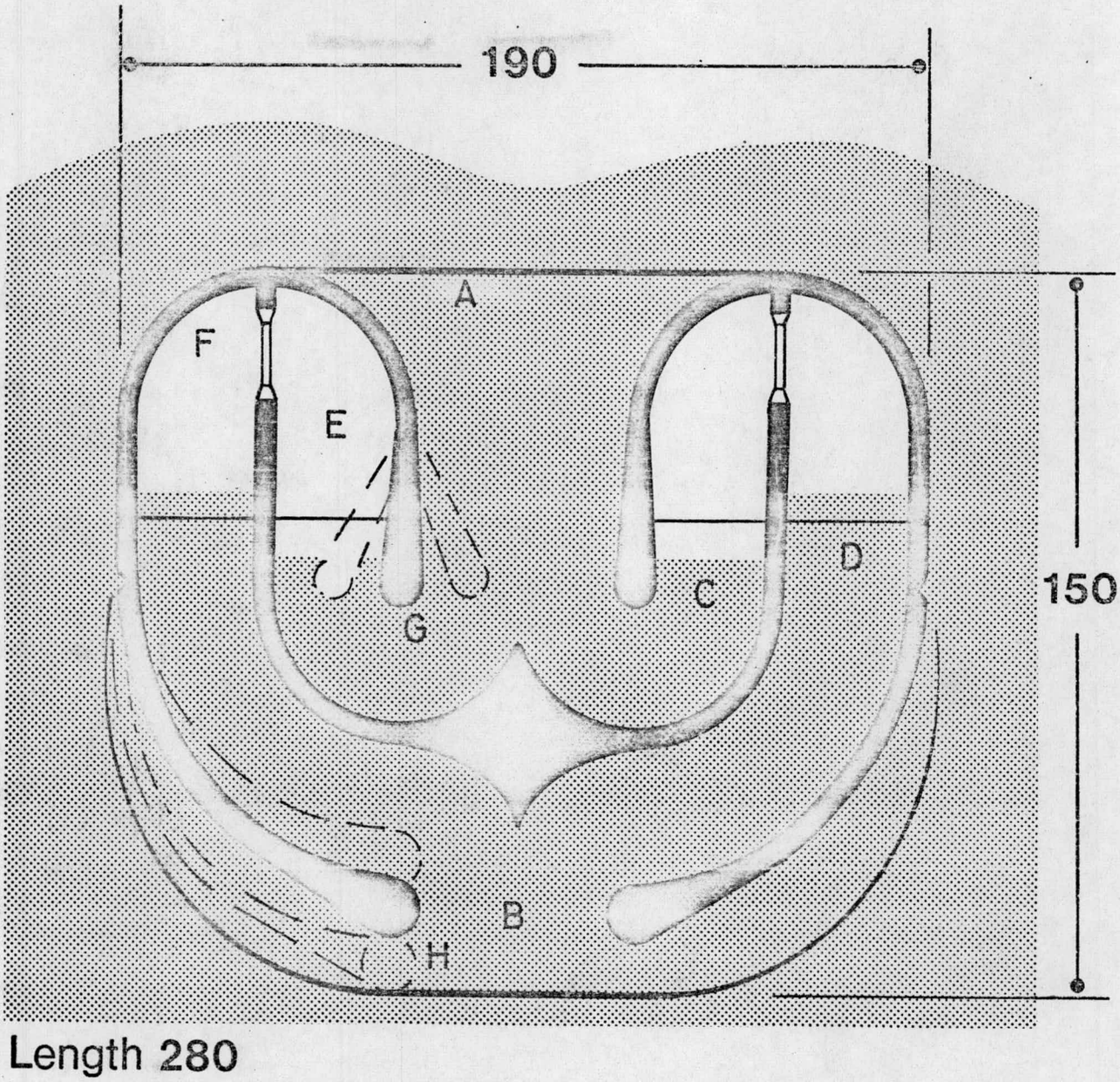

TWIN OSCILLATING WATER COLUMN

TERMINATOR

MODEL

FIG. 1.1.

P.M. SEA DATA

Te(secs)	Hrms	POWER mw/m
.7	.64	226
.8	.57	196.4
.9	.54	199.6
1.0	.52	209.25

THESE SPECIFIC VALUES WERE USED
WITH ALL TESTS USING P.M. SEAS

FIG. 1.2.

Channel 755 wave amp

Maximum	=	1.086	Minimum	=	0.000
Peak-Peak	=	1.086	RMS	=	0.145
Mean	=	0.034			

1.086

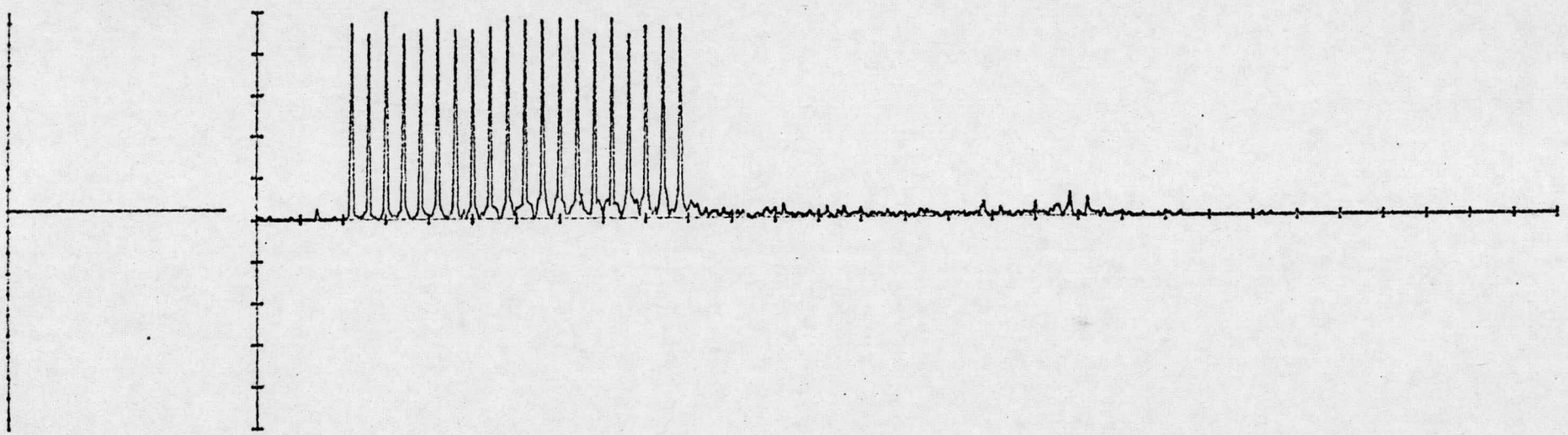

FIG.1.3.

Channel 755 wave amp

Maximum	=	1.071	Minimum	=	0.000
Peak-Peak	=	1.071	RMS	=	0.143
Mean	=	0.032			

1.071

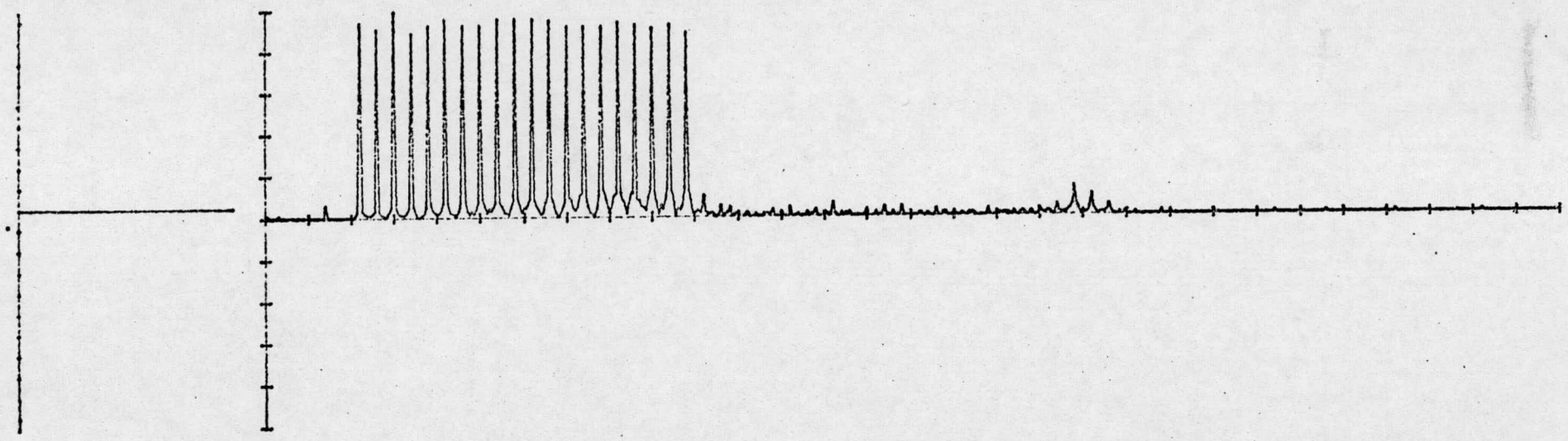

FIG. 1.4.

Edinburgh University Wide Tank Experiment
==========

Experiment Label : 045

Date : 22-NOV-79 Time : 12:20:49

					Position
Channel 300	level information				
Maximum =	20.595	Minimum	=	3.588	1
Peak-Peak =	17.007	RMS	=	13.213	
Mean =	12.674				
Channel 730	pressure (mm)				
Maximum =	4.574	Minimum	=	-4.346	2
Peak-Peak =	8.920	RMS	=	1.247	
Mean =	0.000				
Channel 764	downflowlh				
Maximum =	0.588	Minimum	=	-0.512	3
Peak-Peak =	1.100	RMS	=	0.206	
Mean =	0.000				
Channel 430	pressurerh(mm)				
Maximum =	4.892	Minimum	=	-4.848	4
Peak-Peak =	9.740	RMS	=	1.344	
Mean =	0.000				
Channel 464	downfrh				
Maximum =	0.581	Minimum	=	-0.433	5
Peak-Peak =	1.014	RMS	=	0.186	
Mean =	0.000				
Channel 717	all power(mw)				
Maximum =	0.842	Minimum	=	-0.003	6
Peak-Peak =	0.846	RMS	=	0.033	
Mean =	0.002				
Channel 604	capture (mm)				7
Maximum =	212.295	Minimum	=	0.000	
Peak-Peak =	212.295	RMS	=	9.396	
Mean =	0.658				
Channel 605	resid power (micw)				8
Maximum =	0.029	Minimum	=	0.000	
Peak-Peak =	0.029	RMS	=	0.001	
Mean =	0.000				
Channel 613	impedance				9
Maximum =	6029.657	Minimum	=	-6.993	
Peak-Peak =	6036.650	RMS	=	133.516	
Mean =	3.672				

Experiment remark : %flow error lh

Stack Top 10

2048 4.633

Experiment remark : %flow error rh

11

Stack Top

2048 5.482

Experiment remark : %power error

12

Stack Top

2048 0.993

Experiment remark : sum of all the power

13

Sum = 5.561

FIG. 1. 5.

Channel 604 capture (mm)

Maximum	=	212.295	Minimum	=	0.000
Peak-Peak	=	212.295	RMS	=	9.396
Mean	=	0.658			

212.295

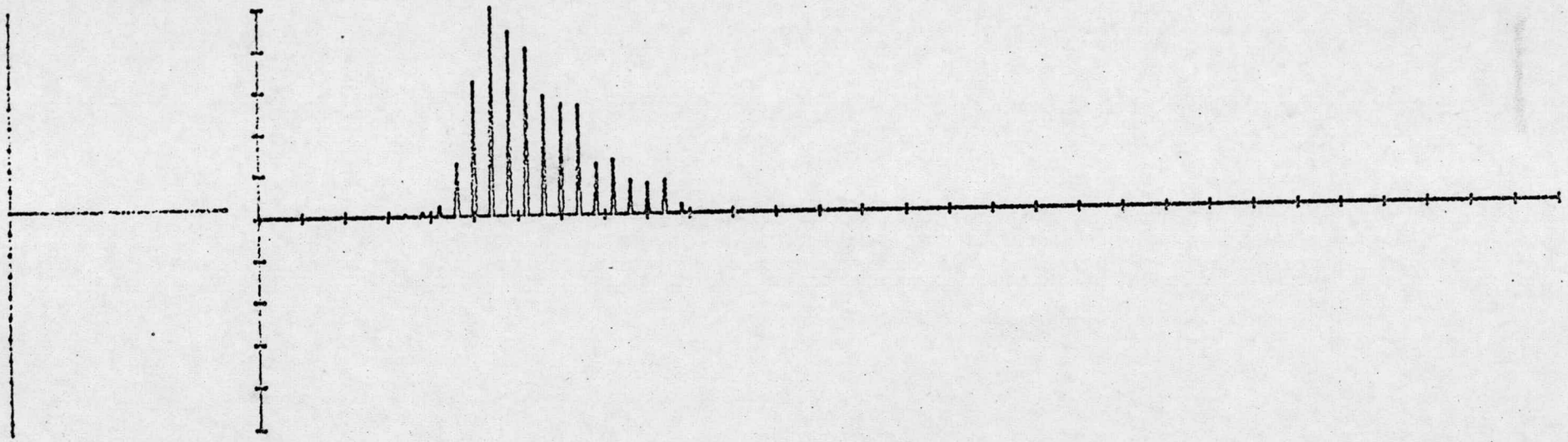

FIG. 1. 6.

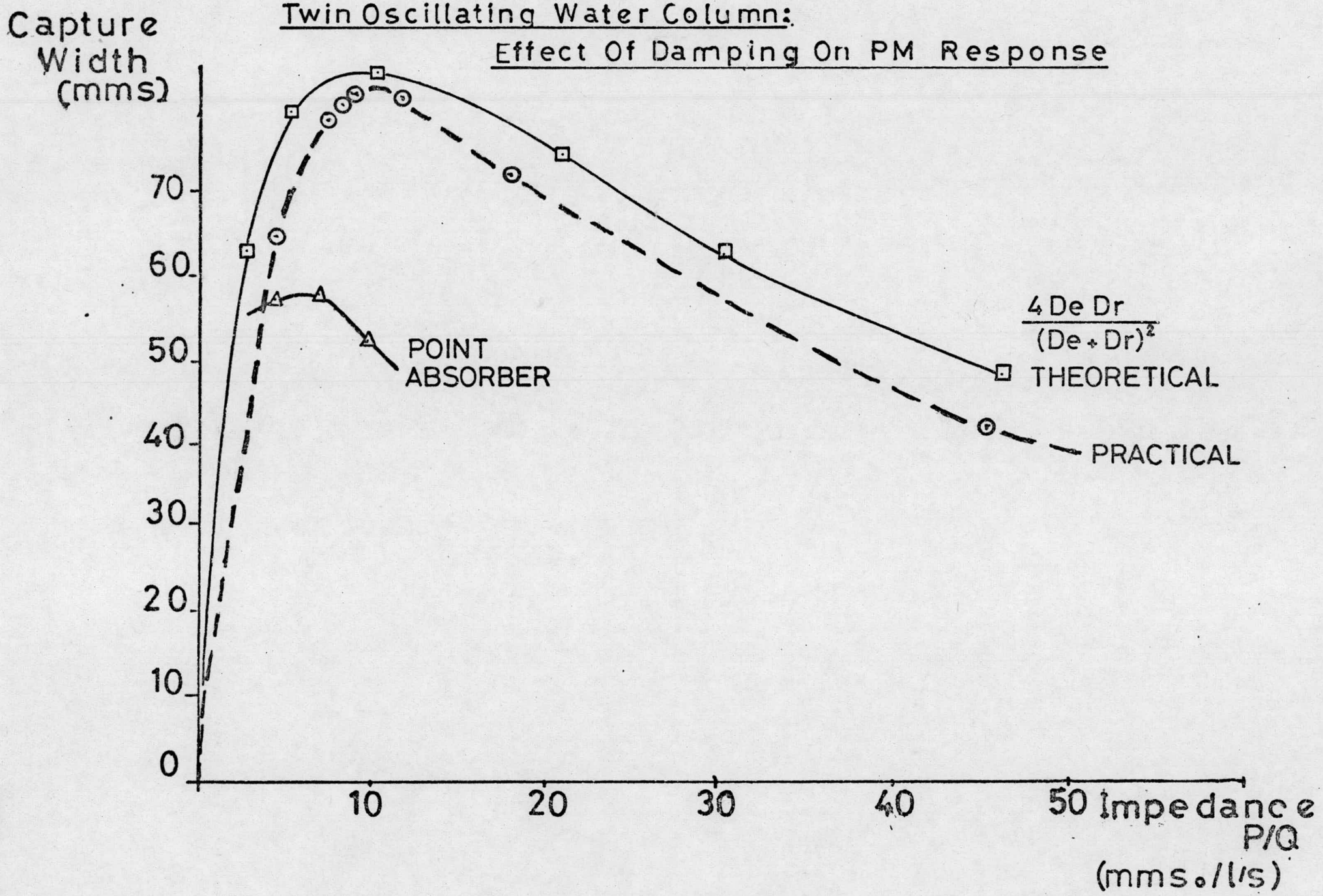
Twin Oscillating Water Column:
Effect Of Damping On PM Response
Capture Width (mms)
70
60
50
40
30
20
10
0
POINT ABSORBER
4 De Dr / (De + Dr)²
THEORETICAL
PRACTICAL
10
20
30
40
50 Impedance P/Q (mms./l/s)

FIG. 1.7.

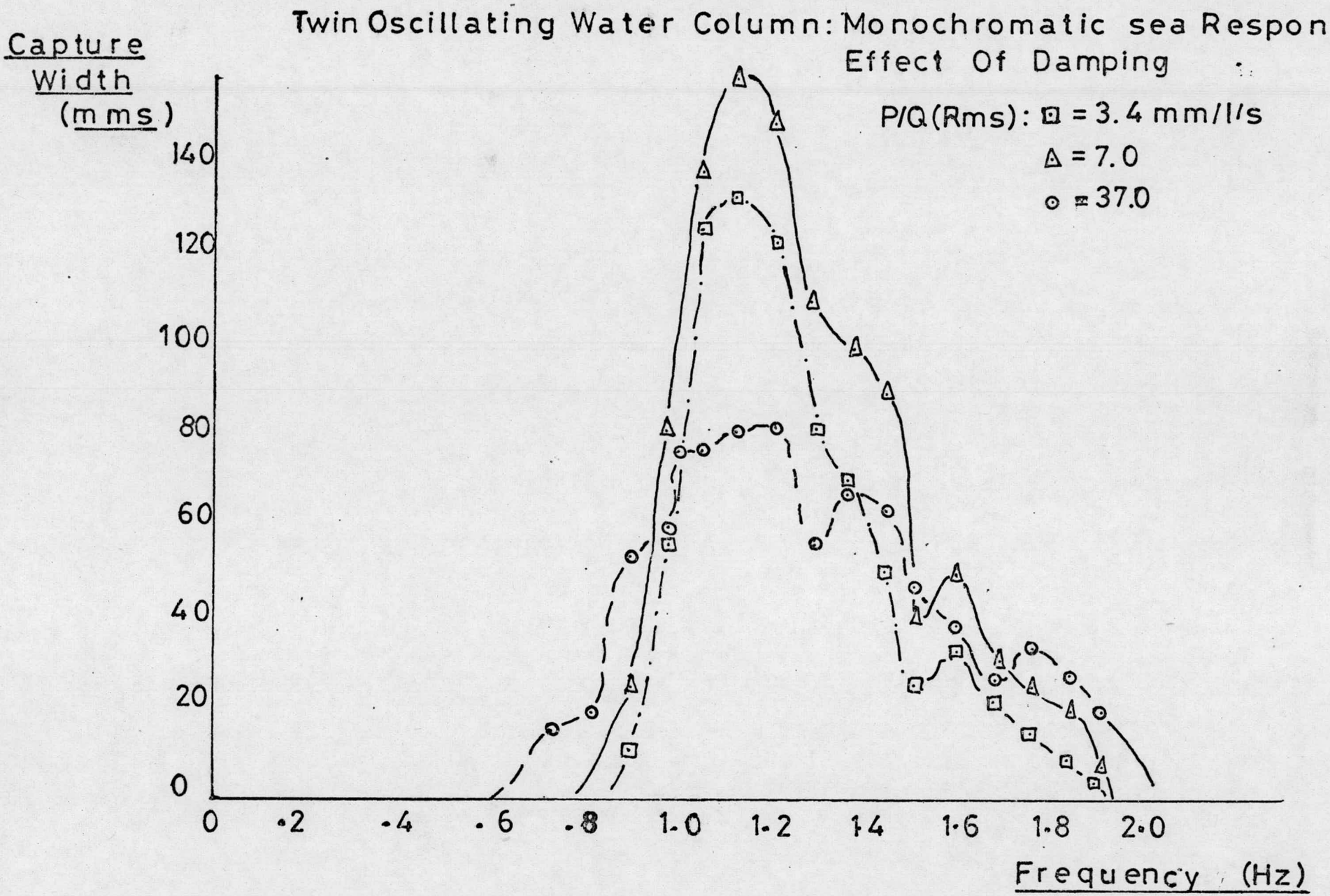
Twin Oscillating Water Column: Monochromatic sea Responce
Effect Of Damping
Capture Width (mms)
P/Q(Rms): ⊡ = 3.4 mm/l/s
△ = 7.0
⊙ = 37.0
140
120
100
80
60
40
20
0
0
·2
·4
·6
·8
1·0
1·2
1·4
1·6
1·8
2·0
Frequency (Hz)

FIG. 1.8.

EFFECT OF WAVEHEIGHT ON DAMPING DUE TO NON-LINEARITIES OF ORIFICE DAMPING

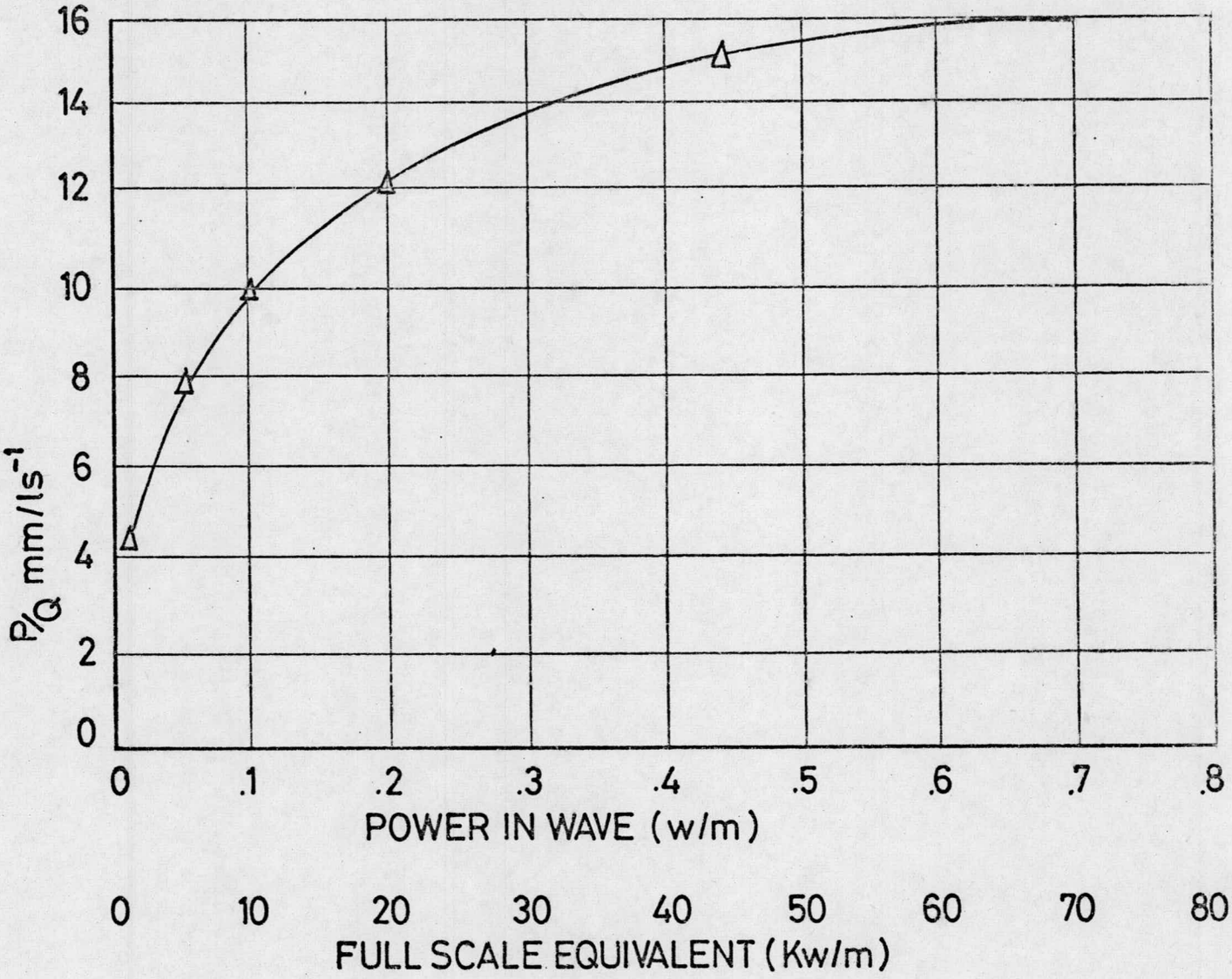

USING: P.M. SEA : Te .8 secs

DEPTH 5cms

FIG.1.9.

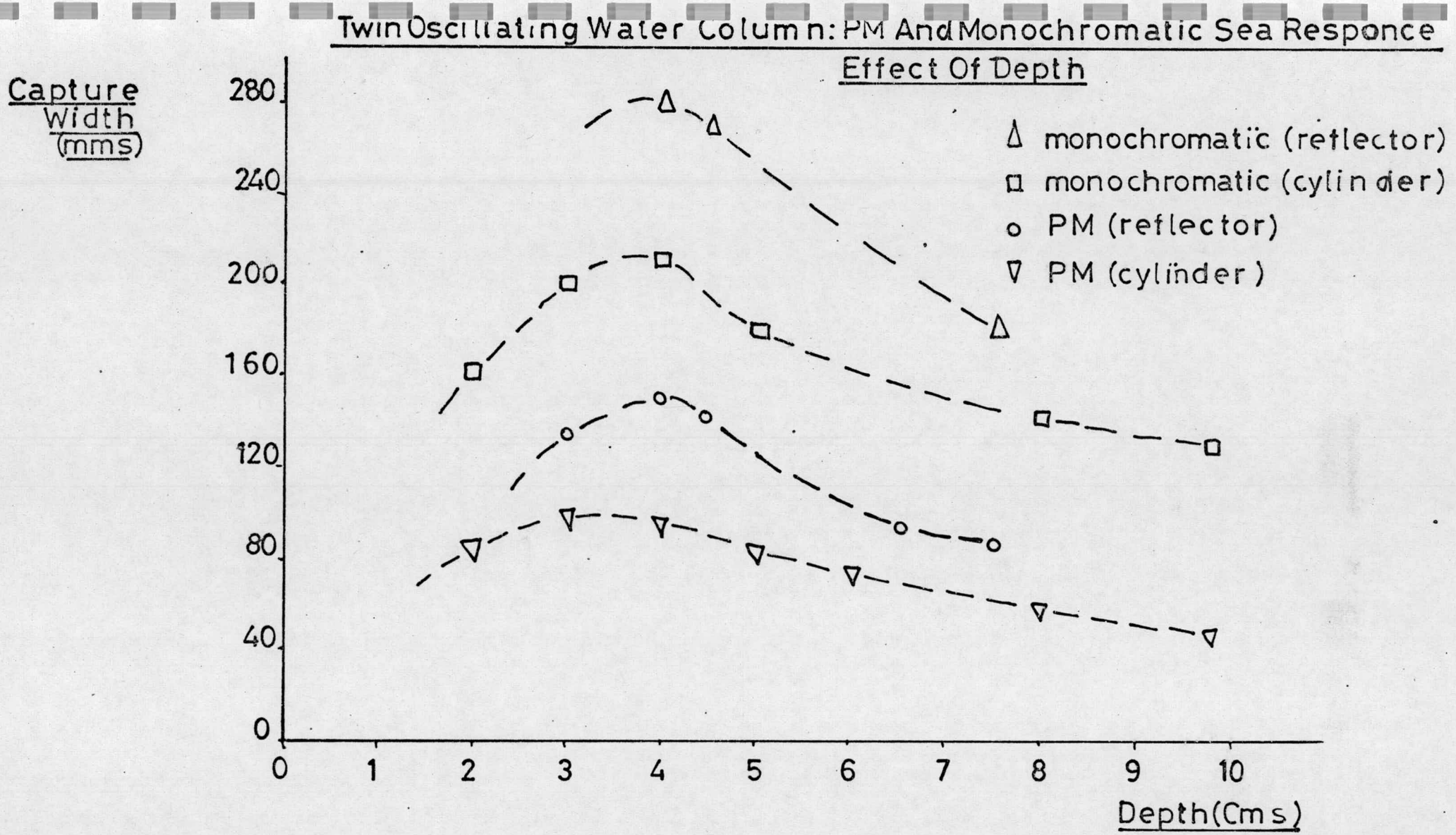
Twin Oscillating Water Column: PM And Monochromatic Sea Responce
Effect Of Depth
Capture Width (mms)
280
240
200
160
120
80
40
0
0
1
2
3
4
5
6
7
8
9
10
Depth(Cms)
monochromatic (reflector)
monochromatic (cylinder)
PM (reflector)
PM (cylinder)

FIG. 1.10.

Twin Oscillating Water Column: Monochromatic Sea Response

Effect of Depth

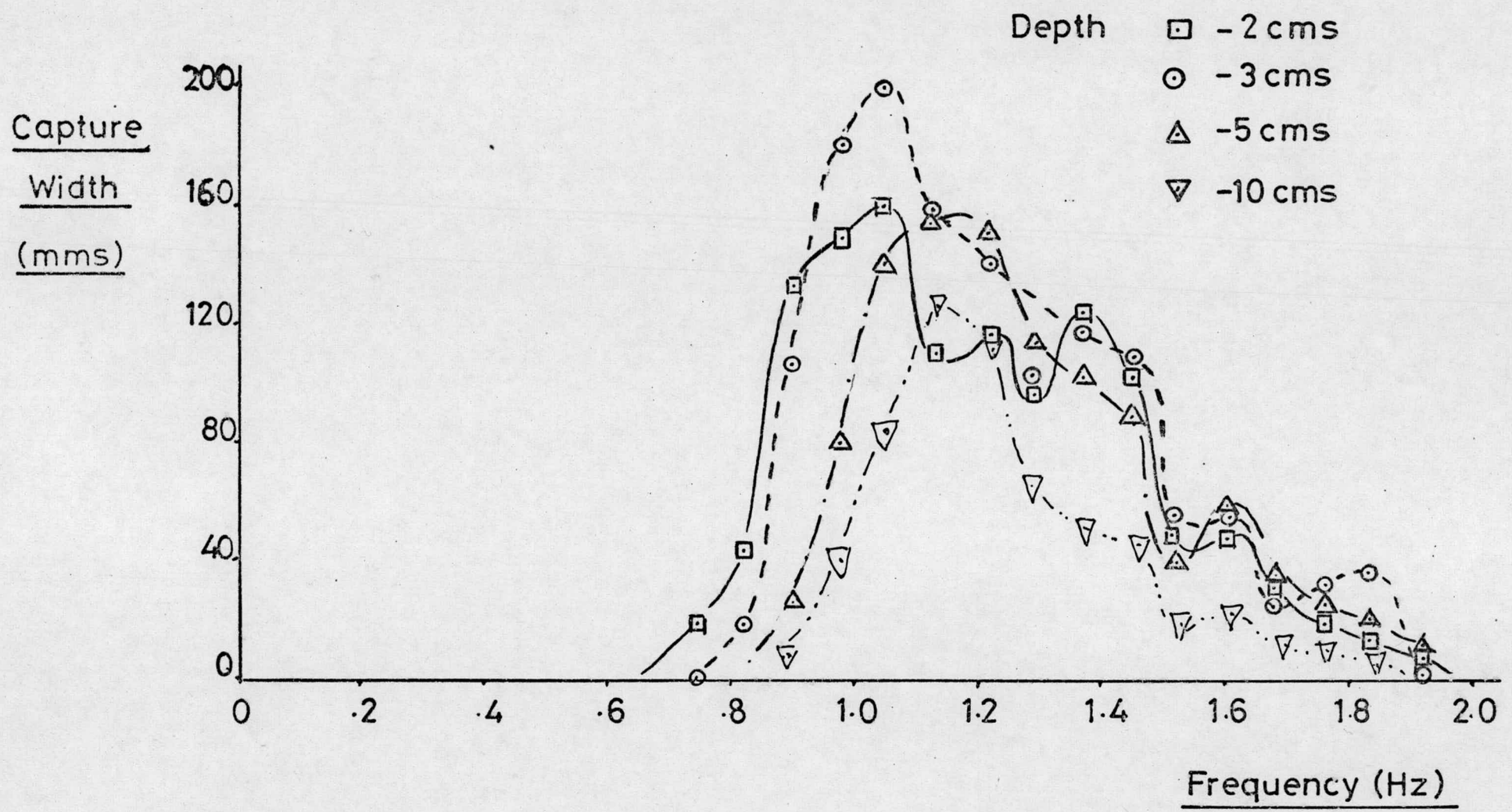

FIG. 1.11.

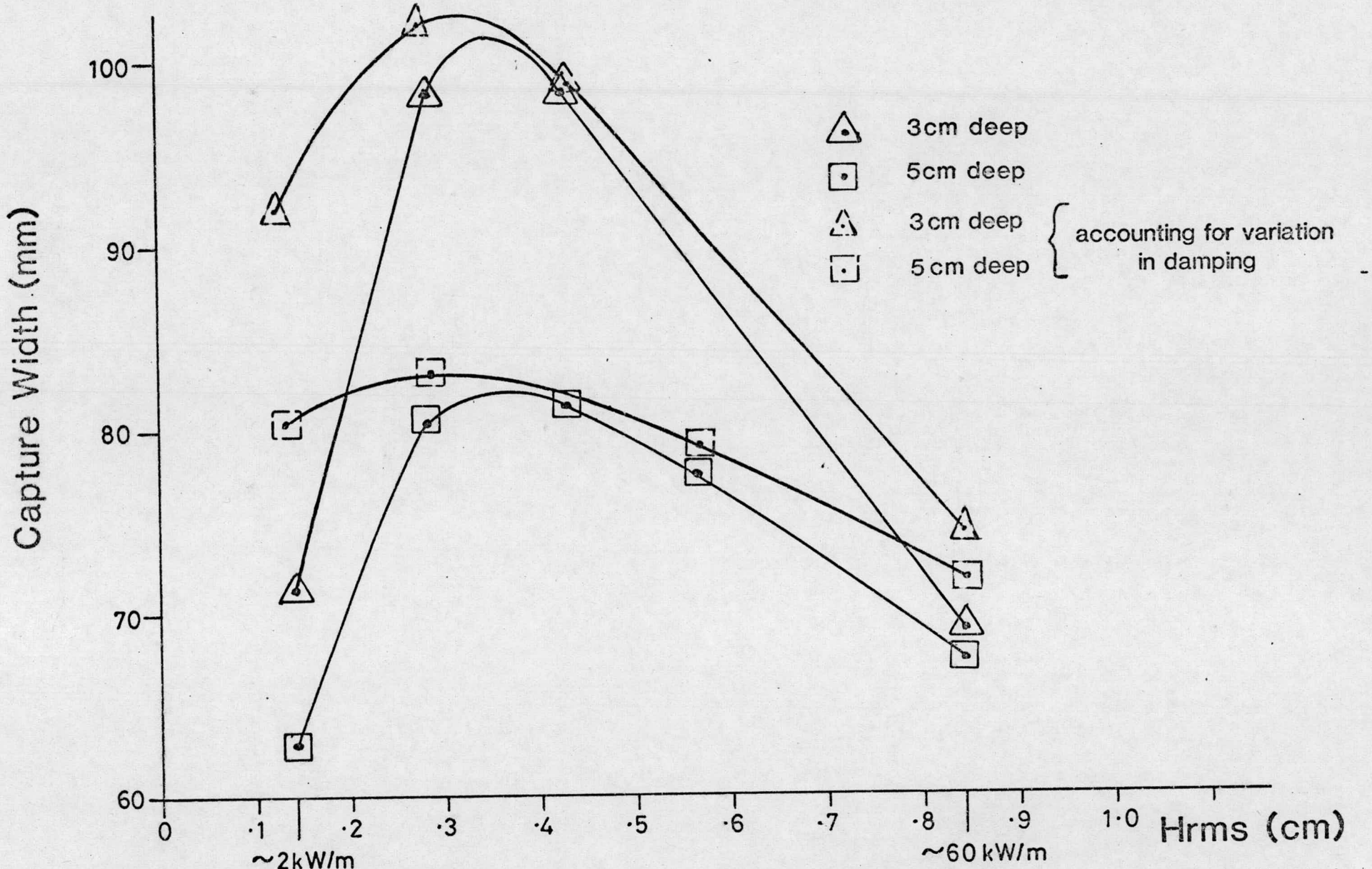

Twin Oscillating Water Column P.M. Sea Response Effect of Wave Height

FIG. 1.12.

Twin Oscillating Water Column: Monochromatic Sea Response
Effect Of Internal Geometry

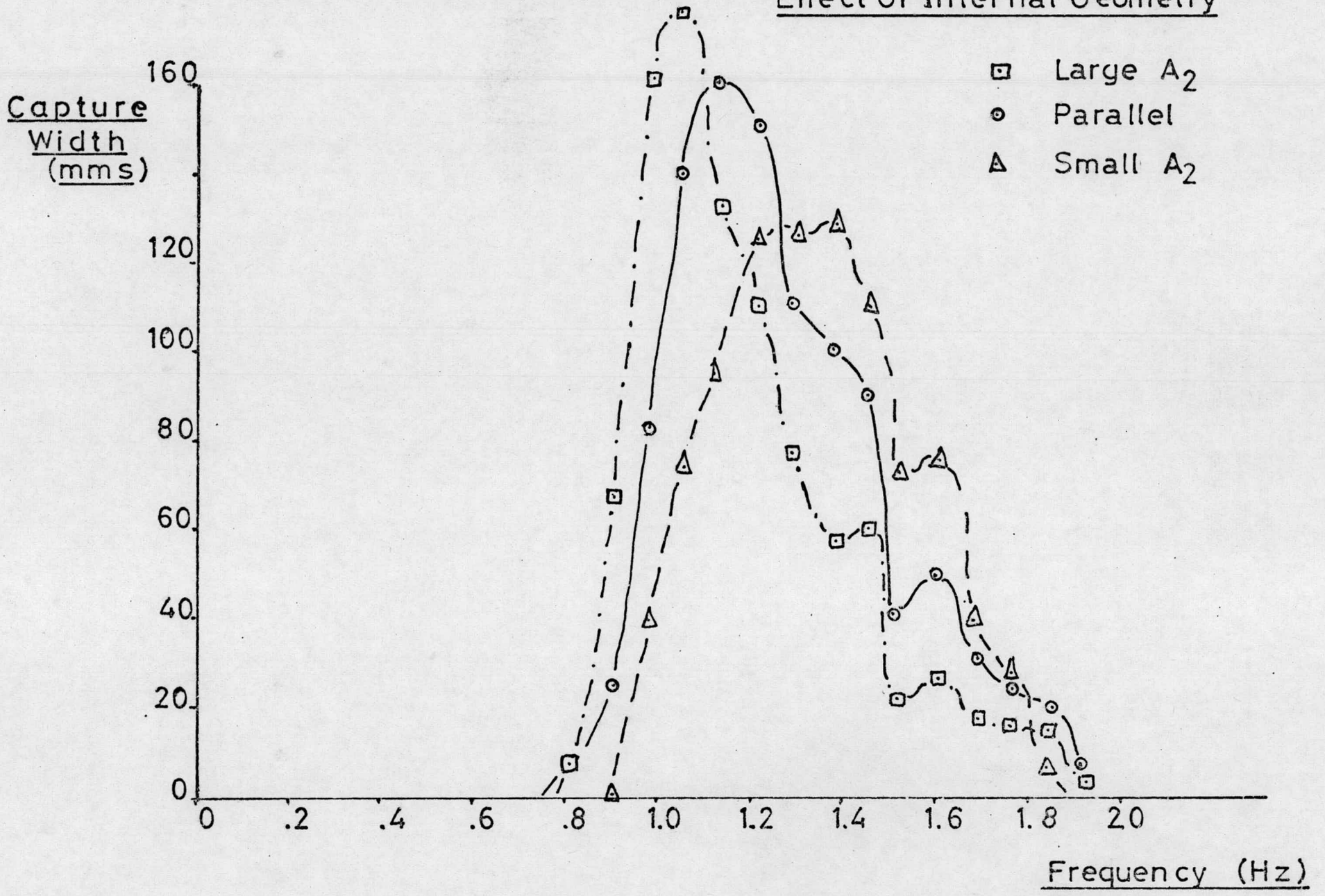

FIG. 1.13.

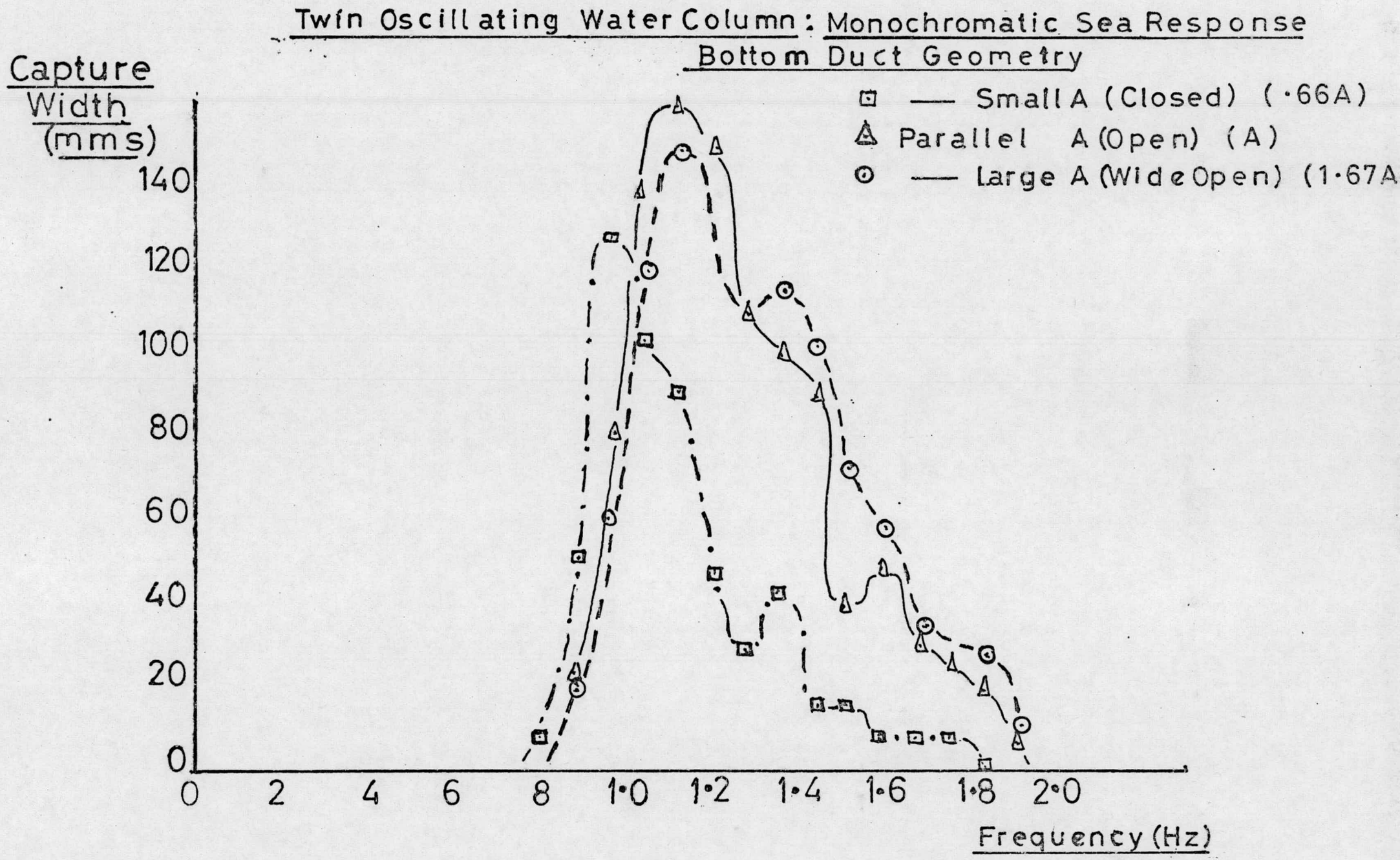
Twin Oscillating Water Column : Monochromatic Sea Response
Bottom Duct Geometry
Capture Width (mms)
Small A (Closed) (·66A)
Parallel A (Open) (A)
Large A (Wide Open) (1·67A)
140
120
100
80
60
40
20
0
0
2
4
6
8
1·0
1·2
1·4
1·6
1·8
2·0
Frequency (Hz)

FIG. 1.14.

By Courtesy of N.E.L.

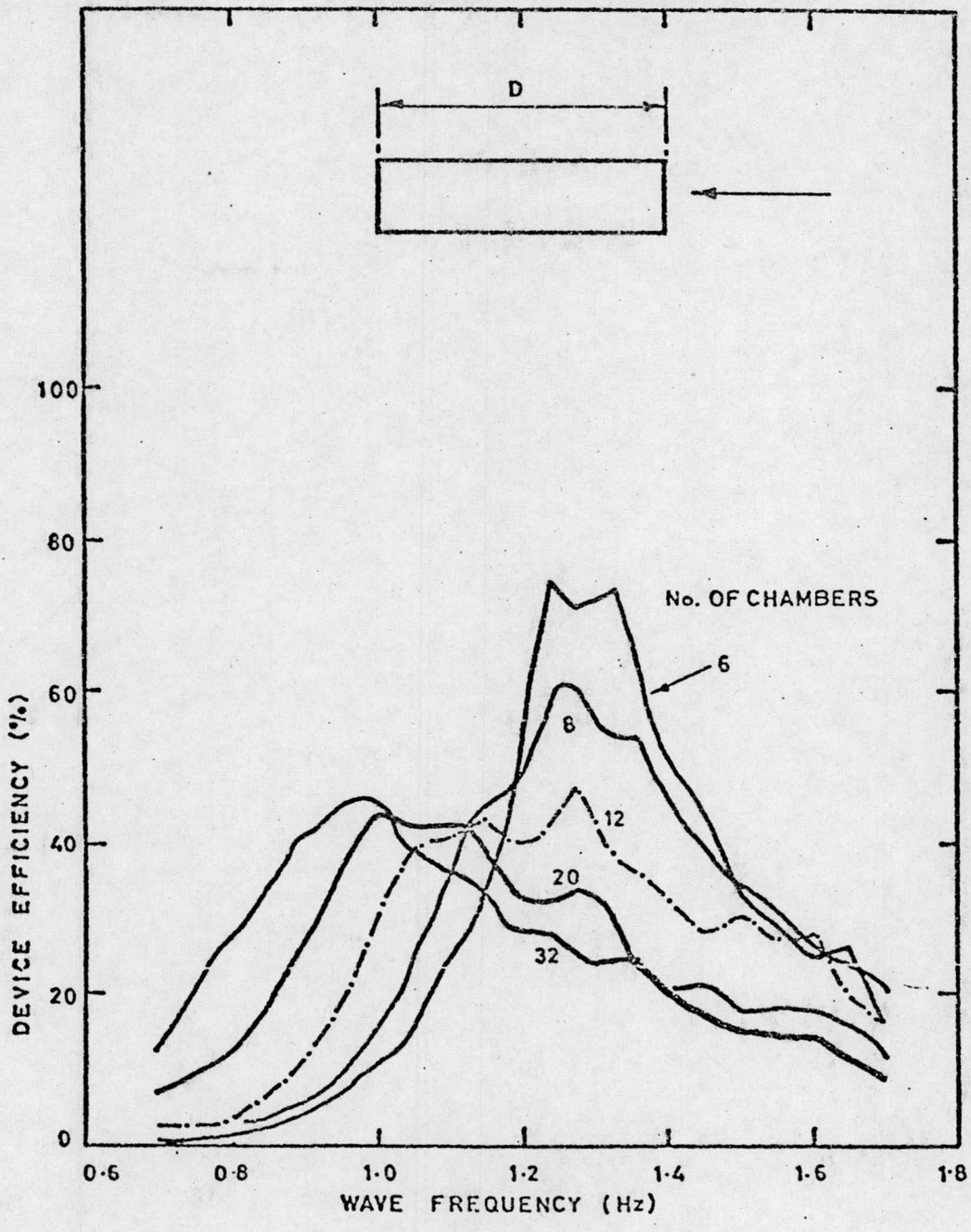

FIG 5 'I' BEAM EFFICIENCY FOR VARIOUS DEVICE LENGTHS

FIG. 1.15.

SURFACE FORCES ON T.O.W.C. TERMINATOR
(SUBMERGED HORIZONTAL CYLINDER)

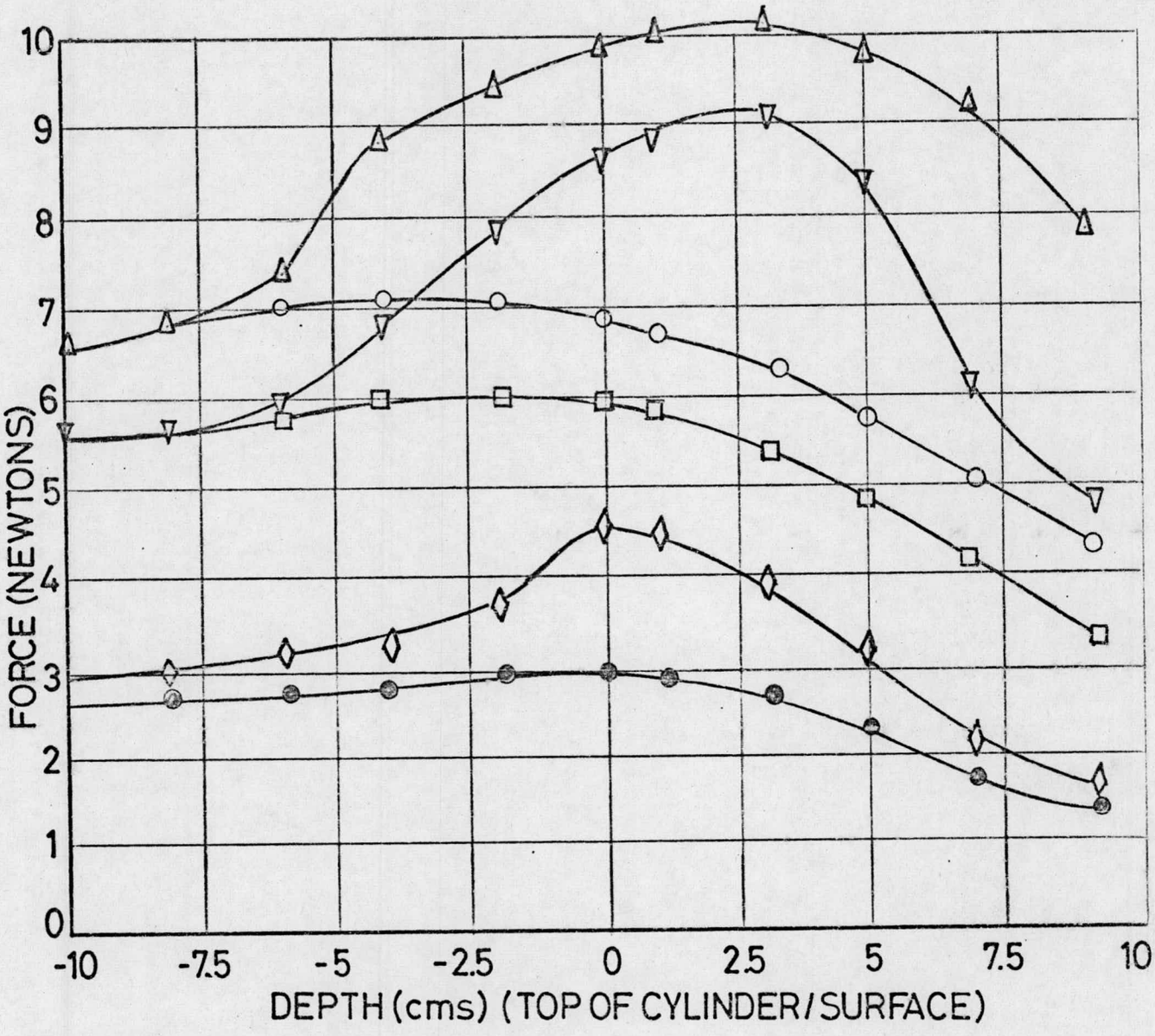

PRACTICAL RESULTS

△ 2.37cms (r.m.s.) WAVEHEIGHT

▽ 4.98cms

◇ 5.84cms

THEORETICAL RESULTS

○ 2.37cms (r.m.s.) WAVEHEIGHT

□ 4.98cms

○ 5.84cms

FIG. 1.16.

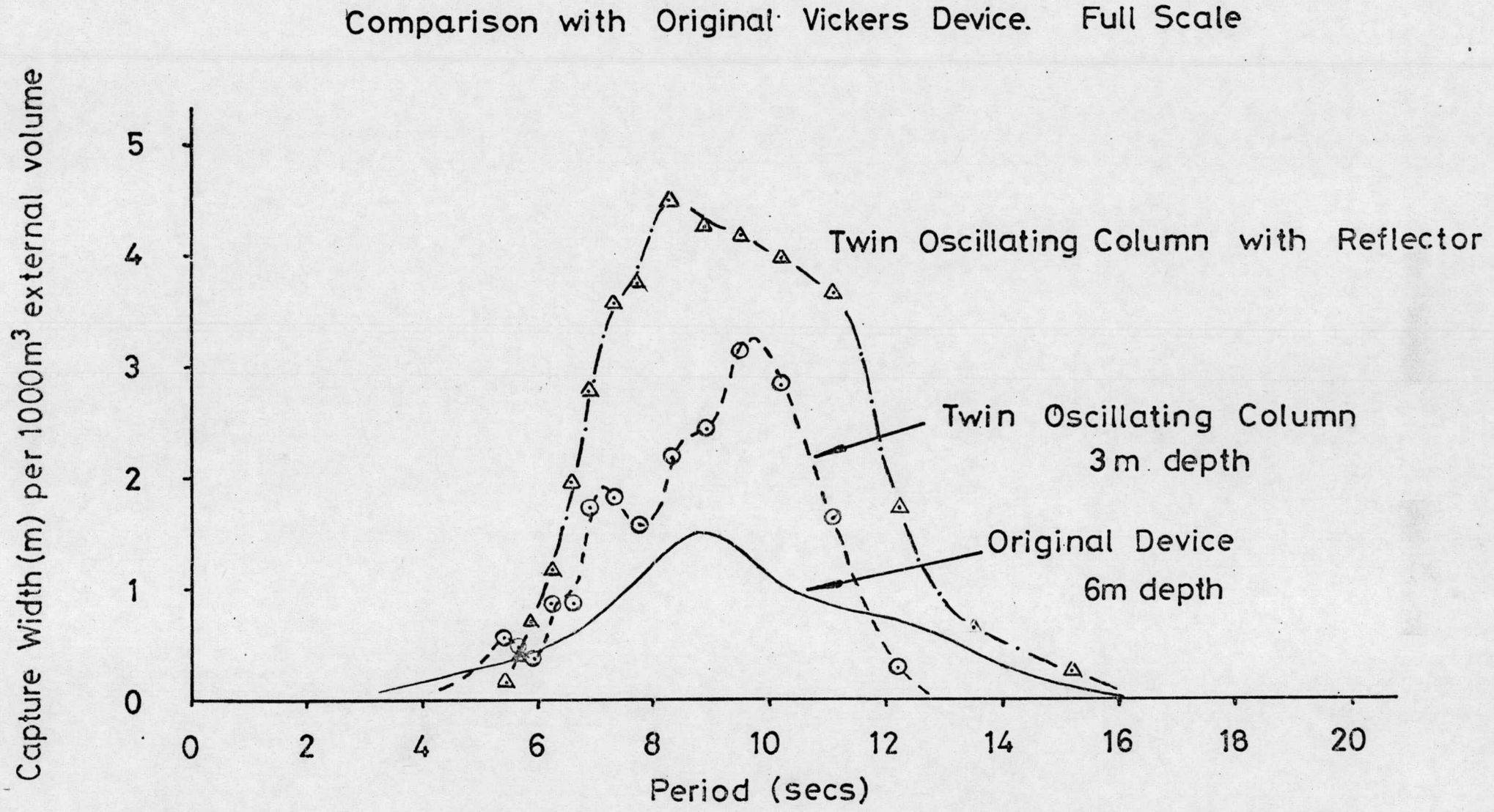
Comparison with Original Vickers Device. Full Scale
Capture Width (m) per 1000m³ external volume
0
1
2
3
4
5
0
2
4
6
8
10
12
14
16
18
20
Period (secs)
Twin Oscillating Column with Reflector
Twin Oscillating Column
3m depth
Original Device
6m depth

FIG. 1.17.

4.2 MODEL TESTS OF THE TWIN OSCILLATING WATER COLUMN POINT ABSORBER

4.2.1 Introduction

The results from the twin oscillating column terminator were so encouraging that it was decided to modify the Vickers Mk 7 device (Point absorber) to operate on the principle of the twin oscillating column. This was simple, a small perspex base being all that was required. The modification did necessitate two compromises, although all the major features of the MK 7 device, e.g. interchangeable bellmouths, adjustable internal geometry, and adjustable column length,etc, were retained.

The first compromise concerned the throttle - the throttle on the original Mk 7 device being mounted well below the model in the air volume. This was obviously impossible in the Twin Oscillating Water Column mode and the final solution lay in adjusting the length of a slot that naturally occurred between the two columns.

The second compromise resulted from the inherited geometry of the Mk 7 device. The downward facing column could only be one half of the volume of the upward facing column. This resulted in unnecessary throttling of the duct but this will be discussed later.

This modified model was also tested in the Edinburgh wide tank. Being very similar in size to the Twin Oscillating Water Column terminator (i.e. 1/100th scale), it was therefore possible to compare the two models with a high degree of confidence.

4.2.2 Description of Model

Figure 2.1 shows the design of the model. The principle is exactly that of the terminator. The model incorporates a large dead space as a result of modifying the original Vickers device. This space will be used for extra water column at full scale thereby lowering the natural frequency of the device. This aspect is discussed in greater detail in the paragraph on Column Length.

4.2.3 Aim

The aim of the programme was to compare the Twin Oscillating Water Column point absorber with the Twin Oscillating Water Column terminator, in order that an effective cost comparison could be made. The point absorber, however, incorporates a number of features that further our understanding of water columns; for instance, it has interchangeable bellmouths, the column length can be altered, and the probes in the bottom duct give us an interesting insight into the way in which water is expelled.

The following variables were investigated:

1. Damping
2. Depth
3. Column length
4. Internal Geometry
5. Bellmouths
6. Directionality of wave spectra
7. Reflector
8. Downward facing duct

4.2.4 Data Processing Progam for Twin Oscillating Water Column Point Absorber

This program is similar to the program developed for the terminator. The major difference is a result of the number and disposition of the wave probes in the bottom duct. It was felt two probes spaced 180° apart were not sufficient. Hence four probes spaced 90° apart were monitored. The format of the print-out is shown in Figure 2.2.

Position 1 shows the level information. This was designed as a brief check to ascertain that the water level did not reach the top of the device or drop to the level where air might blow out.

Position 2 gives the flow from each wave probe. It can be seen that the flows vary, depending on the position of the probe within the duct.

Position 3 was designed to give the % flow error by comparing the error in one pair of probes (180° apart) with the other pair in quadrature. There was typically a ±2.5% error in this value which suggests that the error in actual flow measurement (where the output of all four probes was averaged) was no worse than ±2.5%÷√2 or ±1.76%.

Position 4 shows the values of combined flow. This is the average of the four flow values.

Position 5 gives the pressure drop across the throttle.

Position 6 gives the total power. Each one of the 2048 samples of flow and pressure were multiplied together to give each value of power.

4.2.4 Data Processing Program for Twin Oscillating Water Column Point Absorber (Continued)

Position 7 gives the mean of the 2048 samples in this channel. This was used when the model was tested in Pierson-Moskowitz seas where F.F.T. analysis was not required.

This channel represents power in the wave divided by the power in the sea, as taken from the computer store. The computer store held data of all seas used in experiments, this data was measured with a single probe in the exact position that the model was to be placed.

Position 9 gives the residual power in frequencies outside the frequencies in the particular sea used. If the model had displayed second harmonics these would have been evident here. This residual power never represented more than 1% of the total power.

The last Channel represents impedance in mm/L/sec. As the efficiency of the device is dependent on damping, this was a useful parameter.

4.2.5 Device Experiments and Analysis

4.2.5.1 Damping

Due to the fact that this device was a modification of the original Vickers device, it was difficult to adjust the damping. For this reason only three different values of damping were chosen. Previous tests with the terminator had indicated the most suitable ranges, and three damping values which spanned the peak of this previous graph were chosen. Figure 2.3 shows the monochromatic sea response to these damping values. There is very little variation between the 3.49 and 6.17 values of damping which suggests that these are close to the optimum. This was confirmed by the P.M. data (using larger waveheights) which favoured the 6.17 value and this was subsequently chosen for all further tests. This value resulted in a non-dimensional pressure ratio (r.m.s. pressure/r.m.s. waveheight) of 0.64 - not greatly different from the terminator value of 0.5.

The graph confirms the findings of tests with the terminator. A damping value off optimum does not change the natural frequency but results in loss of peak power and bandwidth.

4.2.5.2 Depth of Submergence

The device was tested at depths that ranged from 1cm to 10cm, representing 1m to 10m at full scale. Figure 2.4a. shows the effect on capture width in a monochromatic sea. There are three interesting differences between this graph and the equivalent graph for the terminator. Firstly the optimal capture width for the point absorber occurs at 2cm rather than 3cm in the case of the terminator.

4.2.5.2 Depth of Submergence (Continued)

Secondly, the frequency shifts from 1.1Hz to 1.35Hz when the depth is increased from 2 to 10cm. This compares with a shift from 1.05 to 1.15 with the terminator.

The frequency shift to higher frequency with increasing depth is a function of the added mass. Theory predicts that the added mass of the point absorber (M. Simon) decays faster with depth than the two dimensional terminator (J. Lighthill) and the graph supports this prediction.

Thirdly, the point absorber displays gross attenuation with depth: the capture width drops by a factor of four from 2cm to 10cm, while the capture width for a terminator drops by 1.6 for the same depth variation.

All three of these features represent disadvantages for the point absorber. The first because it has to be closer to the surface and hence suffers the greater surface forces. The second because cost effectiveness is a function of resonant frequency to the power of four, which implies that the point absorber will become much less cost effective at high tide, and, by implication, at large waveheights. The third because the level of attenuation is 2.5 times that of the terminator, also highly undesirable in these same conditions.

It is important to note that the column lengths of the terminator and point absorber models were designed to be equal. As the natural frequency is higher for the point absorber at 2cm, and the capture efficiency is less than the terminator, it appears that the point absorber exhibits no advantages even at shallow depths.

4.2.5.2 Depth of Submergence (Continued)

Figure 2.4b represents the effect on the model of a Pierson Moskowitz sea at varying depths. At high frequencies it is clear that 3cm gives the optimum capture width but at low frequencies, the frequencies that count for the most cost effective device, 2cm is becoming more cost effective.

Furthermore, the level of attenuation of capture width found in monochromatic seas is confirmed. From 3cm to 10cm it ranges from a factor of 3 at .7 seconds P.M. to 5 at 1 second P.M. This at first appears contradictory as the long wavelength should be attenuated less but it is a feature of the frequency shift.

4.2.5.3 Column Length

The device was designed so that rings could be added to the top of the structure, thereby increasing the column length of the upwards facing duct. Two extension rings were added, one of 60mm depth, the other 100mm.

Figure 2.5 shows the monochromatic frequency response to additions in column length. The frequency is lowered with increasing column length which is to be expected from $T = 2\pi\sqrt{l/g}$. There is also an increase in peak efficiency. The design of the model is necessarily a compromise as it is a modification of the Vickers air volume device. This results in a dead space in the base of the model. The most cost effective way of filling this space is to use it for extra water column. The 10mm toroidal ring represents this extra water column length.

Figure 2.6 shows the response in P.M. seas. These data show that at long wavelengths, which are of greatest importance if a cost effective device is considered, the capture width is improved by 50%

4.2.5.3 Column Length (Continued)

At Te = 1 second, the most cost effective frequency for the device, a length increase from 0 to 6 cms shows a 35% improvement in capture width for a 21% increase in enclosed volume. From 6 to 10cm the cost effectiveness improves by only 12% while the enclosed volume increases by 11%. A 10cm increase is therefore close to the optimum design of column length for a cost effective device.

Some of the improvement with column length could be an effect of lowering the bottom duct and until further tests are made with the final design geometry it is not clear which is the dominant effect.

4.2.5.4 Internal Geometry

The device could be modified to incorporate tapered and antitapered rings to alter the internal geometry. These were so designed to give three different taper angles on the upward facing duct.

The taper angle was designed to be constant from the air-water interface to the bellmouth opening, this requiring additional toroidal inlet rings and modified bellmouths. The three different designs represented taper angles of 15^{o} taper, parallel, and 15^{o} antitaper, while keeping the same overall dimensions of the model.

Figure 2.7 shows the monochromatic frequency response to these geometries. It is evident that antitaper represents improved efficiency (improvement in peak efficiency of 20% against the parallel section) with a slight shift in frequency, which also favours antitaper.

4.2.5.4 Internal Geometry (Continued)

A greater frequency shift is predicted in theory for effectively the gravitational spring constant has been reduced. The results from the Twin Oscillating Water Column terminator exhibited similar improvements in capture efficiency with antitaper but the change in frequency response agreed with theory and was much more pronounced (from 1Hz to 1.3Hz). Three dimensional analysis of ducts (M. Simon) may indicate why this difference obtains.

Figure 2.8 represents the P.M. sea response. It again shows improved efficiency with antitaper - a general improvement of 15% over the parallel section. Again negligible frequency shift is indicated.

4.2.5.5 Bellmouths

Three different shapes of bellmouth were tried. These are shown in Figure 2.9.

There appeared to be no difference between the raised centre section and the standard section. The raised outer section, however, shows a reduction in frequency which is beneficial for a cost effective device. This is due to an effective increase in added mass and is probably depth dependent (less significant with depth), but no depth tests were made with these configurations to test this. The very small variation suggests that bellmouth design on point absorbers is not very critical, and indicates that the focussing effect of a raised centre section bellmouth (e.g. the Lockheed device) is not evident, or is at best outweighed by other effects.

4.2.5.6 Directionality of Wave Spectra

A single test was made with the device in a .8 second, long-crested P.M. sea without Mitsuyasu spreading. The capture width was within 1% of the capture width measured with short-crested seas with Mitsuyasu spreading, as can be expected with a point absorber. It is regrettable that no similar test was made with the Twin Oscillating Water Column terminator. It is interesting to note, however, that the raft displays a 33% reduction in efficiency with short crested against long crested seas. This represents an advantage for point absorbers and indicates that rafts and probably the Twin Oscillating Water Column terminator should be shorter in the wave crest direction. The Twin Oscillating Water Column terminator has a capture width in short crested seas of 50% that in monochromatic seas. The point absorber produces 70% of the monochromatic capture width in short crested seas. As both devices have similar bandwidths it indicates that 20% of the terminator capture width is being lost due to spreading. This could be reduced by having shorter cells in the crestwise direction.

4.2.5.7 Reflector

A semicircular reflector was attached to the inshore side of the device. It was hoped that this would result in improved performance as in the case of the terminator. However quite the opposite occurred; the monochromatic peak frequency was reduced by 50%, as was the bandwidth.

Figure 2.10 shows the P.M. response. There is a shift to lower frequency, but even at this peak the device without the reflector enjoys a greater capture width.

4.2.5.7 Reflector (Continued)

It is not yet clear why this affect is completely different from the terminator. It could be a function of the focussing effect of the reflector, although at first sight this should be advantageous.

It is possible that tests with reflectors encompassing less than half the circumference could produce illuminating results. Possibly a small reflector could be advantageous for a point absorber. Even if this was the case however, the performance advantage could only be small and the disadvantages of a surface piercing device would outweigh it.

4.2.5.8 Bottom Duct

The four wave probes in the duct gave a very interesting insight into the manner in which water is expelled.

Figure 2.11 indicates the direction of the wave relative to the four probes. It was found that the port and starboard probes showed little disparity, which is understandable from symmetry, while the fore and aft probes showed great disparity. The ratio $\frac{Q1}{Q3}$ relates to

the r.m.s. flow

of the aft probe relative to the r.m.s. flow of the foreward probe. For all combinations of depth and frequency the foreward probe shows a greater flow. This could be due to two effects:

1. The direction in which the ducts face
2. The displacement, in the direction of the wave, of the two ducts.

4.2.5.8 Bottom Duct (Continued)

Previous tests with the terminator suggest that directionality of the bottom duct is not an important factor: No attenuation was observed by rotating the mouth of the bottom duct through 180° (fore and aft). It appears, then, that the dominant effect is due to duct displacement.

A possible explanation of this effect is that displacement of the ducts in the fore and aft direction gives the whole device a degree of directionality, thereby enabling some of the surge component of the wave to be removed.

The figure shows that short wavelength seas are affected more than long wavelength seas. This agrees with the directionality theory as the device effectively spans more of a wavelength. Furthermore the ratio approaches unity with increasing depth, which is also understandable as local pressure variations on the surface average out with depth.

This test shows dramatically that a Twin Oscillating Water Column should have its downwards facing duct ahead of the upwards facing duct, thereby making it directional.

This implies that the symmetrical point absorber Twin Oscillating Water Column is not the optimal configuration, as such directional effects cannot be exploited.

4.2.6 Summary of Twin Oscillating Water Column Point Absorber Tests

This series of experimental tests has provided valuable insights into point absorbers, particularly their usefulness as Twin Oscillating Water Column devices. The findings can be summarised as follows:

4.2.6.1 Damping

The effects of variations in damping are similar to those for the terminator device. Either overdamping or under-damping results in reduced peak capture width and less bandwidth.

The optimum r.m.s. pressure drop across the turbine, expressed as metres of water, is .64 of the r.m.s. waveheight in metres.

4.2.6.2 Depth of Submergance

Capture width for this device is highly dependent on depth. It drops by a factor of four when the depth at full scale is varied from 2 metres to 10 metres. This compares with a factor of 1.6 for the terminator.

Natural frequency is also depth dependent. The shift represents a shift from 9 seconds to 7.5 seconds when the inlet depth is dropped from 2 to 10 metres. The natural frequency of the terminator, however shifts from 9.5 to 8.7 seconds. This excessive shift to higher frequency with depth is a further disadvantage for the point absorber.

4.2.6.3 Column Length

Tests showed that the addition of a toroidal ring to the top of the device lowered the natural frequency and improved the capture width.

Analysis of results shows that the addition of the 10cm ring gives optimum capture width for a cost effective device. This 10cm addition will be incorporated into the original shape of the device in place of the dead space which occurred when it was modified from the original Vickers device.

4.2.6.4 Internal Geometry

Results of tests with the Twin Oscillating Water Column Terminator were confirmed in that antitaper provided a 15% improvement in capture width. It is difficult to make a 3 dimensional model infinitely variable in antitaper. However, it is believed that the 15^{o} value is about optimal as greater angles of antitaper will result in excessive duct throttling which previous tests with the terminator have been shown to be undesirable. Natural frequency is not affected to the extent that 2 dimensional theory suggests, but 3 dimensional theory may elucidate this.

4.2.6.5 Bellmouths

The bellmouth with the raised outer section (see graph) gave the best capture width.

4.2.6.6 Directionality of Wave Spectra

The point absorber appeared to be insensitive to directionality and spreading function, unlike the terminator which suffers some 20% loss of capture width.

4.2.6.7 Reflector

A semicircular reflector placed behind the point absorber reduced the capture width. This constrasts strongly with the terminator where it was found to be beneficial. Analysis of 3-dimensional theory may clarify this.

4.2.6.8 Bottom Duct

It was found that the front part of the bottom duct in the direction of wave motion worked harder in all conditions than the rearward part of the duct. This implies that there should be directionality designed into the device which conflicts with the point absorber concept.

4.2.6.9 Conclusions

Figure 2.12 compares the cost effectiveness of the point absorber with the other devices presently being developed at Vickers. It is clear that it is the least cost effective device. This comparison refers to the optimum performance of each device scale up from 1/100th scale.

It is unlikely that further optimisation of the point absorber concept will result in any more than a 20% improvement, while modifications to the terminator mode, utilising the surge component of the wave, could result in the performance already achieved with the reflector but without incurring the disadvantages of the reflector. The symmetry of the point absorber leads to the following disadvantages when compared with terminator performance, as evident from the tests.

4.2.6.9 Conclusions (Continued)

1. Capture width is over-sensitive to depth of submergence, causing excessive reduction of performance at high tide and, by implication at large waveheights.

2. The frequency response is over-sensitive to depth of submergence, shifting excessively towards higher frequencies with increasing depth.

3. An imbalance in flow rates around the bottom duct indicates that the bottom duct should lead the top duct in a wave direction sense, for optimum performance. This implies a non-symmetrical configuration.

On the credit side the point absorber is less susceptable to directionality of sea spectra, although this is taken into account in figure 2.12 which relates to short crested seas with Mitsuyasu spreading. It is also a more robust structure incorporating a cylindrical shape and a toroidal arch but this is counterbalanced by complexity of fabrication.

It is clear that the terminator has great possibilities for development while the parameters of the point absorber, by nature of its symmetry, have been almost fully optimised in this series of tests. Some tests with a model which substitute the dead space for column length could give further insight into top and bottom duct separation but this could only give an improvement of about 10% when the cost considerations of a taller device are considered.

It is therefore proposed that future work should concentrate on development of the terminator design, which has shown great promise.

4.2.7 Future Work on the Twin Oscillating Water Column

Three different Twin Oscillating Water Column designs are considered:

1. Twin Oscillating Water Column Point Absorber

2. Twin Oscillating Water Column Terminator

3. Twin Oscillating Water Column Terminator with Reflector

It is important to relate the theoretical point absorber analysis (M. Simon) to the results of our experimental tests, particularly as the findings are so strikingly different from those of the terminator. Some insights may be gained from this as to how it can be made less sensitive to depth and less sensitive to bottom duct position. Meanwhile it is prudent to assume that these are features of this design and to concentrate effort on the terminator which shows greater promise.

A Twin Oscillating Water Column terminator has been designed which models the artists impression shown in Figure 3.6. This device incorporates the features suggested by the findings of the experimental program.

As it is a two dimensional device it is possible to vary all sections, particularly:

1. Bottom to top duct horizontal separation.

2. Bottom to top duct vertical separation.

3. Cross-sectional area of the air water interface.

4.2.7 Future Work on the Twin Oscillating Water Column Devices (Continued)

4. Taper angle of the inlet duct.

5. Cell length.

6. Spacing of cells.

The versatility of this model will allow every aspect of the device to be explored. The goal is to modify the device to achieve the annual capture width obtained with the reflector by optimising the position of the top and bottom column thereby introducing directionality.

There are also generic studies to be completed. These involve the Safety Chamber, and an automatic latching concept. Patents for both of these have been applied for. Experimental models of each of these features should be developed for incorporation in the Twin Oscillating Water Column terminator design, if test results are favourable.

Optimisation of the Twin Oscillating Water Column could be completed within one year followed by design study of a full-scale device, with indicative costings.

4.3 EFFECTS OF SCALE OF TWIN OSCILLATING WATER COLUMN DEVICES

This chapter describes the effects of scale when related to a cost effective design. Figure 3.1 shows the spectra of monochromatic frequencies that constitute a typical South Uist sea (Mollison, November 1979). The first overlay relates to the capture width that is expected from a 1/100th scale model of the point absorber. It can be seen that only a very small percentage of power in the sea is being removed. Nevertheless it has been found that this is the most cost effective device and analysis will show this later. By comparing overlays it can be appreciated that 1/200th scale is the scale at which resonant frequency matches well the Te of the South Uist Sea. This scale is the most effective as far as resource efficiency is concerned. With Wave Power in its infancy it is reasonable to expect the first devices to be developed with cost effectiveness in mind and it is for this reason that we have discussed all the results of experiments and tests with reference to this scale (approximately 1/100th) rather than the most resource efficient scale (approximately 1/200th).

The product of Figure 3.1 and the first overlay (1/100th scale) gives the annual total capture width in metres at South Uist. This is only 3.3m - a capture width ratio of .14. The product of Figure 3.1 and the last overlay gives the annual capture width at 1/200th scale 11.7m, or a capture width ratio of .24m.

Figure 3.2 shows these capture widths plotted for different scales.

4.3 EFFECTS OF SCALE (CONTINUED)

By measuring the gradient at each point and its accompanying co-ordinates it is possible to read off the appropriate scale against the index selected (See Section of this report referring to scale of the Submerged Wave Chamber).

The index is defined by cost α (scale)^n. If we are interested in capture width per unit volume then n = 3. However, the section of this report dealing with full scale device construction suggests that for a bottom mounted device in shallow water the index should be 2.5. The graph gives the scale for this index as 1/100th.

Referring back to Figure 3.1 with the 1/100th scale film it can be seen that the greater proportion of the power in the wave passes by the device. It is therefore a fallacy to assume that a series of devices will take out all the power in the wave. They will all be competing for the high frequency component in the wave. A cost effective tuned device is necessarily inefficient in terms of resource.

This disparity is not confined to the Vickers device, nor to Water Columns, but is a feature of any tuned wave energy device.

Referring back to Figure 3.2 and its accompanying overlay it is interesting to note that the results achieved from P.M. data [notably capture width in mms of different Te's multiplied by their relevant scales for a 10 second sea] very nearly duplicate the efficiencies at South Uist calculated from monochromatic data. These were short crested P.M. seas with Mitsuyasu spreading but tests with the point absorber indicate that the short crested and long crested seas give the same results to within 1%.

4.3 EFFECTS OF SCALE (CONTINUED)

The only conclusion to be drawn from the co-incident graphs, then, is that a single P.M. sea is a fairly accurate representation of the South Uist sea. Figure 3.3 shows the difference between the two seas. The P.M. sea has a narrower bandwidth but is a close approximation, made closer by the high frequencies we are interested in (for cost effectiveness). Refer again to Figure 3.1 with the 1/100th scale film and also to Figure 3.3. It is clear that for the shared frequencies shown the South Uist spectrum should give more power than the P.M. At 1/150th scale much of the low frequency component is being incorporated in the frequency response which means that the P.M. value should be increasing relative to the South Uist. This is confirmed in Figure 3.2.

Finally at 1/200th scale some of the very low frequencies are included which favour the South Uist spectrum again.

As the P.M. sea closely approximates the South Uist Spectrum it was possible to plot the P.M. data for the terminator, in the knowledge that this is a good approximation to the response of the device to a South Uist sea (See Figure 3.4) This device is affected by short crested seas and annual capture width plotted from monochromatic data would be optimistically high. The graph shows design for optimum cost effectiveness, with an index of 2.5, as 1/115th scale.

As the index scale is sensitive to gradients future tests will be made that cover the P.M. spectrum more rigorously.

4.3 EFFECTS OF SCALE (CONTINUED)

Figure 3.5 shows a graph of capture width ratio for three different devices. This gives a good indication of how effectively each device uses the resource. Also shown is the mean power that the device will be generating in a sea with a mean annual power of 30kW/m. The sizes of the most cost effective point absorber and terminator are shown. Unfortunately not enough P.M. data is available from reflector tests to give the most cost effective size. In absence of this the device has been chosen to be the same size as the terminator, 32m. At this scale the terminator with reflector is producing almost .5MW while the point absorber is producing 1/5th of this.

(THIRD ANGLE PROJECTION - ⊕ -)

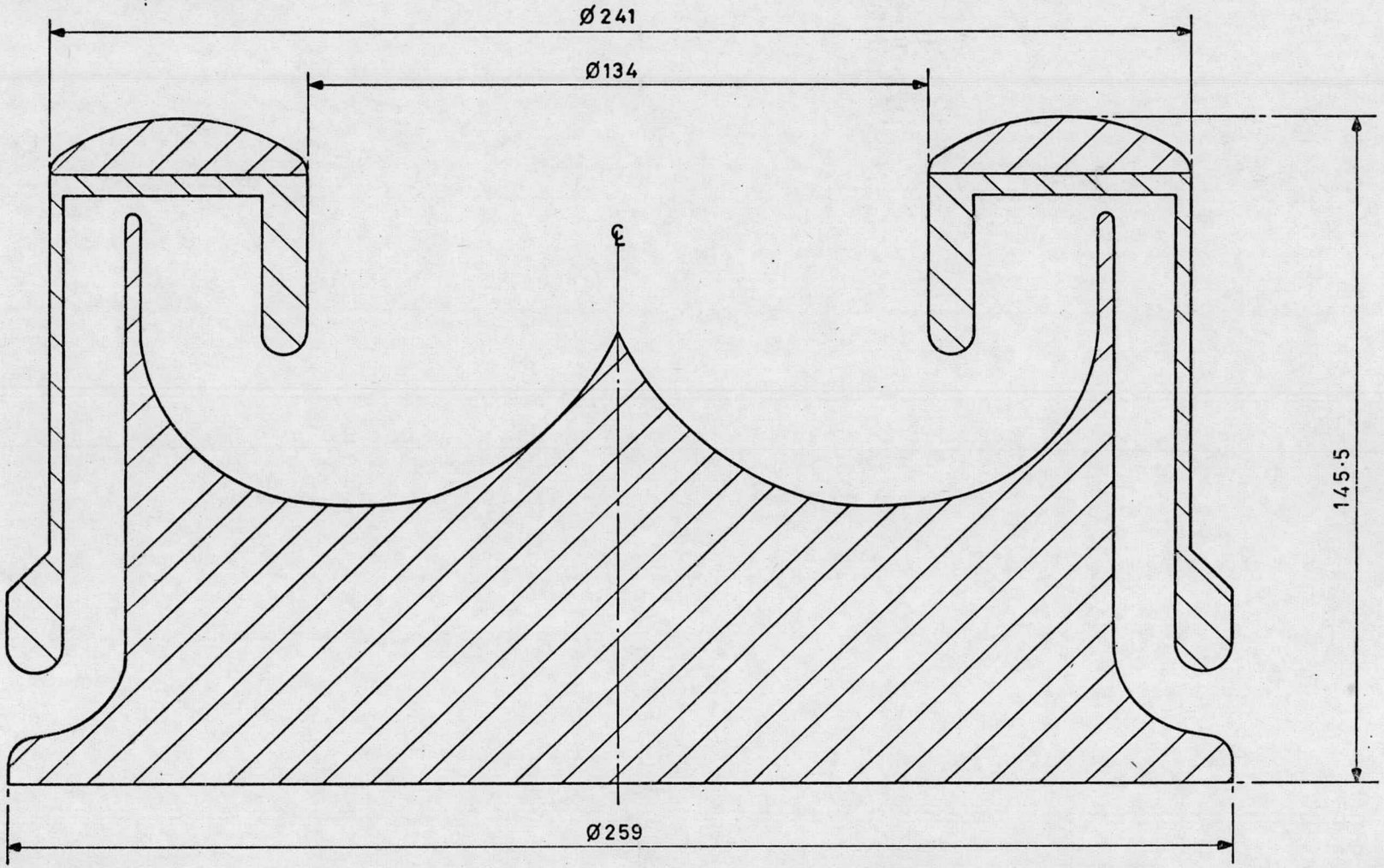

DRAWING No.
T.P. 1204
D C.B./ P.M.M.
C
A
ALTERATIONS

ASSEMBLY DRG.

ALPHABETICAL ISSUE SYMBOLS DO NOT AUTHORISE MANUFACTURE. ALL DEVIATIONS FROM DRAWING TO BE REPORTED TO DESIGN OFFICE.

LIMITS. unless stated

LIMITS. MILLIMETRE unless stated			
NO DECIMALS ± 1	1 DECIMAL ± 0·5	2 DECIMALS ± 0·25	3 DECIMALS ± 0·150

UNLESS OTHERWISE STATED DEBURR R 0·1mm MAX.

VICKERS LIMITED,

DESIGN & PROJECTS DIVISION

VICKERS

SURFACE TREATMENT

SURFACE TEXTURE

No. PER ASSY.

SCALE

MATERIAL & SPECIFICATION

TITLE

CROSS-SECTION OF TWIN OSCILLATING WATER COLUMN POINT ABSORPTION

SHEET OF SHEETS

DRAWING NUMBER

T.P. 1204

ISSUE	DATE
A	8.5.80.

SIZE A3 S.927

B724R/809 OZALID (UK) LTD.

FIG 2.1

Edinburgh University Wide Tank Experiment

Experiment Label : 068

Date : 10-MAR-80 Time : 15:19:16

level information

	a	b	c	d	1
max	1.214	-1.59	10.15	1.607	
mean	-2.94	-7.21	1.461	-4.35	
min	-6.51	-13.1	-7.18	-4.35	

drift
-0.04

2
Channel 3 flow a
MAX= 0.444, MIN= -0.413, P-P= 0.857, RMS= 0.147, MEAN= 0.000
Channel 4 flow b
MAX= 0.621, MIN= -0.552, P-P= 1.173, RMS= 0.198, MEAN= -0.000
Channel 5 flow c
MAX= 0.781, MIN= -0.643, P-P= 1.424, RMS= 0.248, MEAN= -0.000
Channel 6 flow d
MAX= 0.534, MIN= -0.445, P-P= 0.979, RMS= 0.187, MEAN= -0.000

%flow error,ac/bd
2.53
M 3

combined flow
Channel 7 total flow 4
MAX= 0.791, MIN= -0.615, P-P= 1.406, RMS= 0.195 MEAN= -0.000

pressure drop
Channel 10 pressure drop 5
MAX= 4.354, MIN= -3.685, P-P= 8.040, RMS= 1.139, MEAN= 0.000

total power
Channel 105 total power(mw) 6
MAX= 0.309, MIN= -0.003, P-P= 0.312, RMS= 0.016, MEAN= 0.001

sum of the power
2.18 7

capture width
Channel 114 capture (mm) 8
MAX= 126.480, MIN= 0.000, P-P= 126.480, RMS= 6.878, MEAN= 0.509

residual power
Channel 115 residual power(mic 9
MAX= 0.038, MIN= -0.000, P-P= 0.038, RMS= 0.001, MEAN= 0.000

FIG. 2.2.

impedance
Channel 131 impedance mm/l/s 10
MAX= 13.579, MIN= -0.630, P-P= 14.209, RMS= 0.548, MEAN= 0.047

DAMPING

MONOCHROMATIC SEA

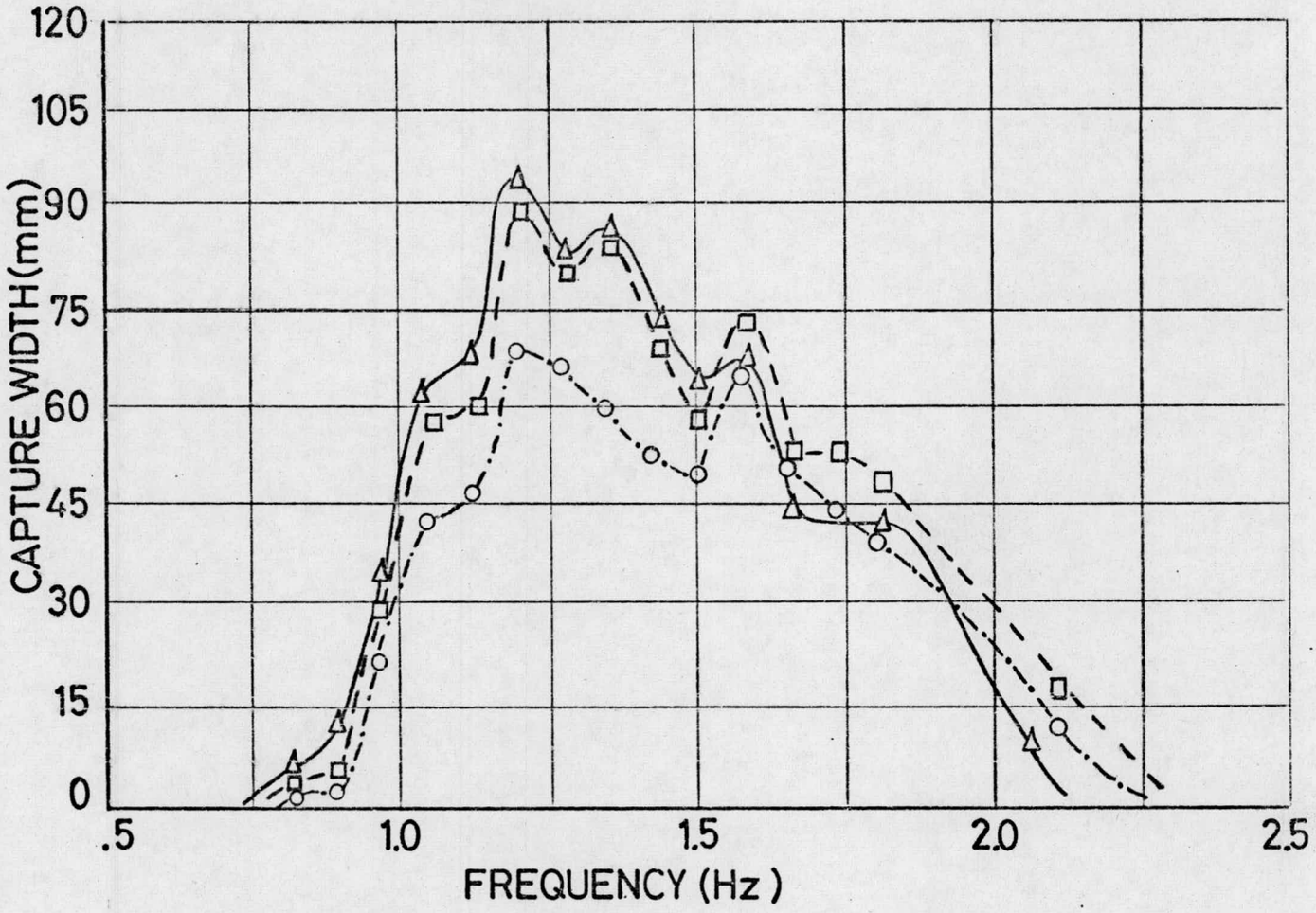

DAMPING

○ 3.49 mm/ls^{-1}

□ 6.17

△ 10.94

FIG. 2.3.

EFFECT OF DEPTH

MONOCHROMATIC SEA

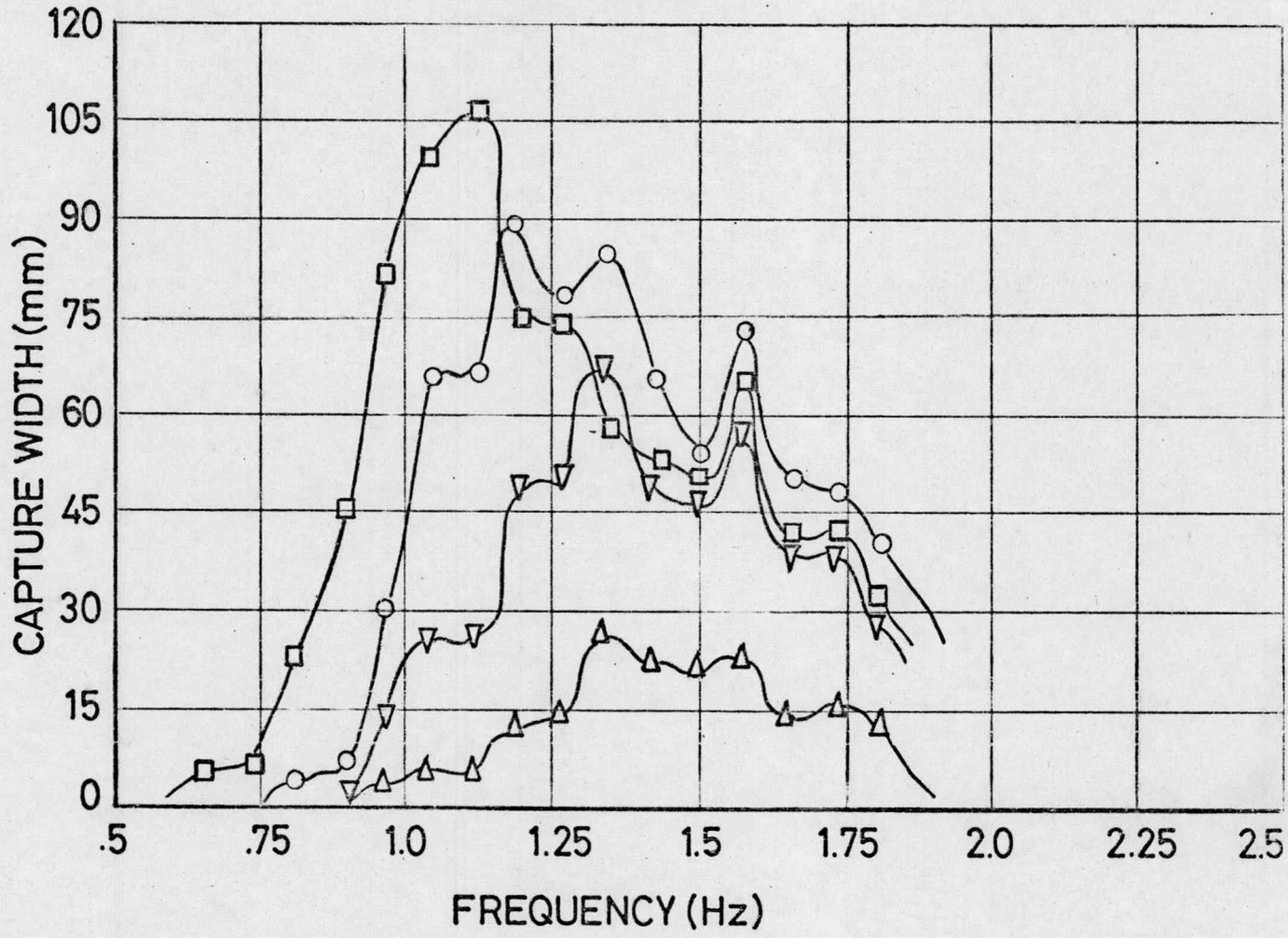

□ 2 cms

○ 4

▽ 6

△ 10

FIG. 2.4.a

EFFECT OF DEPTH

P.M. SEA

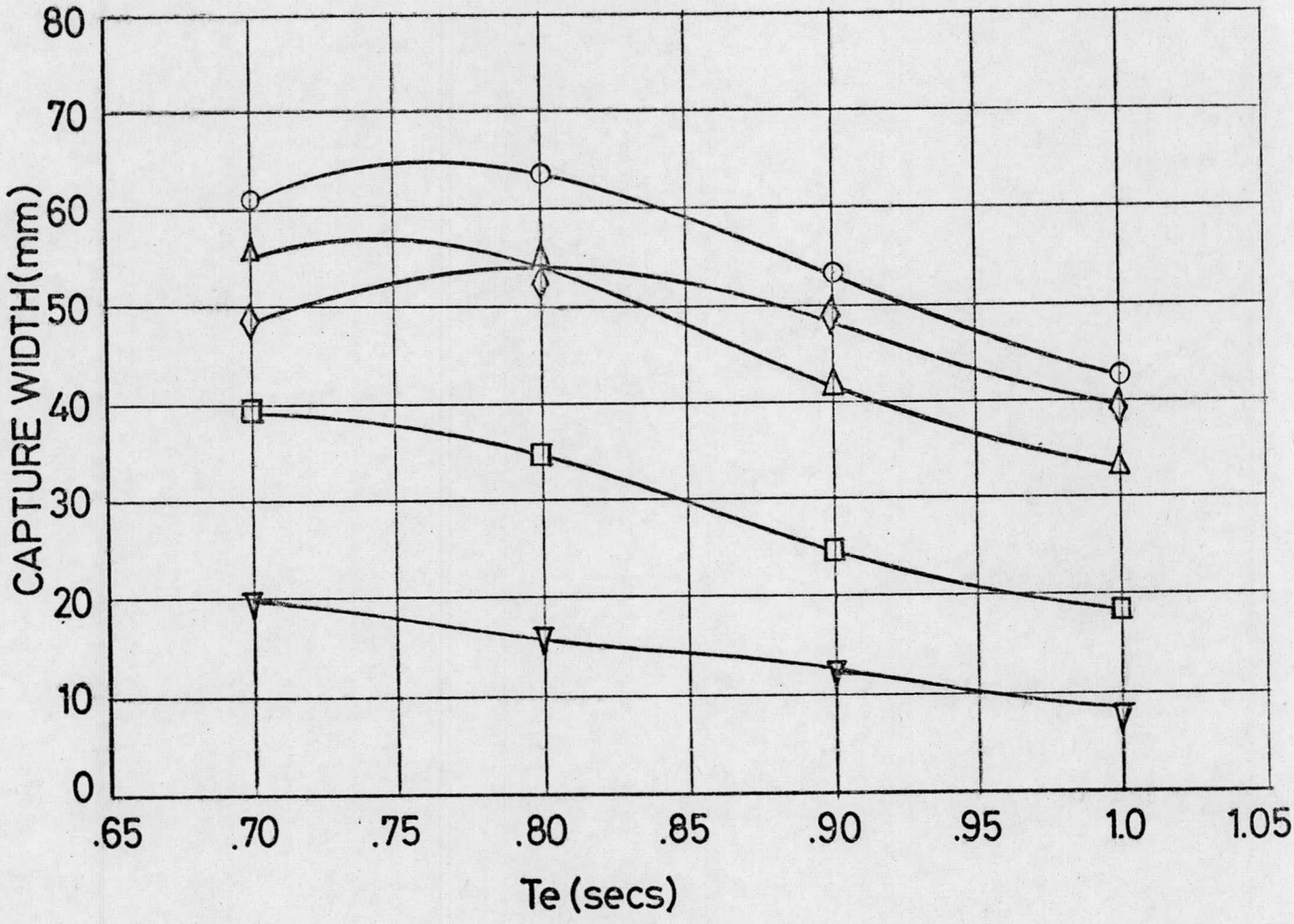

◊ – 2 cms

○ – 3

△ – 4

□ – 6

▽ – 10

FIG.2.4.b.

COLUMN LENGTH MONOCHROMATIC SEA

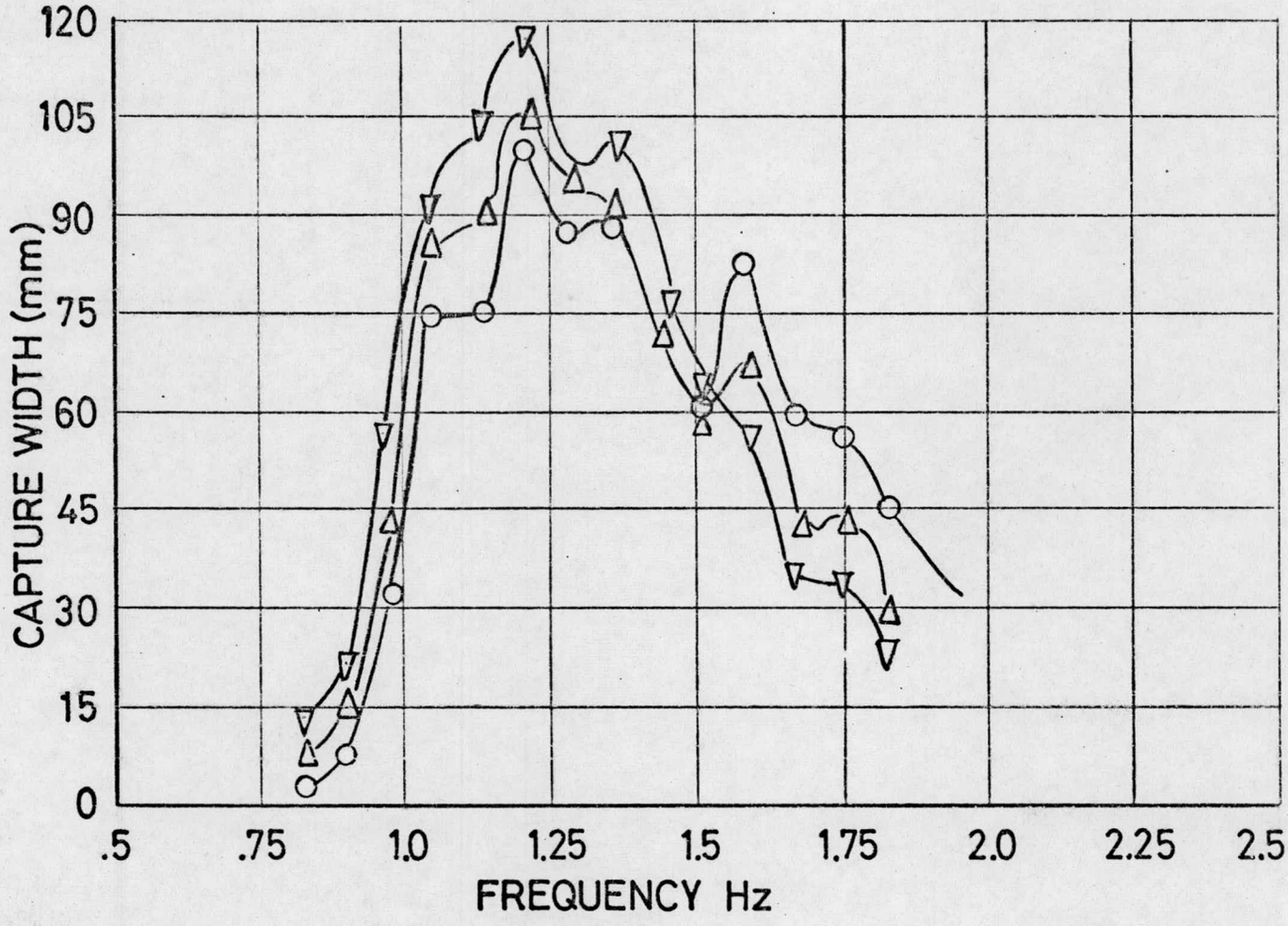

▽ + 10 cms

△ + 6 cms

○ STANDARD

FIG. 2. 5.

COLUMN LENGTH

P. M. SEA

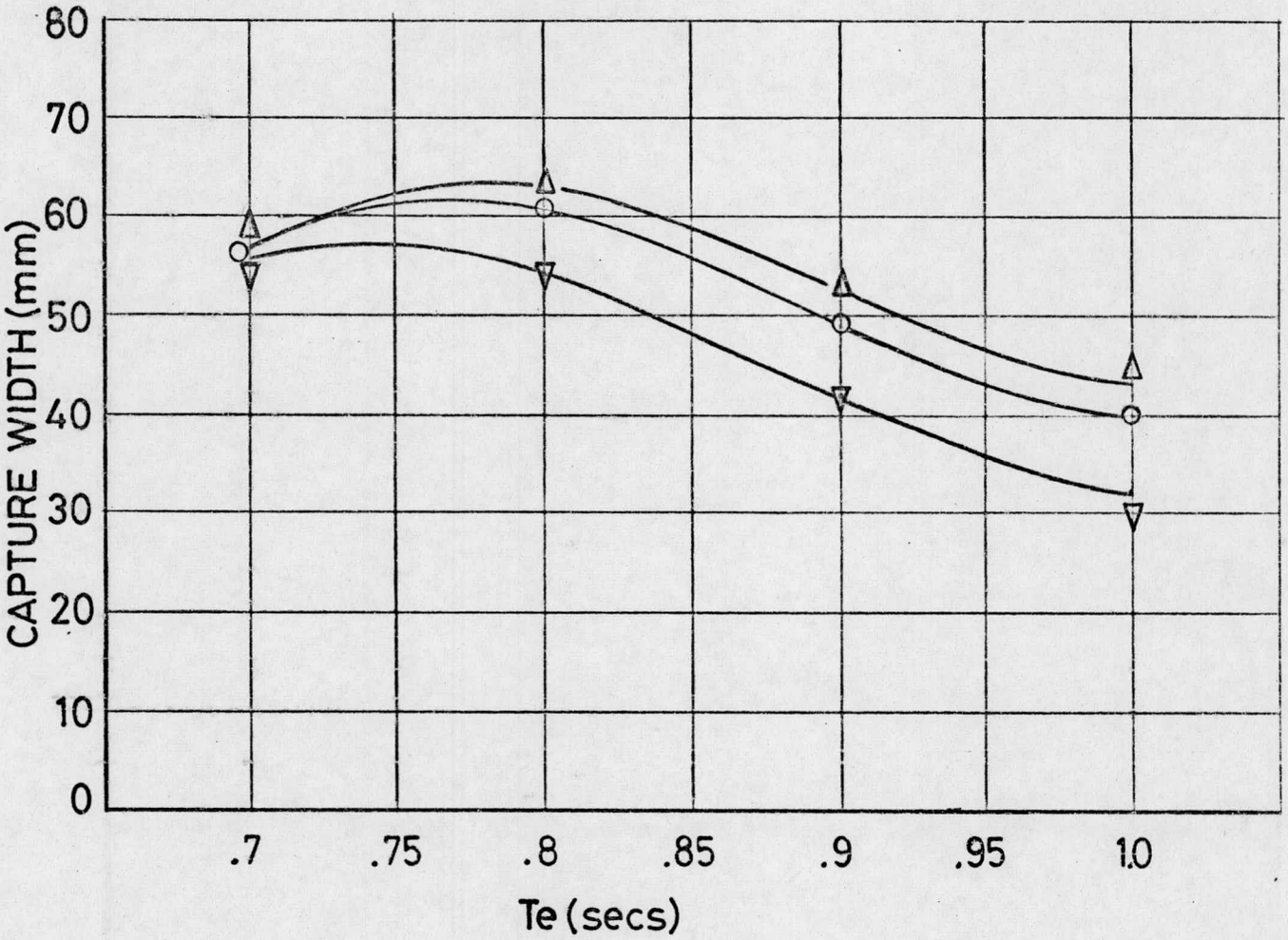

△ +10 cms

○ + 6 cms

▽ STANDARD

FIG 2.6.

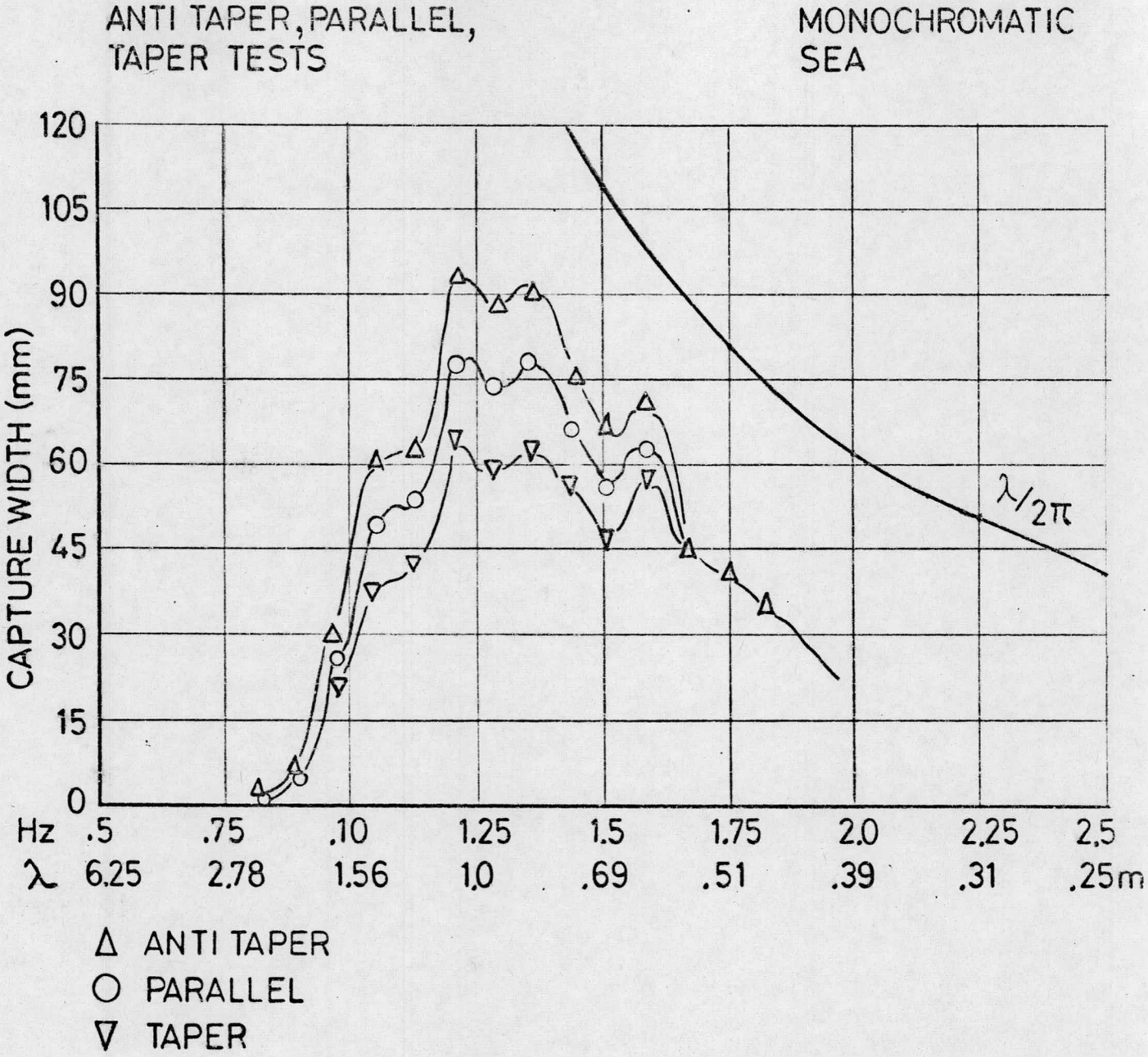
ANTI TAPER, PARALLEL, TAPER TESTS
MONOCHROMATIC SEA
CAPTURE WIDTH (mm)
120
105
90
75
60
45
30
15
0
λ/2π
Hz .5 .75 .10 1.25 1.5 1.75 2.0 2.25 2.5
λ 6.25 2.78 1.56 1.0 .69 .51 .39 .31 .25m
Δ ANTI TAPER
○ PARALLEL
∇ TAPER

FIG. 2.7.

ANTI TAPER, TAPER, PARALLEL TAPER TESTS

P.M.SEA

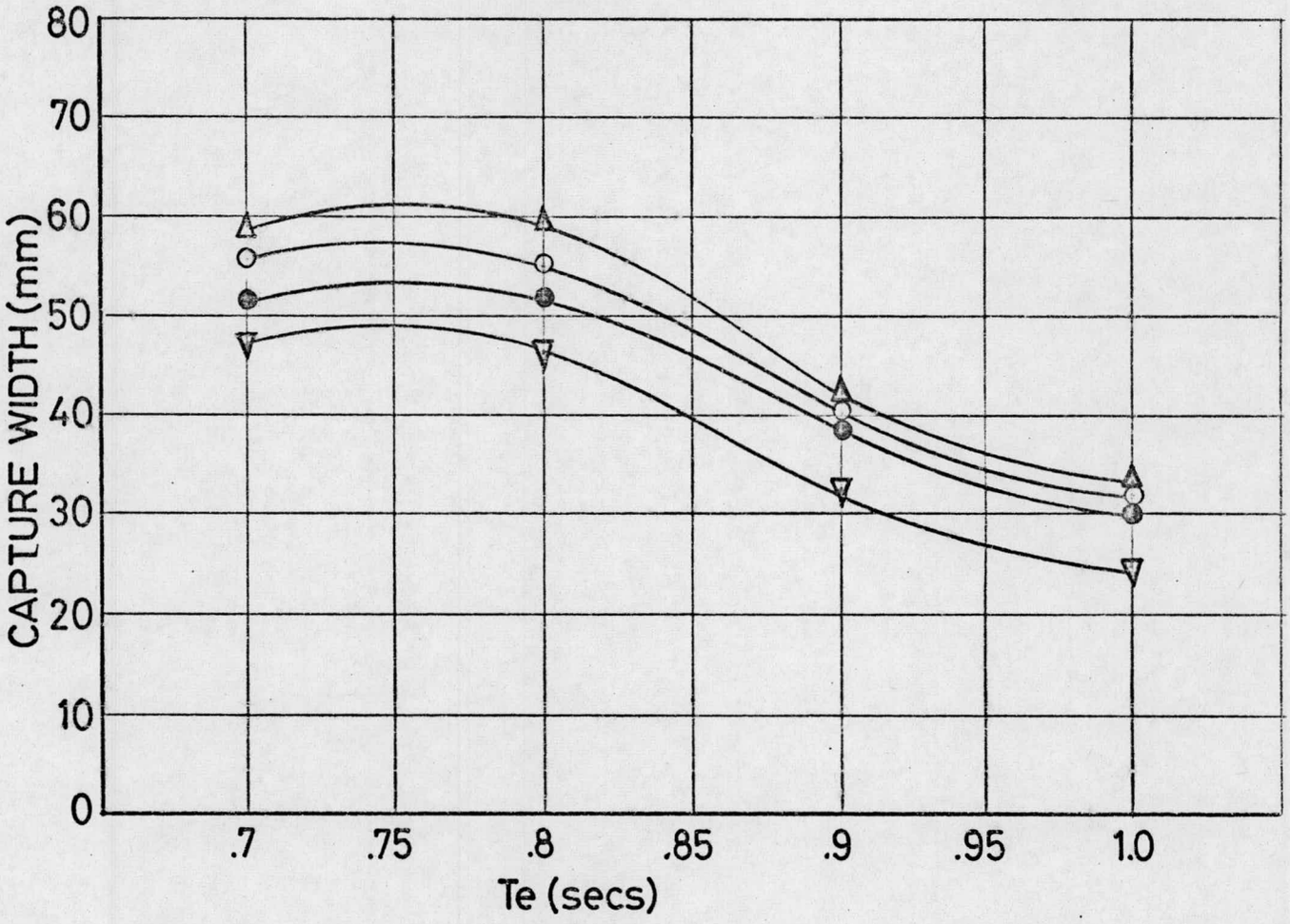

△ ANTI TAPER

▽ TAPER

○ PARALLEL (WIDE SECTION)

● PARALLEL (NARROW SECTION)

FIG. 2.8.

BELLMOUTHS

MONOCHROMATIC SEA

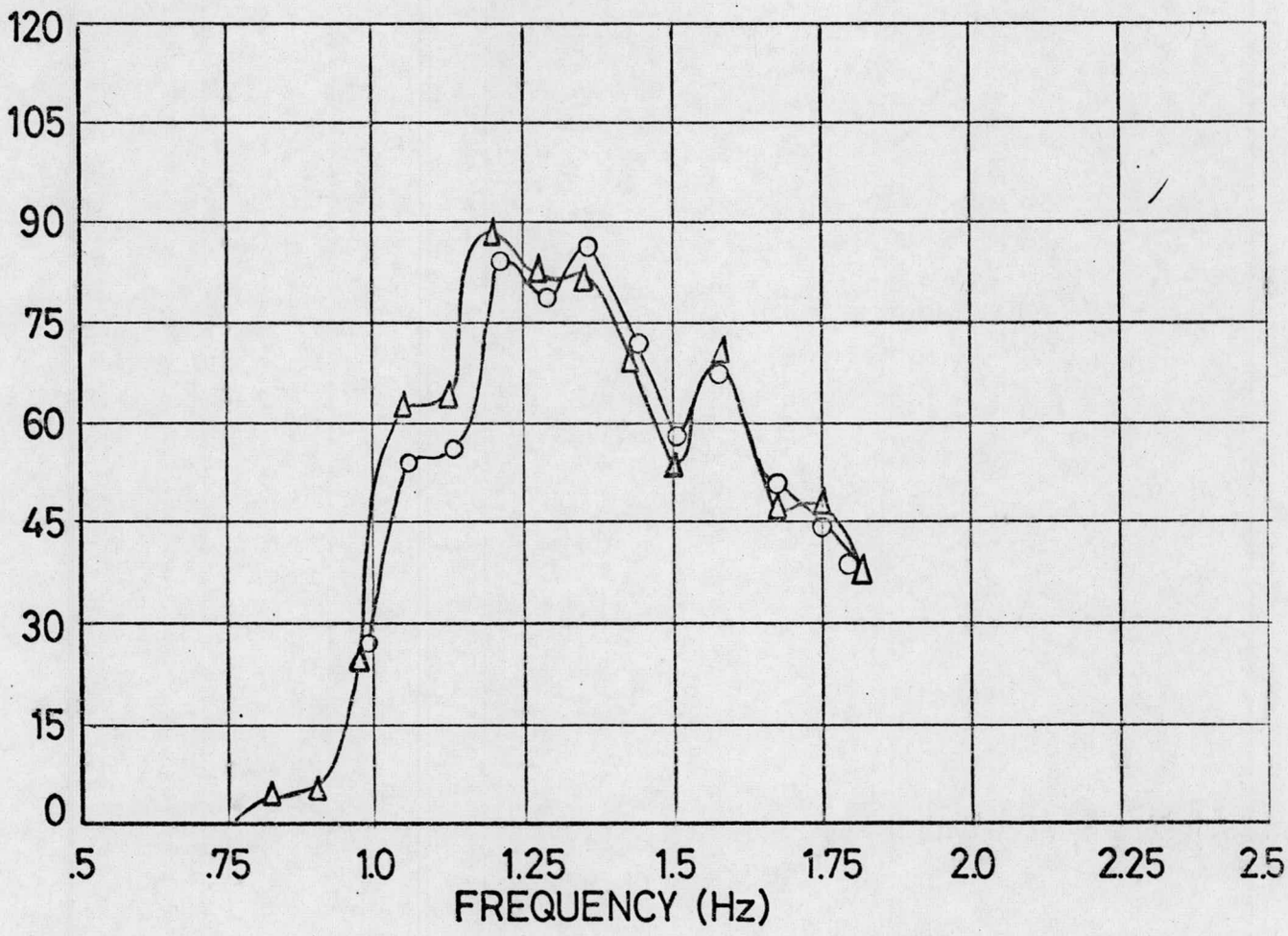

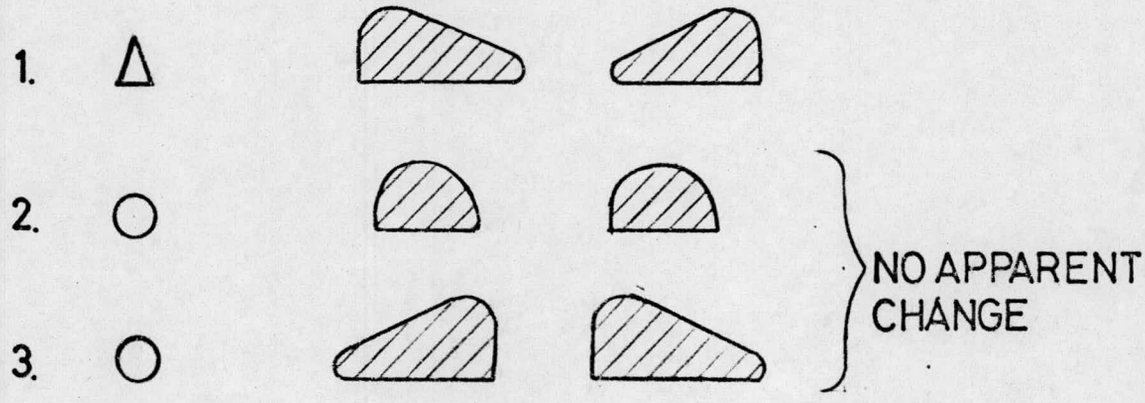

FIG. 2.9.

REFLECTOR TEST P.M. SEA

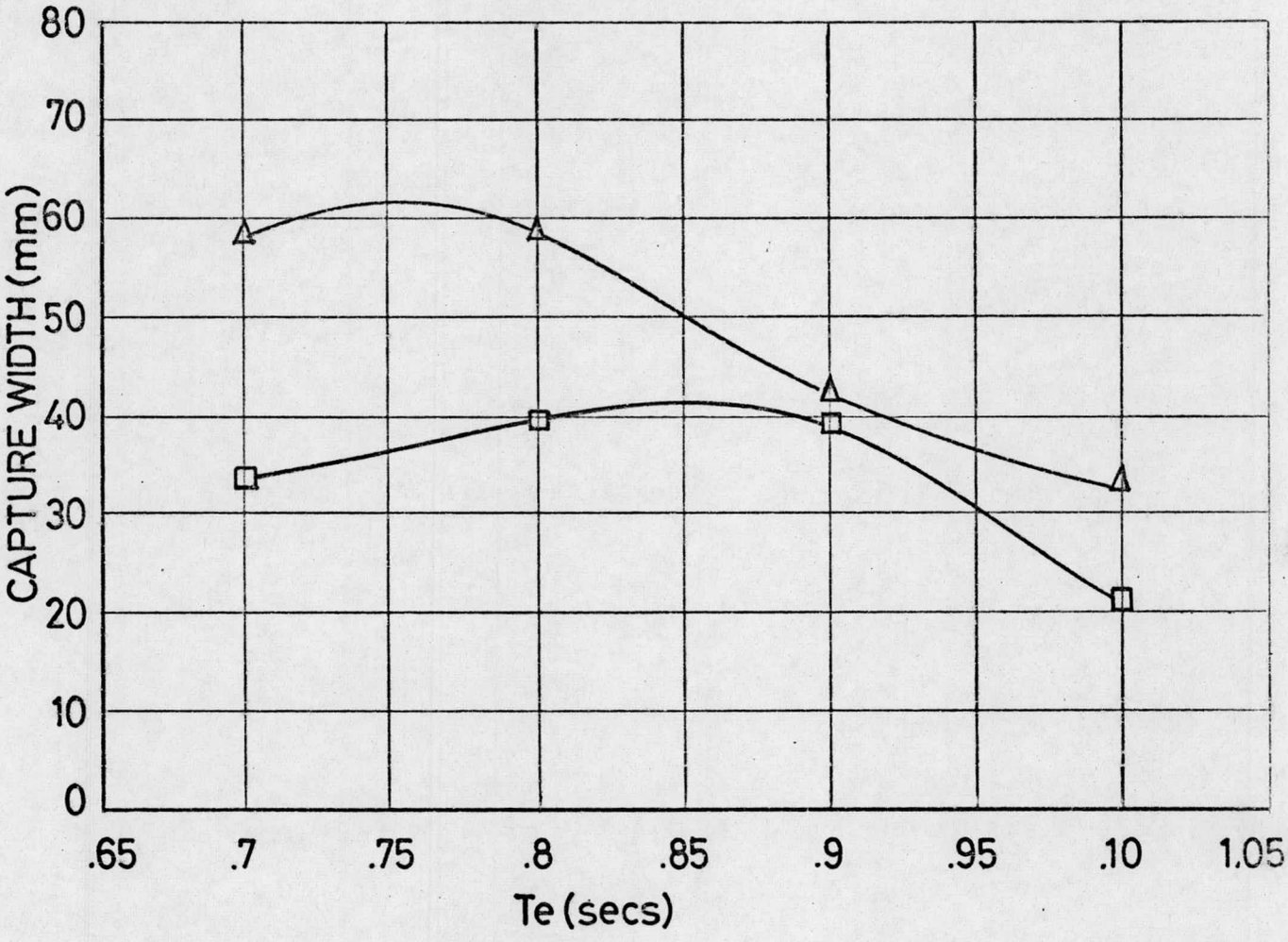

△ ANTITAPER

□ ANTITAPER WITH REFLECTOR [◎]

FIG. 2.10.

FLOW RATIO OF DOWNWARD FACING DUCT

P.M. SEA

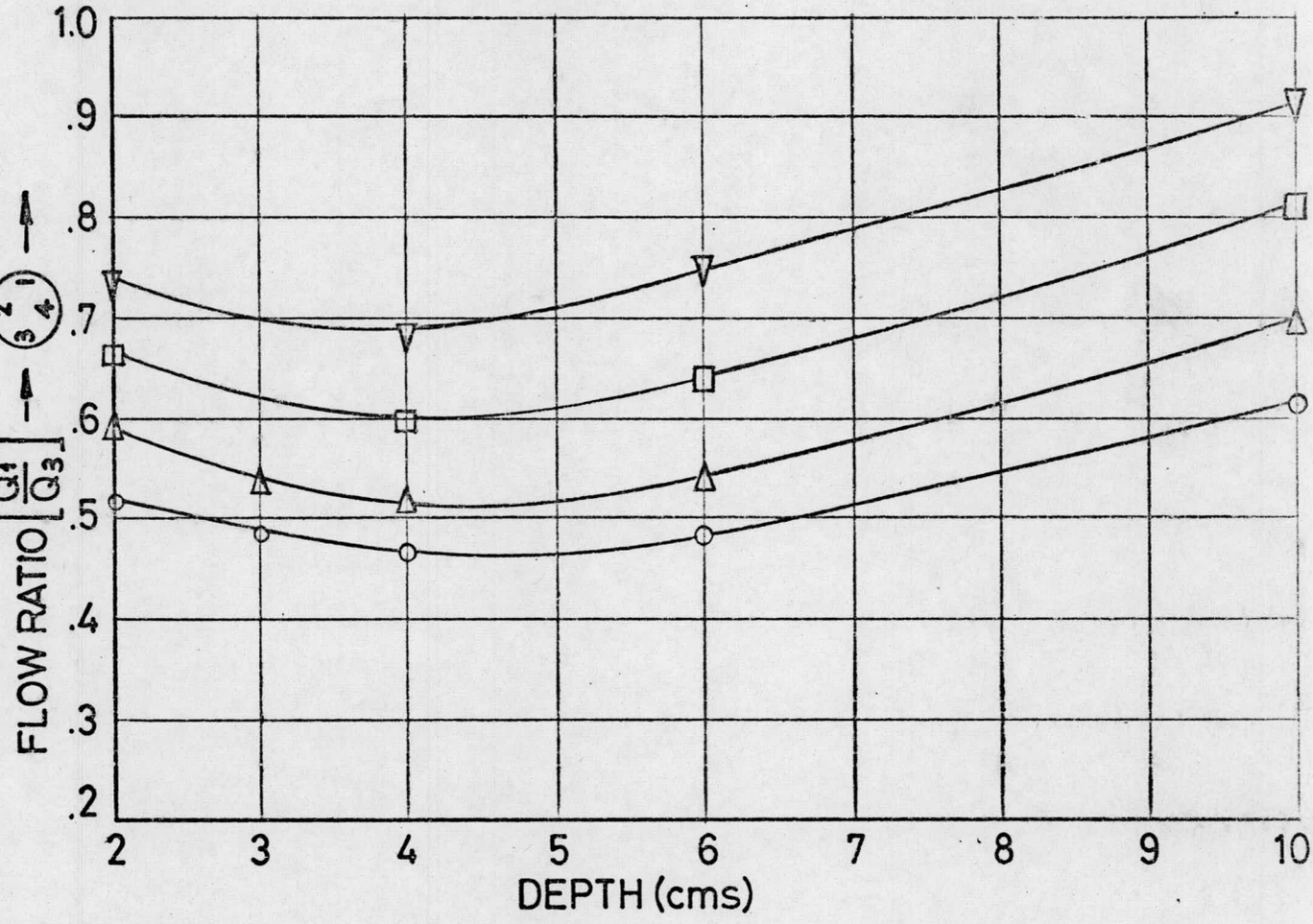

▽ Te = 1.0 secs

□ Te = .9 secs

△ Te = .8 secs

○ Te = .7 secs

FIG. 2.11.

COST EFFECTIVENESS COMPARISONS P.M. SEA

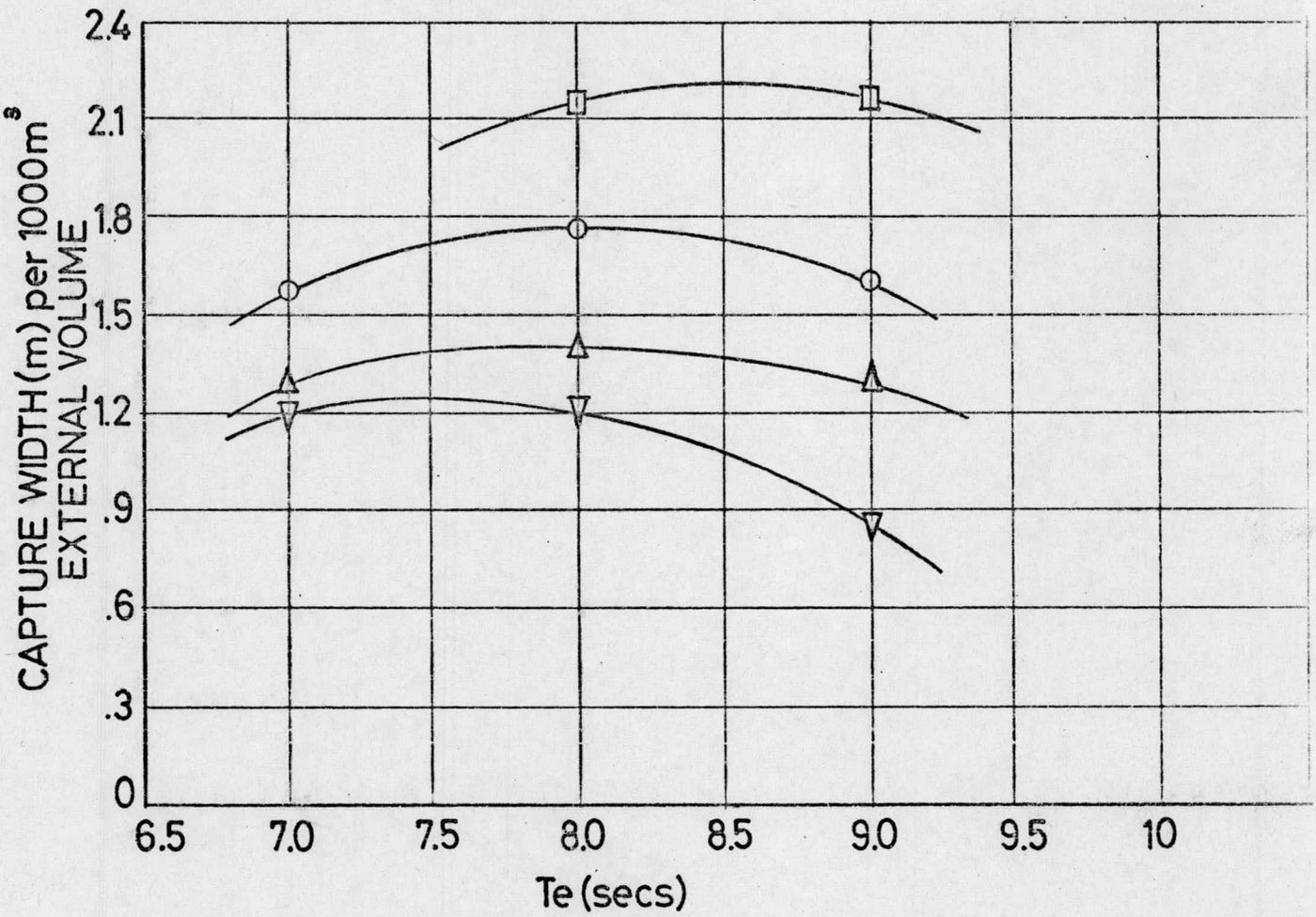

□ T.O.W.C. WITH REFLECTOR

○ WAVE CHAMBER

△ T.O.W.C. : TERMINATOR

▽ T.O.W.C. : POINT ABSORBER

FIG. 2.12.

FIG. 3.1.d

FIG. 3.1.c.

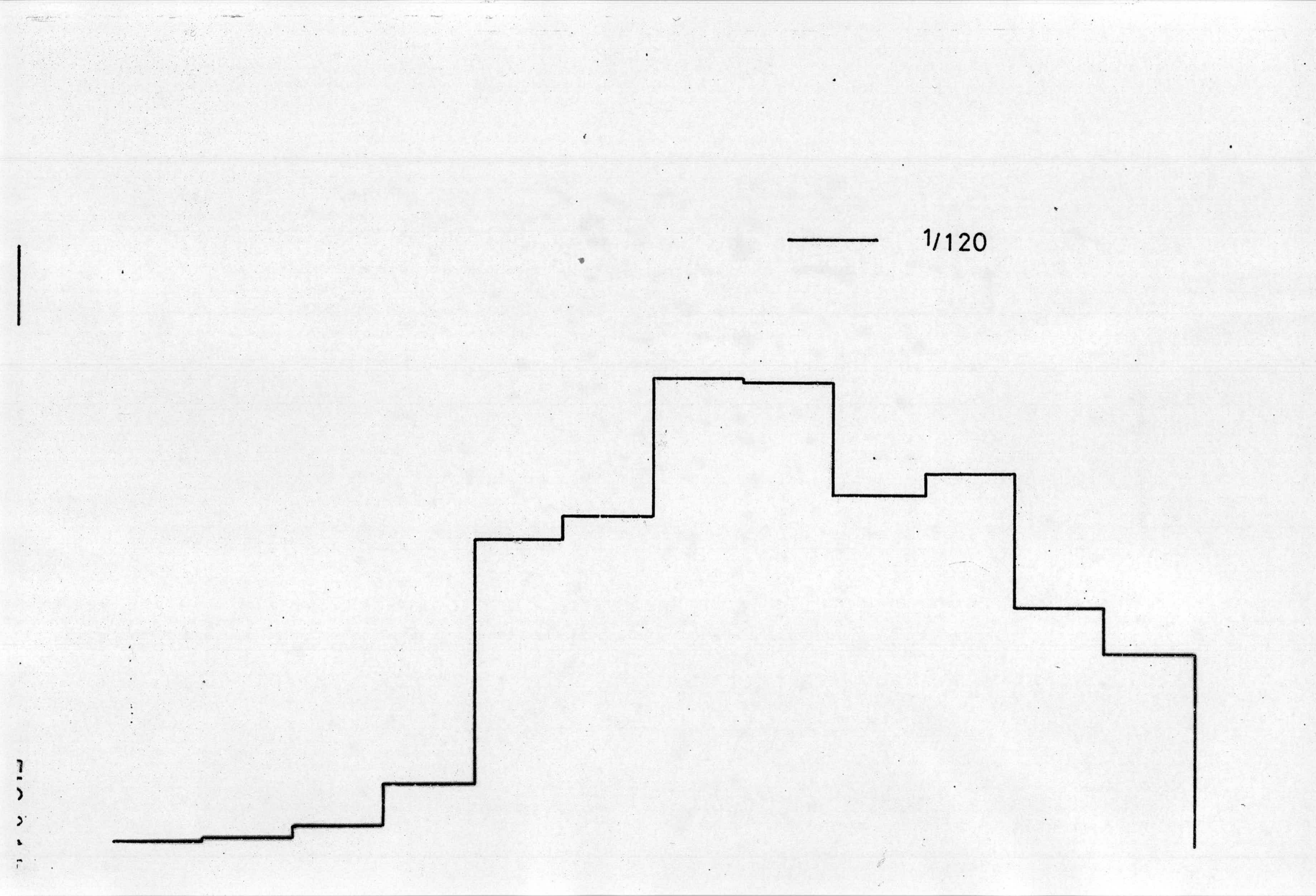
1/120

FIG. 3.1.a.

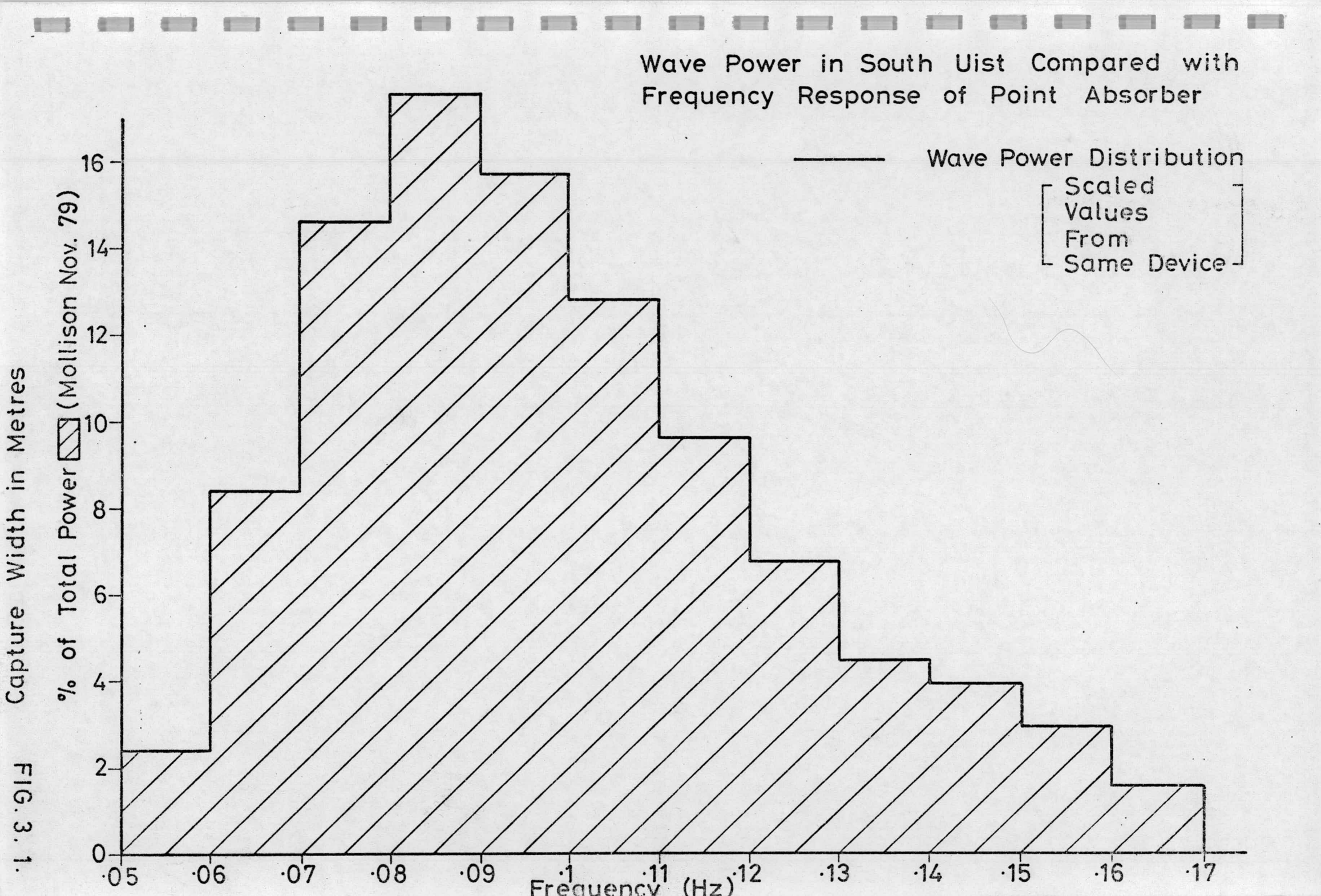
Wave Power in South Uist Compared with Frequency Response of Point Absorber
Wave Power Distribution
Scaled Values From Same Device
% of Total Power (Mollison Nov. 79)
Capture Width in Metres
0
2
4
6
8
10
12
14
16
·05
·06
·07
·08
·09
·1
·11
·12
·13
·14
·15
·16
·17
Frequency (Hz)

FIG. 3. 1.

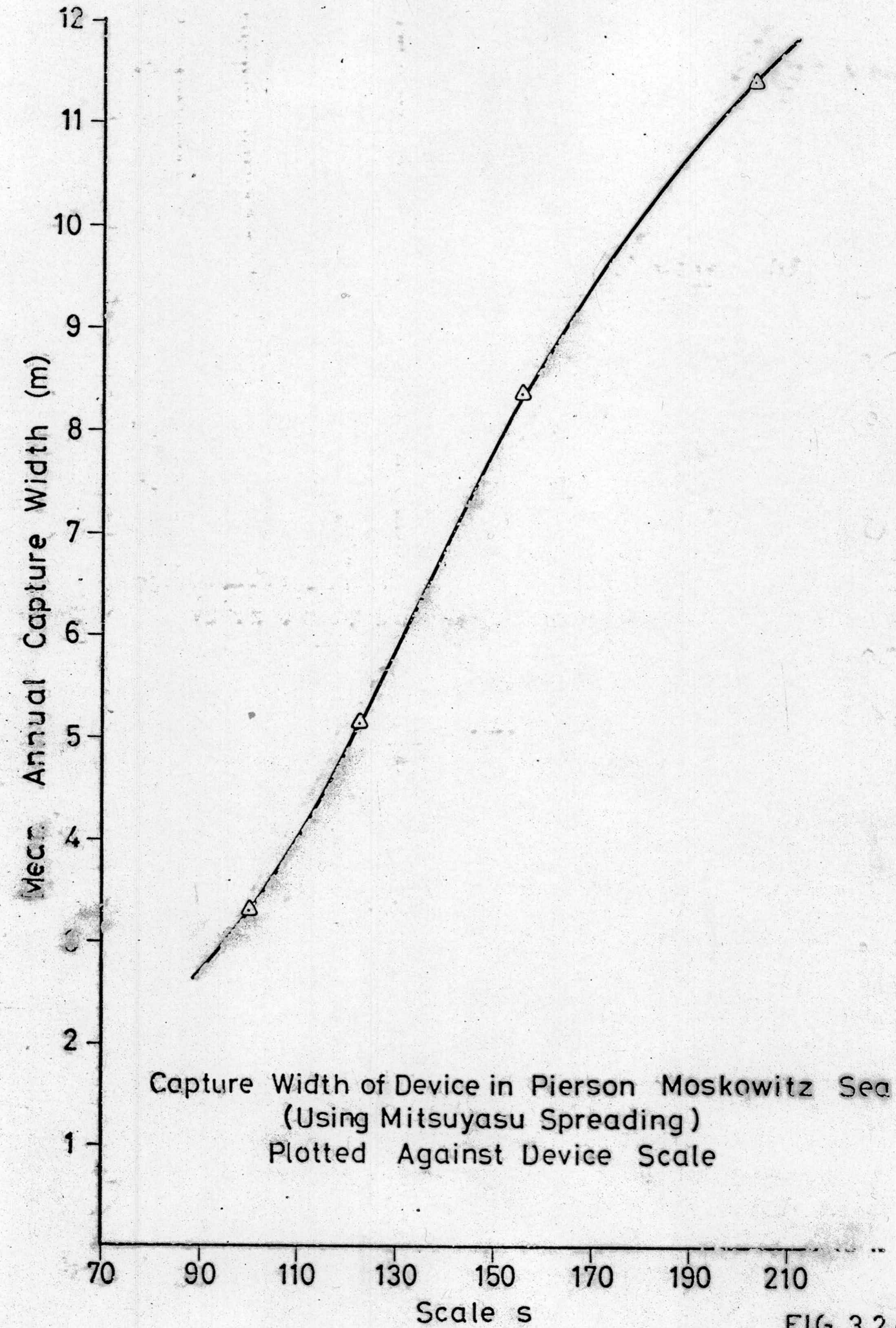

Capture Width of Device in Pierson Moskowitz Sea
(Using Mitsuyasu Spreading)
Plotted Against Device Scale

FIG 3.2a.

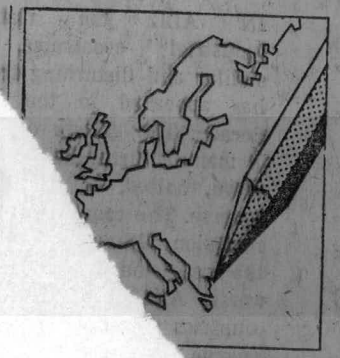

Product of Monochromatic South Uist Sea Data (Off-shore Buoy) and Device Capture Width Plotted Versus Device Scale

TOWC Point Absorber

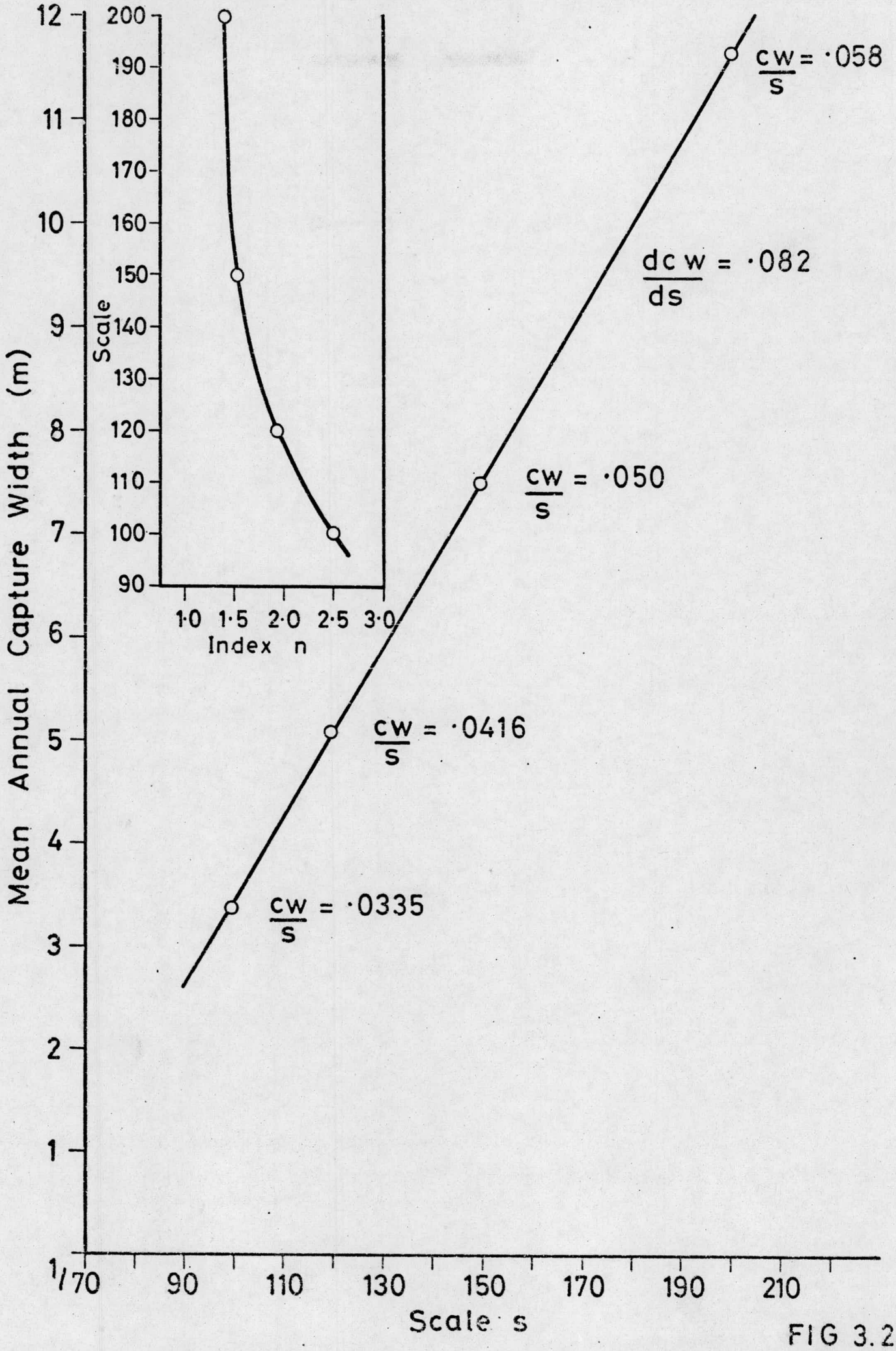

FIG 3.2.

Comparison of Monochromatic Complement of South Uist Sea
With Monochromatic Complement of Pierson Moskowitz Sea

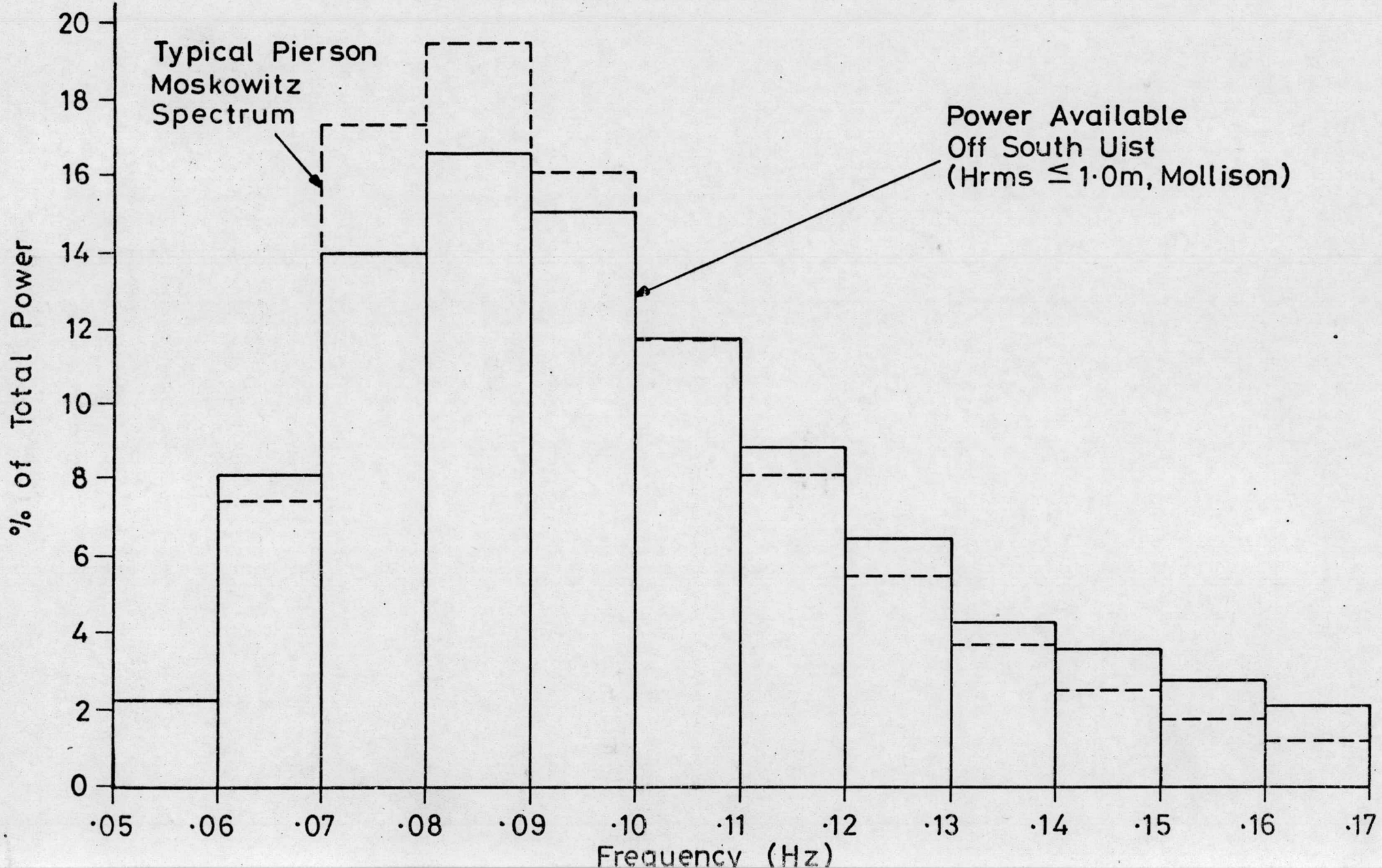

FIG. 3.3.

Projected Capture Width at South Uist for T.O.W.C. Terminator

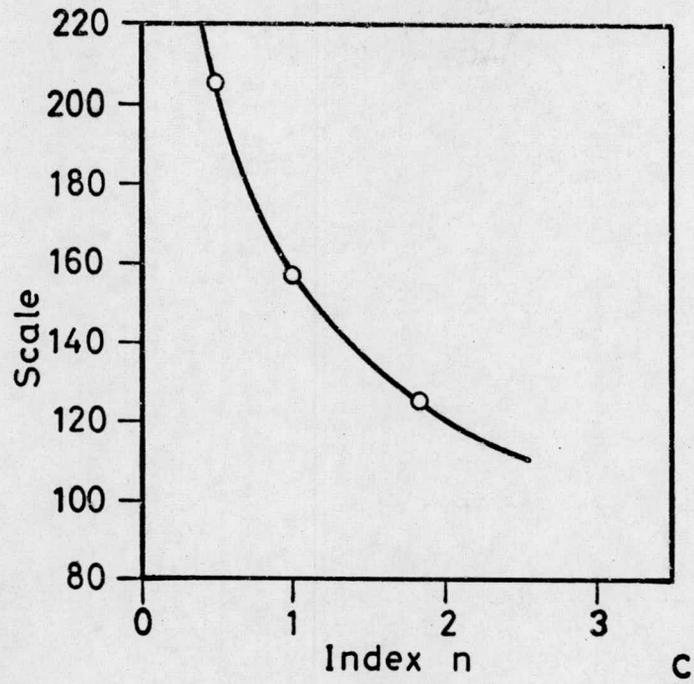

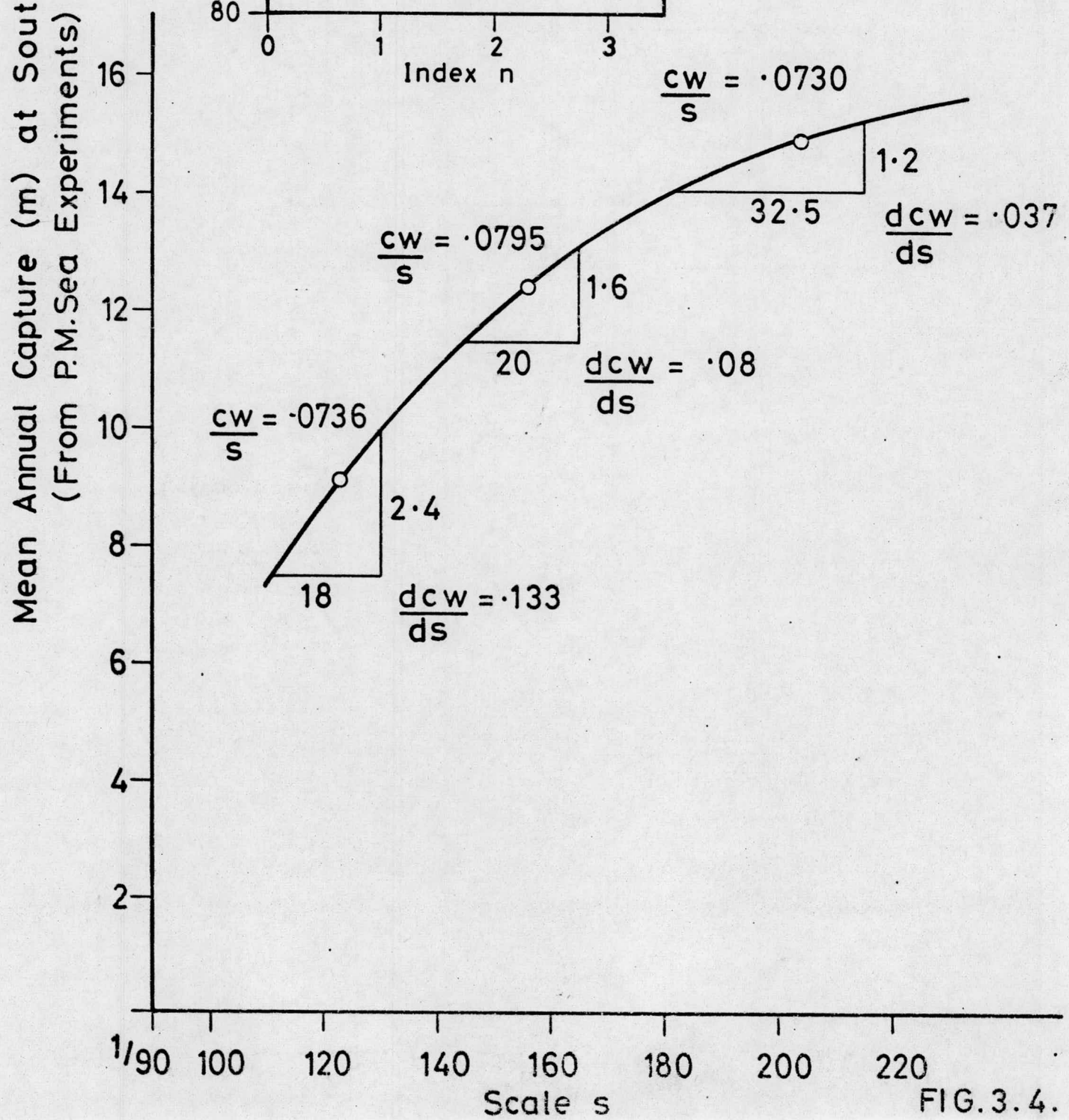

FIG. 3.4.

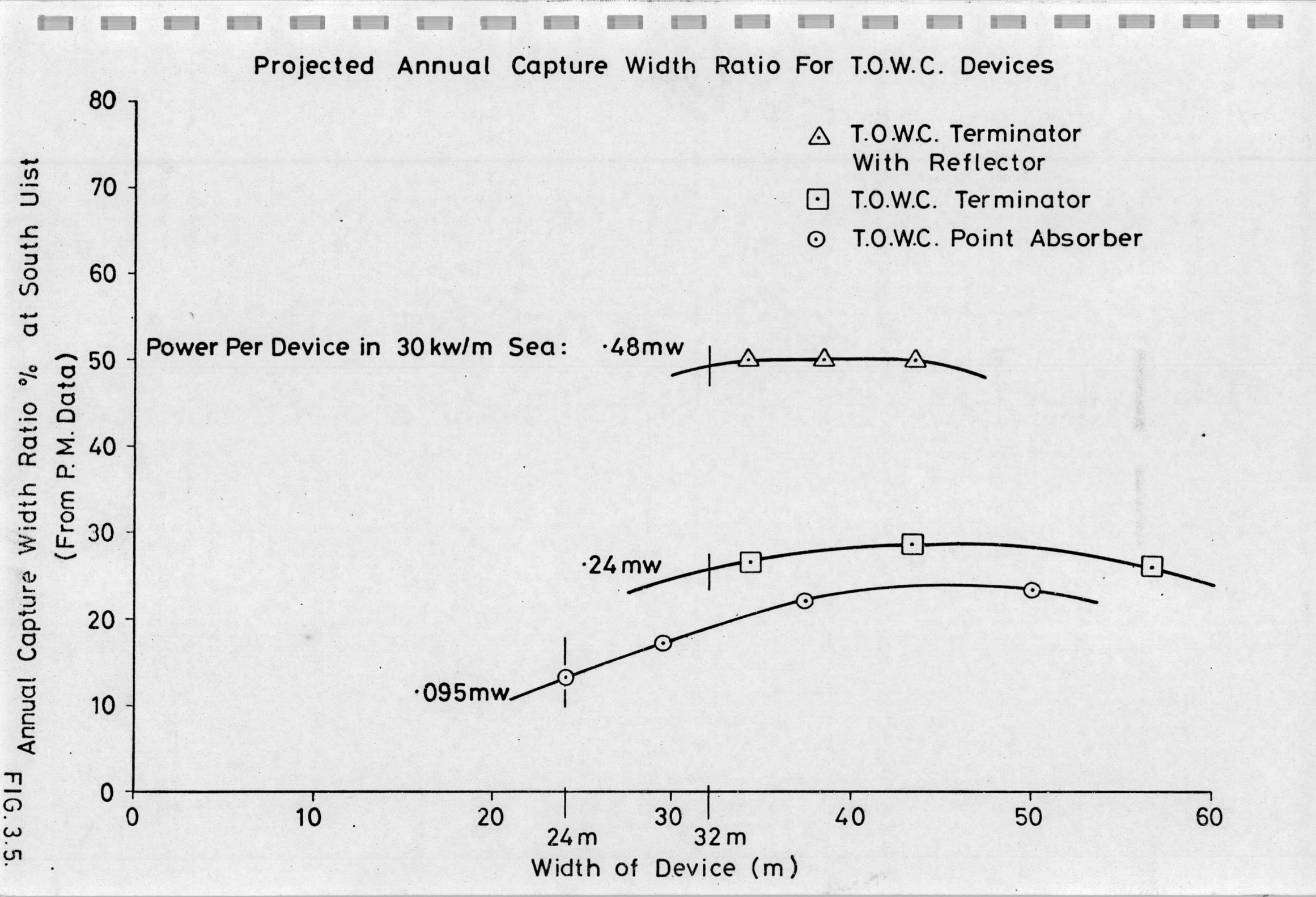
Projected Annual Capture Width Ratio For T.O.W.C. Devices
T.O.W.C. Terminator With Reflector
T.O.W.C. Terminator
T.O.W.C. Point Absorber
Power Per Device in 30 kw/m Sea: ·48mw
·24mw
·095mw
Annual Capture Width Ratio % at South Uist (From P.M. Data)
Width of Device (m)
24m
32m
0
10
20
30
40
50
60
70
80

FIG. 3.5.


Twin Oscillating Water Column
TERMINATOR MODE
Vickers

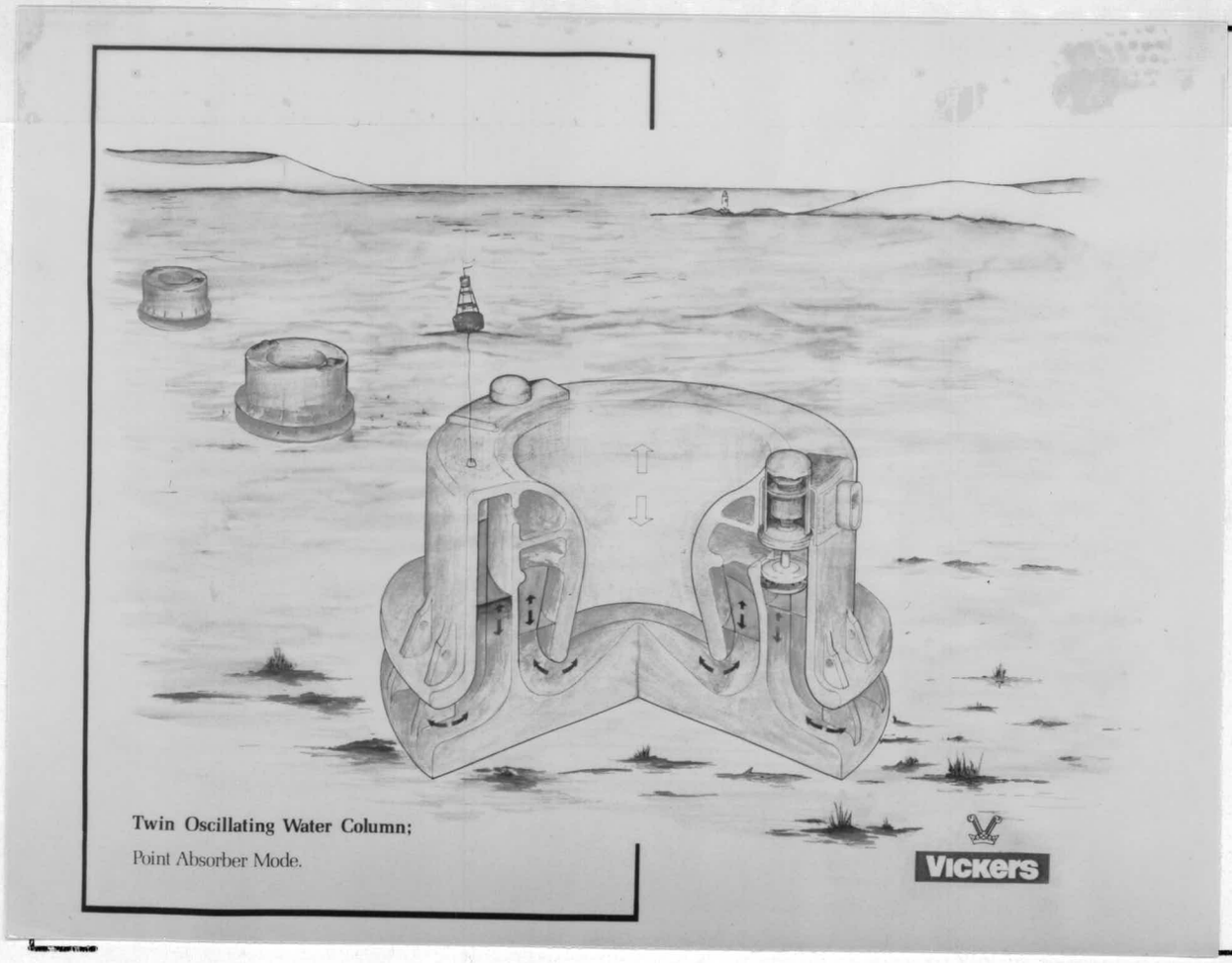
Twin Oscillating Water Column;
Point Absorber Mode.
Vickers

Figure 3.6

4.4 MODEL TESTS ON THE SUBMERGED WAVE CHAMBER

4.4.1 Introduction

The Submerged Wave Chamber device was tested in the Edinburgh wide wave tank together with the Twin Oscillating Water Column device. This report describes the Submerged Wave Chamber concept and the of tests conducted to assess the potential of the device.

Aim

The aim of the experimental programme was to compare the performance of the Submerged Wave Chamber in rectified and unrectified modes of operation, and to assess the effects on performance of device length, damping, chamber segmentation, and inlet depth.

These variables were selected as being those most likely to influence the cost effectiveness of the device, providing a preliminary indication of potential performance, and suggesting the most promising areas for further investigation and development.

4.4.2 Description of the Submerged Wave Chamber Principle

The Submerged Wave Chamber (SWC) can be regarded as a means of generating a secondary wave in an underwater chamber, which then provides a frame of reference and environment within which the energy conversion system operates.

Essentially an inverted horizontal trough orientated along the direction of wave motion, the Submerged Wave Chamber (Figure 4.1) responds to overhead wave pressures sensed along its upwards-facing inlet ducts which forms a secondary wave within the chamber.

The amplitude of this secondary wave is maximised by suitable selection of chamber length, height, and inlet duct geometry. With adequate length the total air volume remains essentially constant, unlike the original Vickers device which depended on compression of a relatively large air volume for its operation. The Submerged Wave Chamber has a much smaller air space, can be more compact and hence less costly to build.

The device can be configured to produce either rectified or alternating air flows. In the arrangement for alternating air flow, the chamber is divided into cells by a number of transverse bulkheads. As the wave travels along the chamber air is forced through bi-directional turbines located between the cells (Figure 4.2a) or connected via a manifold (Figure 4.2b).

4.4.2 Description of the Submerged Wave Chamber Principle (Continued)

In the arrangement for rectified air flow (Figures 4.3a and b), the chamber air space is divided by fences which extend from the roof of the chamber to cut into the wave crests, forming seals. The air entrapped between crests is forced to travel by "peristaltic" effect towards the inshore end of the chamber whence it is returned to the front compartment via a return tube and air turbine. This arrangement has the advantage of requiring only one turbine which operates at relatively higher pressure due to the mechanism of rectification, thereby enabling the use of a compact turbine and generator installation.

Alternatively, the chamber is divided as for the alternating flow arrangement, but instead of providing each cell with its own turbine, they feed a common turbine via non-return valves. This arrangement has the added complexity of valving, but retains a single turbine and generator installation. In addition, the use of valves provides the opportunity for the introduction of phase control with its potential low frequency performance enhancement.

The Submerged Wave Chamber, as an attenuator-type device, is inherently stable due to its orientation to the wave motion and its force balancing length. The device can therefore be moored in relatively deep water, on taut moorings or tension legs, to take advantage of the greater wave energy resource available. (Figure 4.4).

The Submerged Wave Chamber also benefits from the improved survivability of a submerged device avoiding slamming and differential buoyancy forces, without making any sacrifice in efficiency for this privilege.

4.4.3 Testing Procedure

A single nominally 1/100th scale model was tested (Figure 4.5), mounted on a purpose-built stand on which inlet depth and slope can be adjusted.

For mixed sea testing a range of Pierson-Moskowitz spectra with the Mitsuyasu spreading function were used, of energy period from .7 to 1 seconds. In addition an artificial sea was used, which contained 20 equispaced frequency components of 1mm amplitude, from .43 to 1.91Hz. With this the frequency response of the device could be generated using the Fourier analysis technique.

In order to calculate the efficiency of the device, the power content of each component of the sea incident on the device must be measured. This was achieved using three wave-probes lying along the line on which the model was to be sited.

Pressure and water level data were recorded in each test. Pressure was measured with Furness Micromanometers, flow was calculated from pressure measurements across orifice plates pre-calibrated in steady air flow. There was some doubt as to the validity of the method of flow measurement in alternating flow, but a comparison of flow measurement derived from wave probes and orifice plates on the TOWC (Figure 4.6) allayed any fears.

Water level was measured for qualitative purposes at four locations within the chamber using Churchill two-wire wave probes. The data was logged and processed on the Edinburgh PDP11/60 system, which could be simply programmed to calculate information such as power, capture width etc.

4.4.3 Testing Procedure (Continued)

Data was recorded for each cell individually which, due to the limited instrumentation available, typically involved running each sea two or three times and accumulating the data from each run on the computer .Processed data was finally displayed on teletype and graph plotter.

4.4.4 Alternating Flow Mode

The bulk of the testing on the SWC has been in the alternating flow mode using the common manifold method, since this is most easily arranged experimentally and gives a very good indication of the linear performance of the device.

The parameters investigated in this mode were:-

- Damping
- Partitioning of the Inlet Duct
- Cell Length
- Device Length
- Inlet Depth
- Waveheight
- Duct Taper
- Distribution of Power Output between Cells.

Damping

Damping was adjusted by interchanging the pre-calibrated orifice plates, which were attached to the model magnetically for ease of removal.

Performance is fairly sensitive to changes in damping as indicated by Figures 4.7a and b which show its effect on frequency response and capture width in mixed seas. A 25% deviation from the optimal damping results in only a 10% reduction in capture width. The damping figures relate to the ratio of the square root of pressure drop to flow, which are linearly related for an orifice plate. This represents a rather greater deviation in the ratio of pressure to flow of approximately 33%.

Damping (Continued)

This insensitivity to damping is to be expected from theory, (Simon [2]) :-

$$\text{Capture width, } W = W_{max} \times 4 \frac{DeDr}{(De+Dr)^2}$$

De, Dr internal and radiation damping.

The optimal orifice diameter is 9mm for a 200mm cell length, this varies with cell length to maintain a ratio of orifice area to cell waterline area of about 125.

With this degree of damping the fluctuating pressure across the orifice plate expressed as an r.m.s. head of water is between .4 and .5 of the r.m.s. height of the wave generating it, a useful non-dimensional figure which can be applied readily to full scale.

Partitioning of the Inlet Duct

In the rectified mode the central chamber of the S.W.C. must necessarily be partitioned into cells, and the frequency of this partitioning is dealt with in the following section. In principle however, this partitioning need not continue into the inlet ducts, that is beyond the maximum excursion of the internal wave, although for structural reasons they are desirable. Tests were therefore conducted to investigate how these partitions, which tend to channel the water into vertical oscillations only, effect the performance of the performance of the device.

Partitioning of the Inlet Duct (Continued)

Figures 4.8a and b show the effect on frequency response and mixed sea capture width. An improvement throughout of about 15% is derived from introducing these partitions.

Cell Length

Tests were carried out with the chamber divided into 150, 200 and 300mm length cells. Figures 4.9a and b show an overall improvement in performance by reducing from 300mm to 200mm. The trend is most pronounced at high frequency, reversing slightly at low frequency. In mixed seas the improvement is 6% at 1.1 seconds energy period to 12% at 0.8 seconds.

This improvement does not however continue with further sub-division of the chamber into 150mm cell lengths. (Figures 4.10a and b). The same effect of an improvement at high frequency occurs, but the break even point has now shifted much higher up the bandwidth. In mixed seas a reduction in capture width of up to 7% consequently results with the shorter cell.

An optimum cell length of about 200mm is therefore indicated to match the response of the present model. This represents a ratio of wavelength at resonance to cell length of about 6 which agrees closely with the analyses by Lighthill and Simon [1,2]. They predict that the maximum pressure amplification occurs for a single submerged resonant duct at a similar value of $\lambda/6$. Evidently the more complex case of an attenuator differs very little in this respect.

Device Length

The model tested has a fixed length of 1.2m, but the performance of a reduced length device was investigated by blocking off various lengths of the inlet ducts with foam rubber at their leeward end. This technique models quite accurately the internal behaviour of a shorter model, but inevitably creates a distorted flow pattern outside. It is hoped that a blockage at the rear of the model has less effect on its performance than one at the front.

The results of these tests are displayed in Figures 4.11a and b. The effect of a reduced length is to attenuate the response to lower frequencies. This has a considerable effect on mixed sea performance, where an almost linear improvement in capture width per unit length, with length, is observed.

Attenuation of the lower frequencies occurs due to the suppression of net upward and downward motion by the relatively incompressible air space within the chamber.

This effect is quantified in Figure 4.12, in which the change in air volume of a freely vented chamber (a measure of the suppression of an enclosed chamber) is plotted against device length/wavelength. Superimposed is the bandwidth of the current model with its full 1.2m length, and it is apparent that at the lower end considerable suppression is still taking place. From this analysis it appears that significant improvements in productivity can be expected for at least a further 50% increase in device length. The performance improvements arising from an incresed device length must however be balanced against structural considerations, which will be discussed in a later section.

Inlet Depth

The performance of the S.W.C. was investigated at a range of inlet depths from 40mm, the optimal depth, to 150mm, by which power output was attenuated typically by a factor of two. Figure 4.13a shows the effect on frequency response, from which it is evident that the natural frequency, and general shape of the response remains unchanged. Figure 4.13b shows the effect of depth in mixed seas. The shorter energy periods are effected most severely, attenuating by a factor of 2.5, greater sensitivity at high frequency where depth, z is large compared with wavelength, λ, is expected since the existing pressure fluctuation is given by:

$$P = P_o e^{-2 \pi z / \lambda}$$

A further graph, figure 4.14 plots the ratio of frequency responses at the two extremes of depth, and shows clearly how the reduction in performance at depth varies with frequency. The increasing sensitivity to depth at high frequency, discussed above, is quite marked, the ratio of capture width falling from 1 to .1 across the bandwidth. The overall trend agrees quite closely with the exponential law governing the decay of power with depth, which has been superimposed on the graph. A further effect however is also apparent, the fall off with frequency is modulated by a resonant effect, offsetting the exponential decay of power. At its peak the ratio is almost twice the exponential function. This is well in accordance with theory (Lighthill [1]), which indicates that for an idealised device with no internal losses and linear damping this resonant effect can be more marked to the point where at its peak no attentuation with depth is incurred.

Waveheight

The SWC was tested in two mixed seas, 0.8 and 1 second energy period, and r.m.s. waveheight was varied between 1.5 and 10mm. The results are presented in Figure 4.15
In both seas the device performed most efficiently in a waveheight of 4mm r.m.s. Above this, efficiency decays gradually due to increasing frictional losses arising from high fluid velocities within the device, but the effect is fairly minor amounting to only 10 and 15% in the range tested.

Below the optimum waveheight, efficiency falls away more rapidly. This is possibly due to surface tension, which creates a pressure on the water column comparable with the orifice pressure drop at these waveheights, in which case the effect will dissappear at larger scale. Moreover, whatever the cause of this phenomenon, in view of the low power content of these waves, a low efficiency is of little significance. By matching the device to a typical wave climate it can be shown that this lapse of efficiency is responsible for a loss in total annual energy output of less than 1%.

In the mid range of waveheight the optimum orifice diameter for a 200mm cell length is 9mm as reported earlier. This does not hold good throughout the range of waveheight however, as the optimal diameter increases slightly with waveheight to compensate for the square law pressure flow relationship of an orifice plate, which tends to increase damping with waveheight.

Duct Taper

The taper of the inlet ducts of the model tested can be adjusted by pivoting its outside walls (Figure 4.5). The device was tested with these walls upright, swung out at 15°creating tapered ducts, and swung in at 7.5° to form antitapered ducts. The results are presented in Figures 4.16a and b, in which the capture width scales have been adjusted to take account of the different cross-sectional areas of the three configurations.

From parallel to antitaper there is a discernable shift in response towards lower frequencies. This is reflected in mixed seas where antitaper performs better above .85 seconds energy period. Improved performance at low frequency is of particular value, due to cost implications which will be discussed in the section on Scaling. The predominant effect of pivoting in the walls however was a reduction in bandwidth, which is mainly due to the reduction of the size of the inlet.

The converse effect, of increasing bandwidth due to the wider inlet of the tapered duct, unfortunately swamped the true effects of taper alone, and little can be concluded about these from the test. The test does however suggest that, judging from the high mixed sea efficiency with taper, there is scope to increase duct widths and hence the cross-sectional area of the SWC, with a worthwhile return in power output.

In order to isolate the effects of duct taper from duct size, far greater adjustability of duct geometry is required, which is discussed in the section on Future Work.

Distribution of Power Output between Cells

The data presented hitherto relates to gross figures for the device as a whole. For all tests however, the contribution of each cell was also recorded.

Figure 4.17 shows how each cell contributes to the total frequency response of the device, and it can be seen that the distribution is very uneven. With an improved distribution, higher efficiencies might be achieved, and certainly the maximum water column oscillations which need to be accommodated will be smaller, leading to a smaller device. An understanding of the cause of the irregularities is first required, and an insight is given in Figure 4.18, which plots the r.m.s. pressure fluctuations, non-dimensionalised against waveheight for four mixed seas. It is apparent that the variations in pressure are not erratic, but follow very smooth curves, which could be described as standing waves. This is reinforced by the fact that the wavelength of these waves tends to increase with energy period. The irregularity of the standing waves is only to be expected since the seas which give rise to them are irregular. A common feature in all seas is that the standing waves originate from an antinode at the rear of the device. This provides a clue to a possible method of eliminating the waves, to taper the width of the device at the back end so that no reflective end face is provided.

4.4.5 Rectified Flow Mode

Limited testing has been conducted on the peristaltic method of generating a rectified flow of air, the parameters tested were:-

Damping
Fence and Partition Spacing
Device Length

Similar trends existed as for the alternating flow mode. Performance peaked with damping equivalent to a single 10mm orifice for the entire device, providing a relatively higher degee of damping.

The ideal fence and partition spacing was 200mm as for the alternating flow mode, and performance increased steadily with overall device length.

The performance of this mode in mixed seas is compared with the alternating mode in Figure 4.19. The capture width of the rectified flow mode is only 65% of that for the alternating flow mode. Experimental work in the near term consequently will be concentrated on the alternating flow mode to assess the potential of the device, but the advantages of rectification warrant further work at a later stage.

4.4.6 Future Experimental Work

Future experimental work will be concentrated on the following topics:-

(1) Device Length

The effect of further increases in device length will be studied with the next model which will be comprised of 200mm detachable modules.

(2) Duct Taper and Width

The effects of duct width, and a change in duct width from inlet to air water interface will be studied in isolation. This will be achieved with the ability to adjust the width of the inlet duct and the central chamber width independently.

(3) Power Distribution between Cells

Work will be directed towards achieving a more even distribution of the power output between cells.

(4) Rectification

The next model will be designed to accept simple flap valves for rectified flow tests, to examine the potential for phase control. By measuring the pressure and flow within each cell as in the alternating flow experiements the total power generated can be determined. Similar measurements after rectification will establish the losses in the valves, but these will not be very representative of the full scale device.

4.4.6 Future Experimental Work (Continued)

(5) Motion as a Tethered Device

The model will be given extra buoyancy and moored by taut lines simulating a tension leg mooring system. The motion of the device in waves, and the effect of this motion on performance will be measured.

(6) Internal Stresses and Mooring Forces

These will be measured using strain gauges and load cells.

(7) Array Effects

Initially the performance of a device in an infinite array will be simulated with the use of reflector walls to provide lines of symmetry. Later, when the device has been more fully optimised, arrays of three or more models will be tested, particularly in angled seas, to assess the effects of the directionality of arrays.

(8) The Submerged Wave Chamber as a Terminator

The SWC was originally envisaged as an attenuator, gaining pneumatic and force balance by spanning waves in their direction of motion. In theory however, if sufficiently long to achieve a pneumatic balance in a crestwise direction, the SWC could operate as a terminator, though in this mode it would necessarily become a bottom mounted device.

Some tests will therefore be carried out in short crested seas on the SWC in this mode, to assess its performance and cost effectiveness compared with the attenuator mode.

4.4.7 Selection of the Full Size Device Scale

In order to optimise the scale of a full size SWC relative to the present model, it is necessary to compare its frequency response with the wave climate data at its proposed site.

Figure 4.20a shows the projected frequency response of the SWC at a depth of 6 m, for devices 100, 120 and 150 times the present model dimensions with its full 1.2 m length.

Superimposed is the distribution of power off South Uist, a favoured site, in waves up to 1 m r.m.s. height, collated by Mollison[3]. The application of a wave height limit will be discussed in a later section.

It can be seen that the response of the X100 device is far higher frequency than the wave power distribution, and even at X150 the match is not perfect. However, further analysis shows that a good match between response and wave climate is not necessarily a desirable feature.

Also included on this graph is a Pierson Moskowitz spectrum chosen for the best fit with the South Uist data. The shape of the distribution is very similar but bandwidth is reduced by about 20%.

The fraction of power in each group of the distribution was then multiplied by the mean capture width in that frequency band for each of the three devices. The resulting distributions are plotted in Figure 4.20b Each value can be considered as the contribution within the given frequency band towards the mean annual capture width expected in this wave spectrum, which is then calculated from the sum of the contributions.

4.4.7 Selection of the Full Size Device Scale (Continued)

The mean annual capture width is plotted against scale in Figure 4.21. It is important to note that the gradient of the curve decreases with increasing scale, in other words increasing scale brings diminishing returns".

At this point some measure of the capital cost of the SWC must be introduced. In the top insert of Figure 4.21 a typical curve relating cost to scale is superimposed on the capture width curve, with scales chosen so that the curves just touch. At the point of contact of the two curves, cost/capture width is a minimum, that is the device is most cost effective, since by increasing or decreasing scale the two curves diverge cost increasing faster than capture width. At this point it can be said by inspection:-

$$\frac{\frac{dc}{ds}}{\frac{c}{s}} = \frac{\frac{dw}{ds}}{\frac{w}{s}}$$

c capital cost
w capture width
s scale

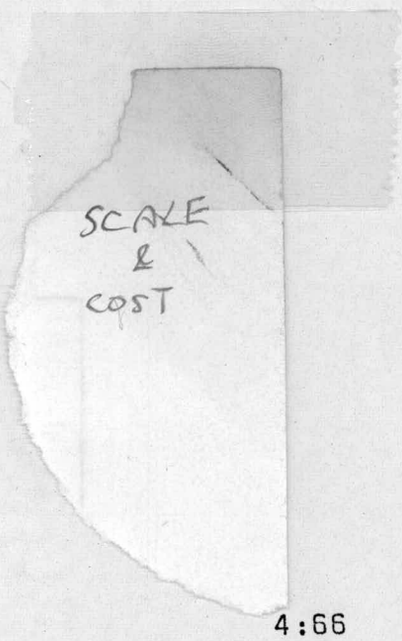

4.4.7 Selection of the Full Size Device Scale (Continued)

Now assuming that cost is related to scale by a function of the form:-

$$c = Ks^n$$

$$\frac{dc}{ds} = Kns^{n-1} = \frac{c}{s^n} ns^{n-1} = n \frac{c}{s}$$

$$\therefore \frac{\frac{dc}{ds}}{\frac{c}{s}} = n = \frac{\frac{dw}{ds}}{\frac{w}{s}}$$

Therefore, at the point of maximum cost effectiveness:-

$$\frac{\frac{dw}{ds}}{\frac{w}{s}} = n$$

The index has been calculated for the three scales and the values plotted in the lower inset of Figure 4.21, which represents the optimal scale for any cost index. A realistic index is likely to lie between 2.5 and 3, implying an optimal scale factor of 110.

The comparison was drawn earlier between the South Uist data and a single P.M. distribution. In fact if the same procedure is carried out using the P.M. distribution, the mean annual capture width of the X150 device is increased by only 4.2% due to the reduced bandwidth, and is actually 1.3% lower for the X100 device since the response falls on the shoulder of the wave power distribution. In view of this the scale analysis was also applied to mixed sea tank test data.

4.4.7 Selection of the Full Size Device Scale (Continued)

Assuming a representative energy period of 10 seconds, mean capture widths have been calculated for three scales of device and are plotted in Figure 4.21. These figures are only 60-70% of the equivalent values calculated by synthesis of the distributions. The cause of this disparity can only be the spreading function applied to the mixed seas, making them short crested.

The main object of the analysis however is to establish the optimal scale of the device, and if the cost index is calculated as before, a second curve of optimal scale is produced which crosses the original curve in the region of interest, again indicating an optimal scale factor of 100 - 110.

Utilisation of Resource

The above analysis is aimed at maximising the cost effectiveness of the SWC. If, instead, the goal is to make the best use of the wave energy available, then different and rather conflicting criteria are involved. The relevant index is now 1 and the optimum scale, at which response and wave energy distribution are now matched, occurs at about 175.

The discrepancy between optimal scales is not peculiar to the SWC : it is inevitable if device response and wave energy distribution have finite bandwidths.

4.4.7 Selection of the Full Size Device Scale (Continued)

Device Capacity

In the scale optimisation, the assumption was made that the SWC would function only in waves less than 1 m r.m.s. height. This is a reasonable first estimate with the limited data available; a device 100 times the present model scale could indeed operate satisfactorily in waves in this range, but by similar reasoning the X120 and X150 devices could operate up to 1.2 and 1.5 m with a resulting increase in the overall resource utilisation. This would bias the optimal scale upwards.

Furthermore, this assumption of a waveheight limitation is a rather course one since it implies that above the limit power output will cease. The waveheight limit is applied to take account of the limited capacity of the SWC. This is set by two factors, the rated output of installed plant, and its 'maximum swept volume', that is the maximum amplitude of oscillation of the water columns that can be accommodated. In higher waveheights however, power output would not actually cease. A better assumption is that with further increases in height the SWC continues to generate the rated plant output, and the water column oscillations are limited to the maximum swept volume by a throttling system, thus dumping excess power.

Figure 4.22 presents the percentage of wave energy available off South Uist to a wave energy device operating at its predicted capture width up to a given waveheight, and at a constant power above, plotted against the waveheight at which the transition occurs. The data is taken from total wave energy available off South Uist between March 1976 - February 1978 collated by Miller and Hogben[4].

4.4.7 Selection of the Full Size Device Scale (Continued)

Now the swept volume of a device 100 times the model scale which could accept up to 1m r.m.s. wave height represents about 25% of the total structure cost, and the plant about 10%. Therefore, for a given scale of device, if these costs are considered proportional to the transition waveheight, the overall cost would rise as the dotted line in the Figure 4.22. On this basis an improvement in cost effectiveness will be expected at a 30% increase in capacity.

With the data available at present it is not possible to analyse the effects of device capacity on cost effectiveness very accurately, but the points discussed above will be taken further in future work.

4.4.8 Conclusions

The Submerged Wave Chamber is proving itself a promising derivative of the original Vickers device. It compares well with the other derivatives in terms of performance (Figure 2.12), whilst benefiting from the force balancing properties of an attenuator, which allow it to be moored in deeper water if the economics are favourable, to avail itself of the larger wave energy resource available. A detailed costing has yet to be undertaken, but after comparing the performance data with that for comparable devices, we conclude that a figure of 6p/kw hr is entirely realistic.

The prospects for future work are exciting, with great potential for further improvements in efficiency and cost effectiveness promised by optimisation of device length, duct width and taper, the distribution of power output within the device and by the introduction of phase control. Meanwhile, in coordination with the theoretical work in hand, experimental work will be initiated on the dynamics and stressing of the SWC, in order to assist in the design of a full scale structure and mooring system.

The Submerged Wave Chamber

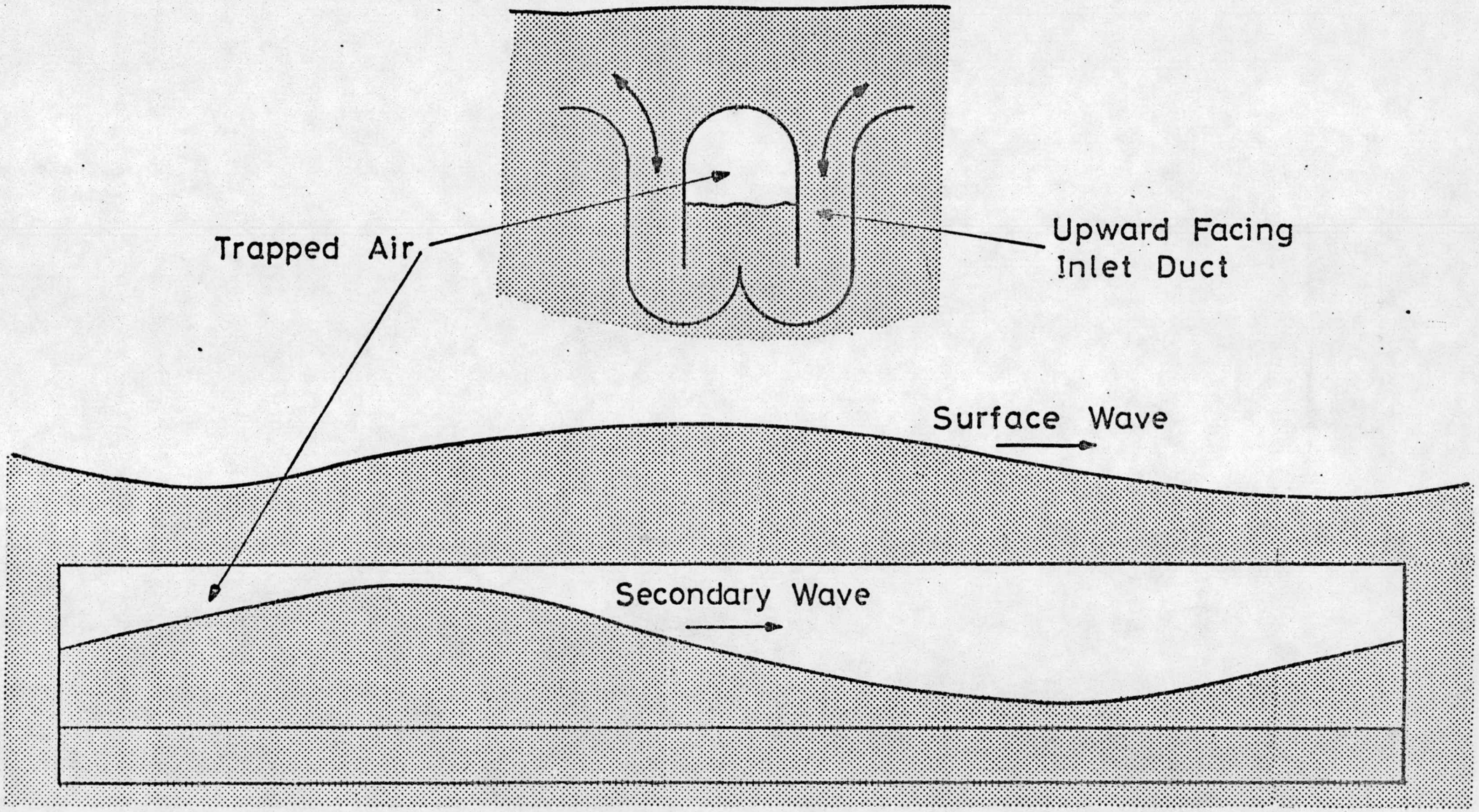

FIG. 4.1:

(a)

FLOW FROM CELL TO CELL

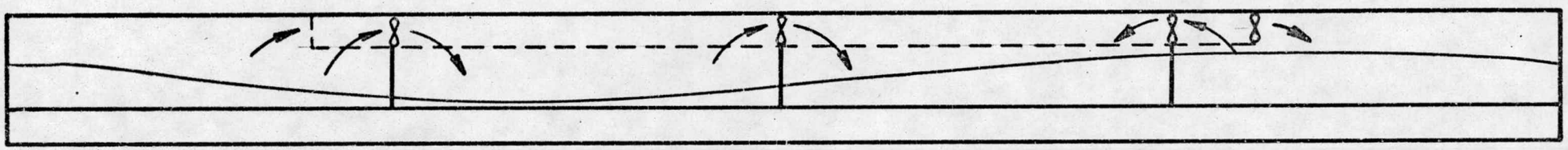

(b)

FLOW VIA A MANIFOLD

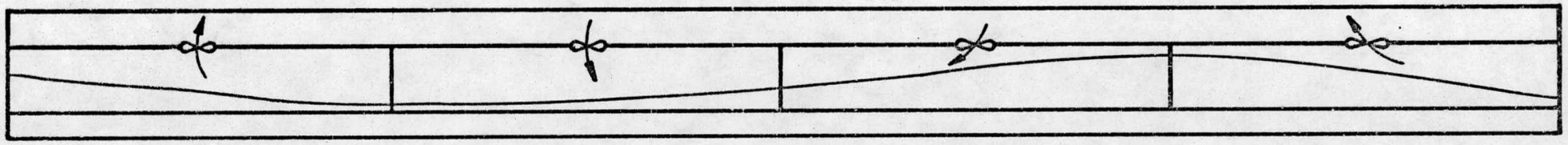

FIG. 4.2.

THE SUBMERGED WAVE CHAMBER
ENERGY CONVERSION BY BI-DIRECTIONAL AIR TURBINES

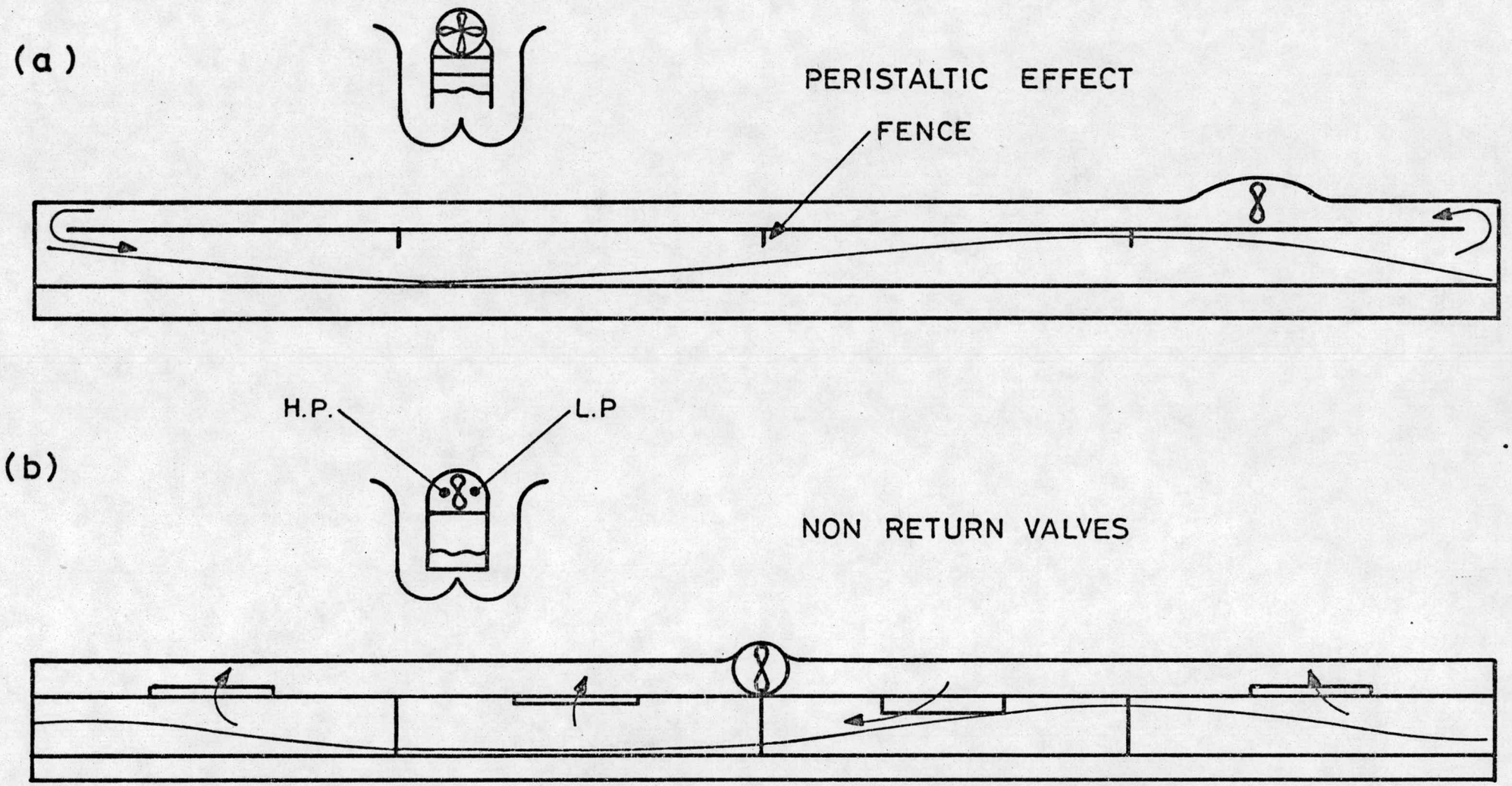

ENERGY CONVERSION BY UNI-DIRECTIONAL AIR TURBINE

THE SUBMERGED WAVE CHAMBER

FIG. 4.3.

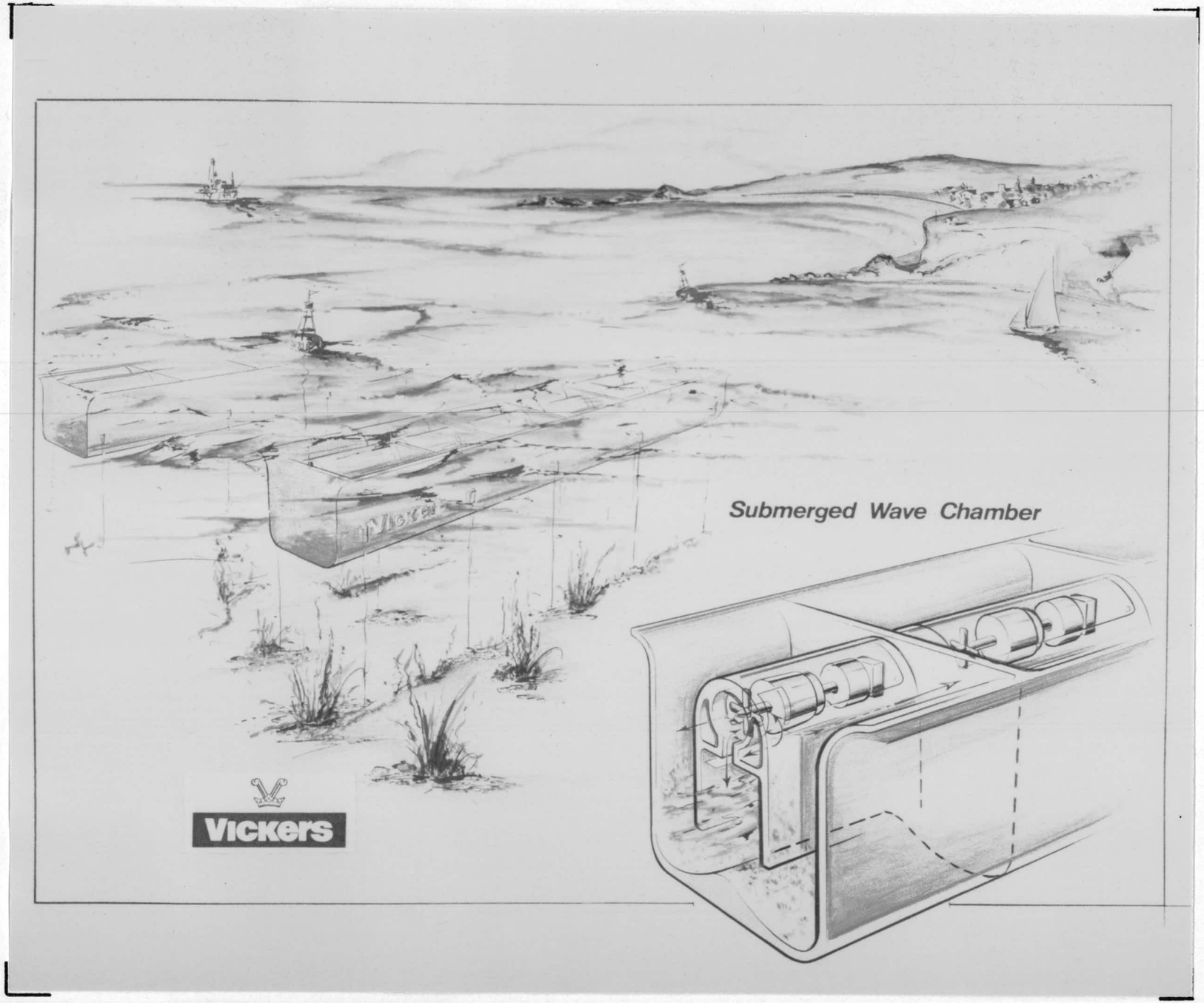

Figure 4.4

Cross-Section of Submerged Wave Chamber
Test Model.

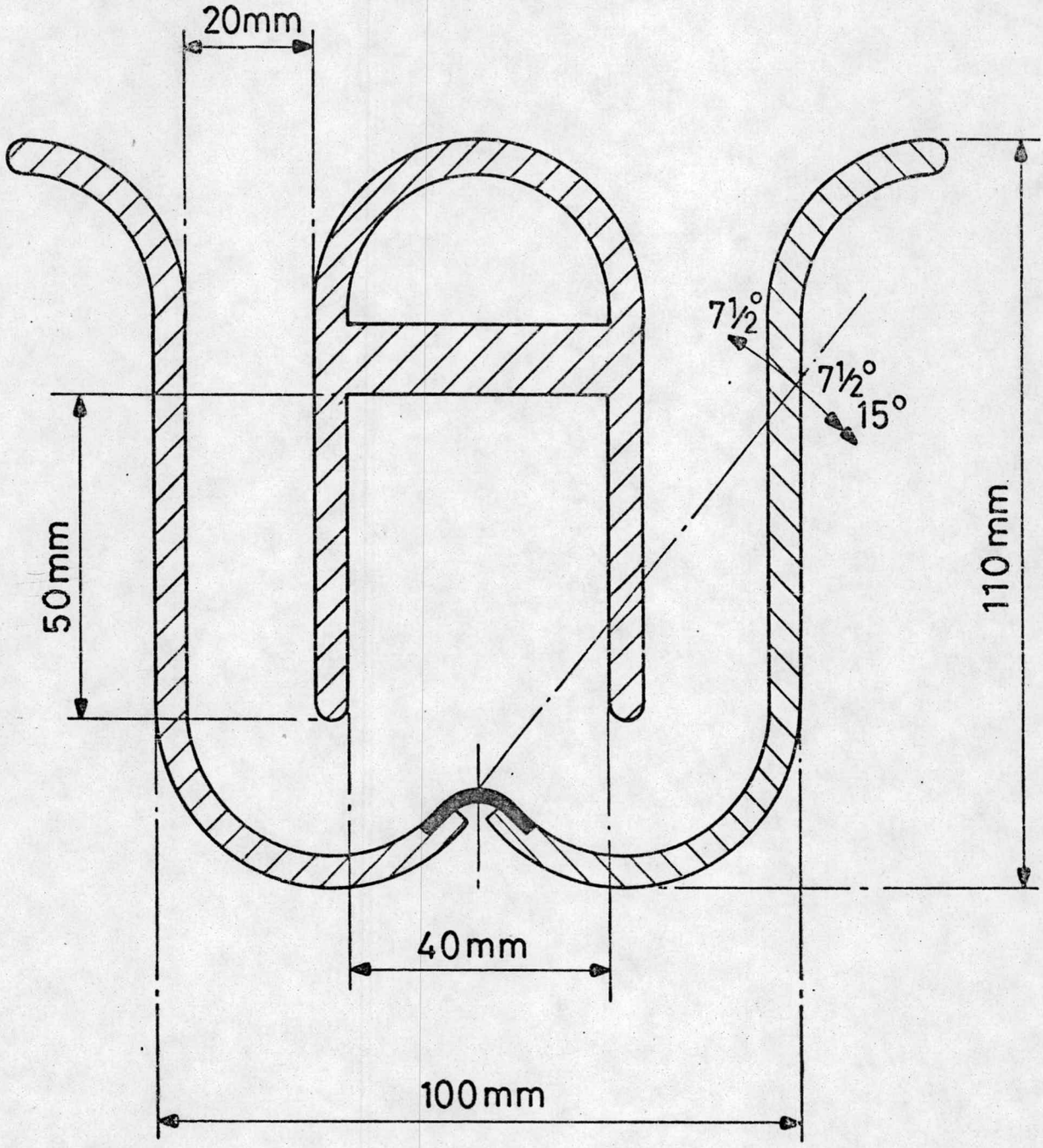

Scale 1:1

Full Device Length 1·2m

FIG. 4.5.

Comparison Between Flows Computed From Water Level and Orifice Pressure Drop.
– Twin Oscillating Water Column.

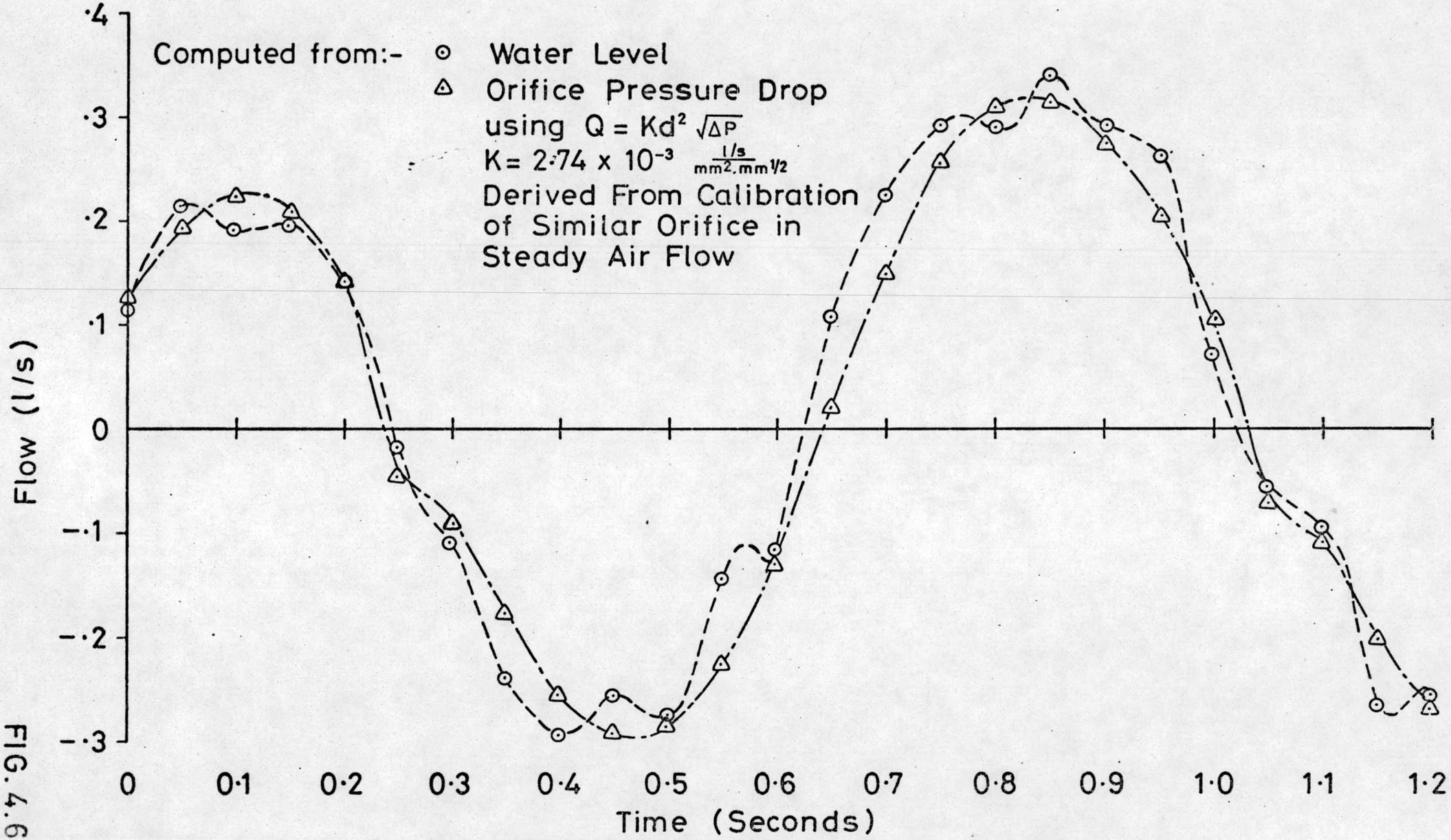

FIG. 4.6.

(a)

Submerged Wave Chamber. Effect of Damping on Frequency Response.

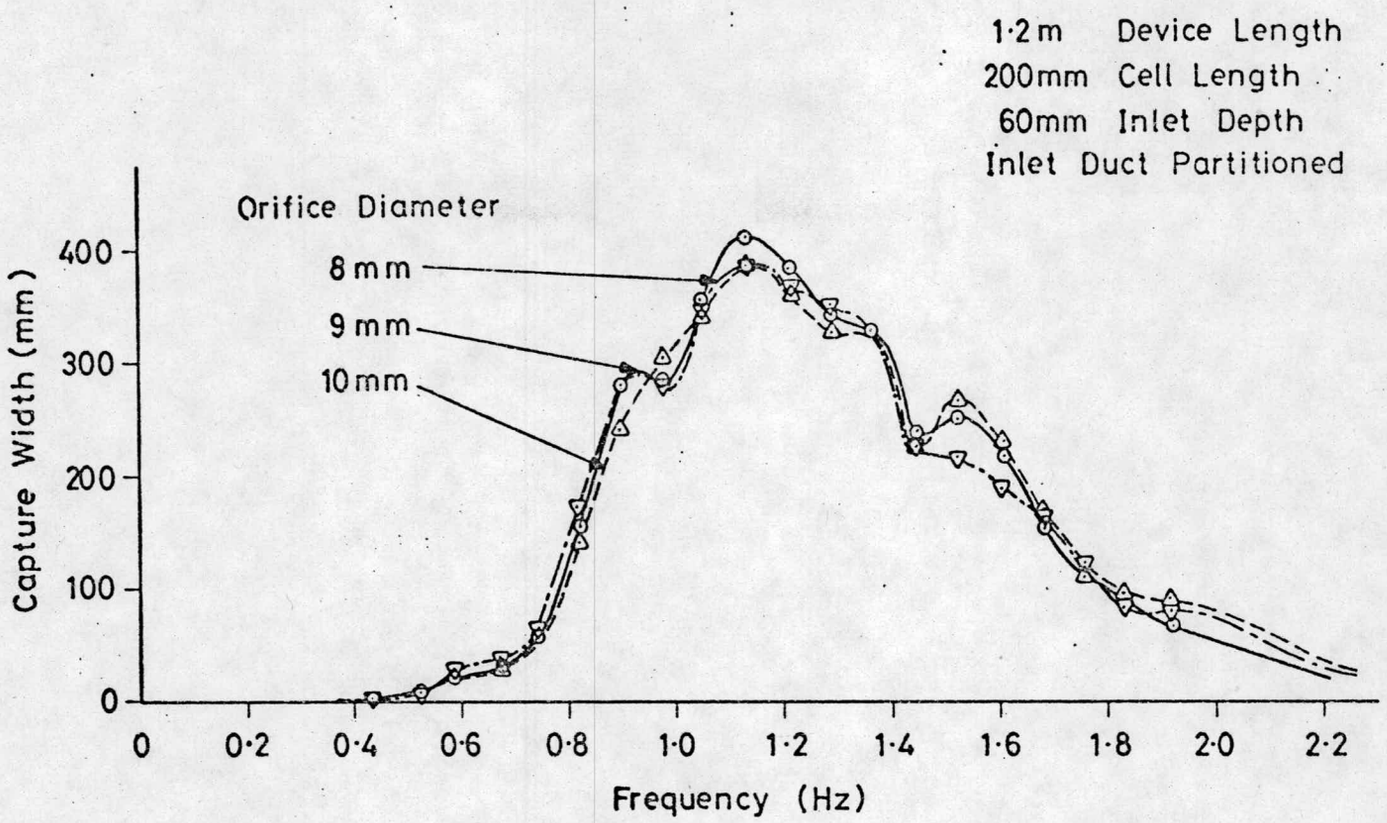

(b)

Submerged Wave Chamber. Effect of Damping on Capture Width in Mixed Seas

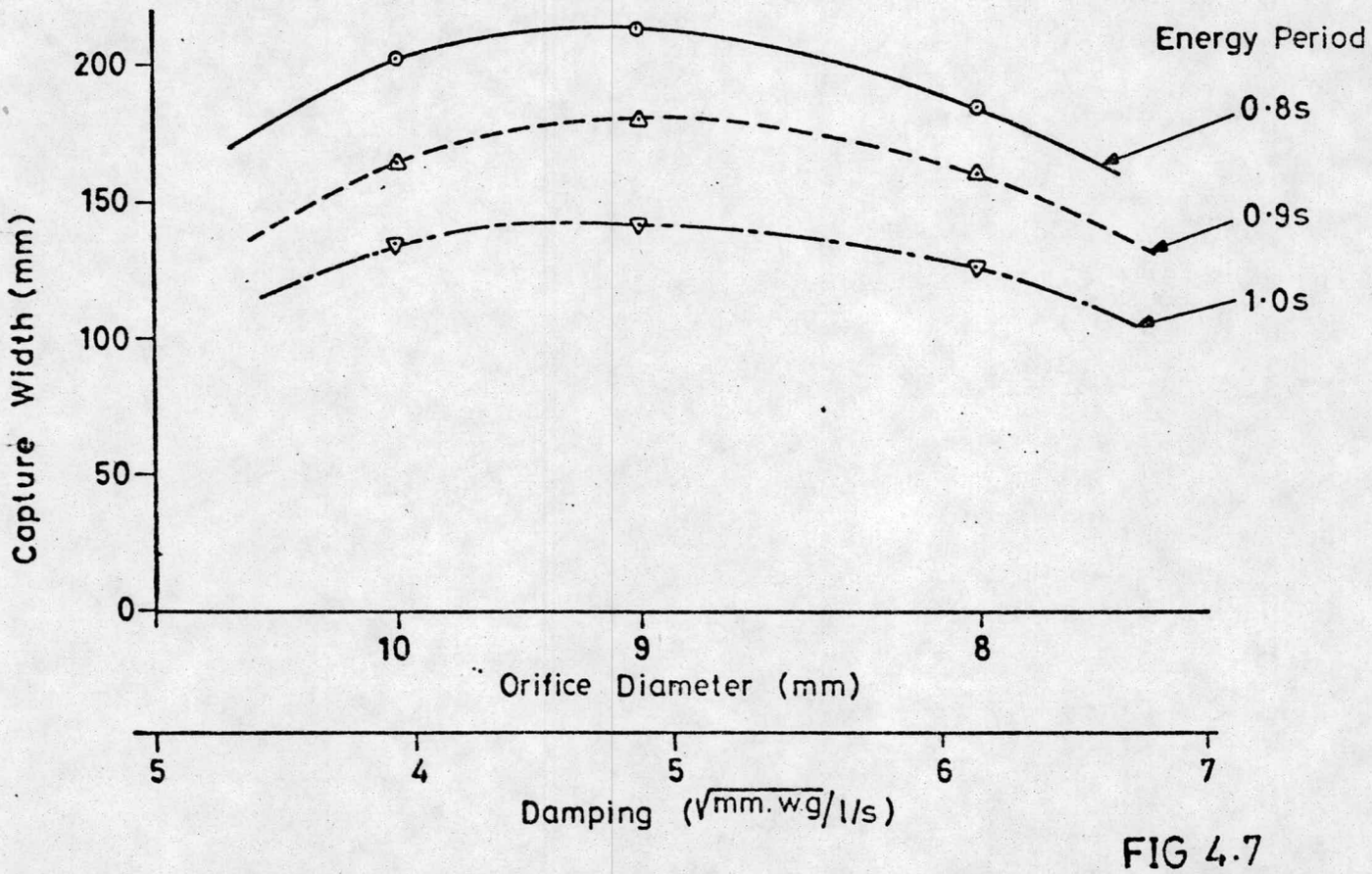

FIG 4.7

(a)

Submerged Wave Chamber. Effect of Partitioning Inlet Duct on Frequency Response.

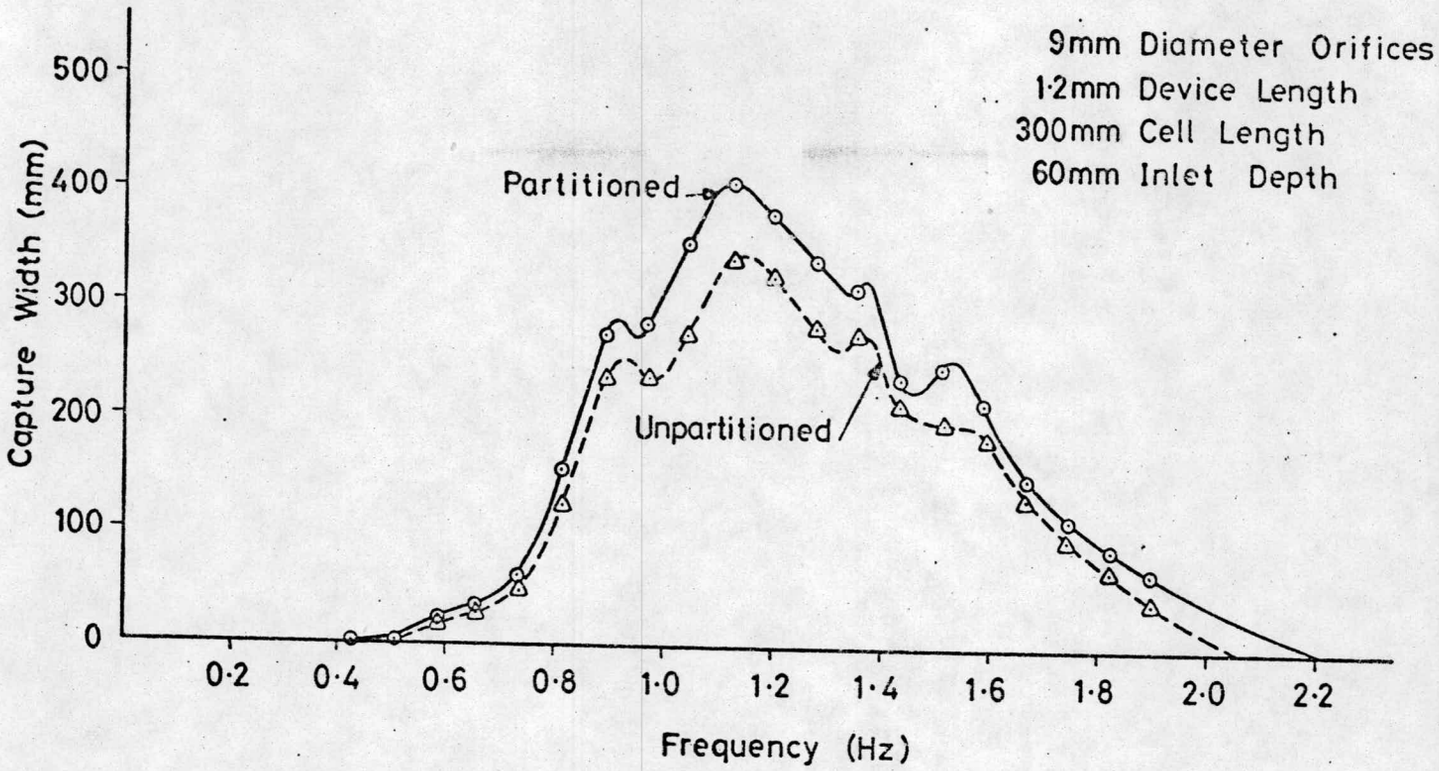

(b)

Submerged Wave Chamber. Effect of Partitioning Inlet Duct on Capture Width in Mixed Seas.

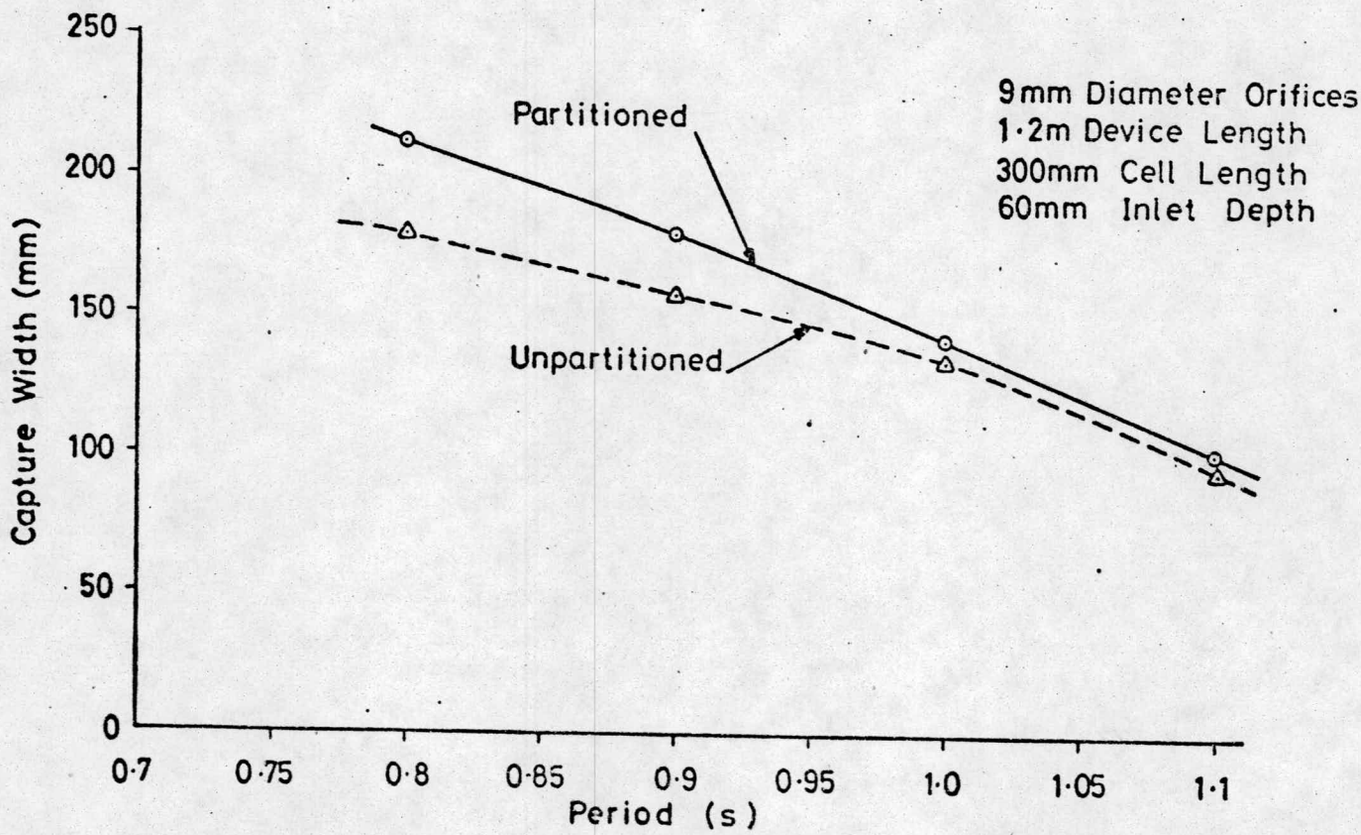

FIG 4.8

(a) Submerged Wave Chamber. Effect of Cell Length on Frequency Response.

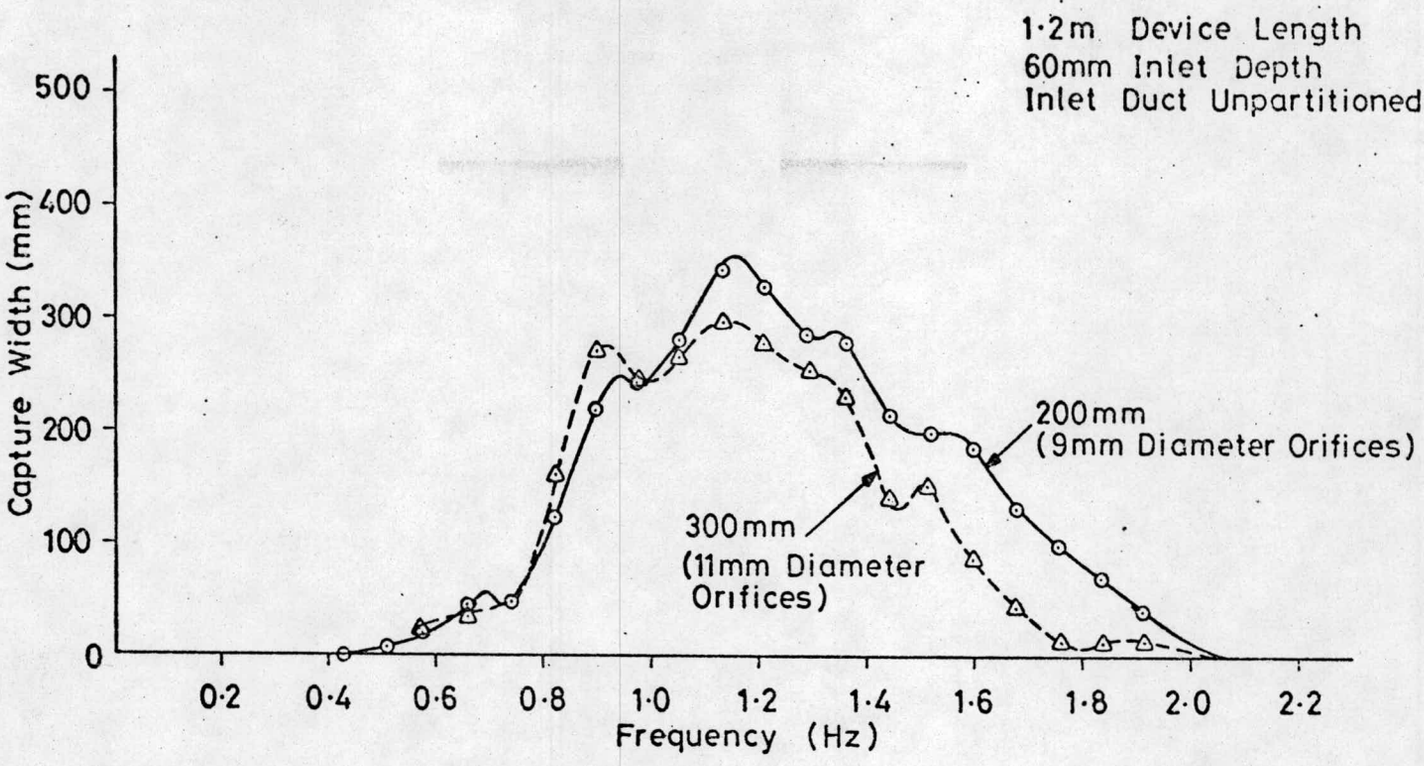

(b) Submerged Wave Chamber. Effect of Cell Length on Capture Width in Mixed Seas.

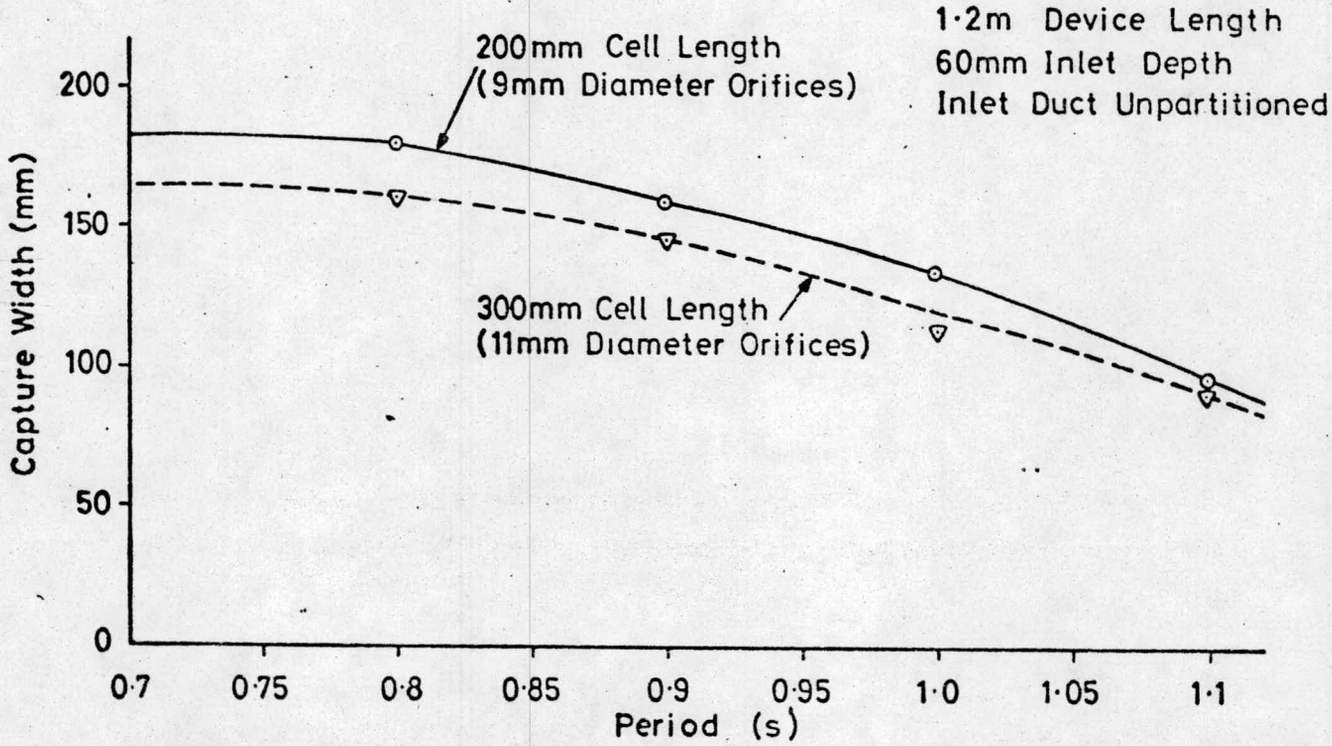

FIG 4.9

(a) Submerged Wave Chamber. Effect of Cell Length on Frequency Response.

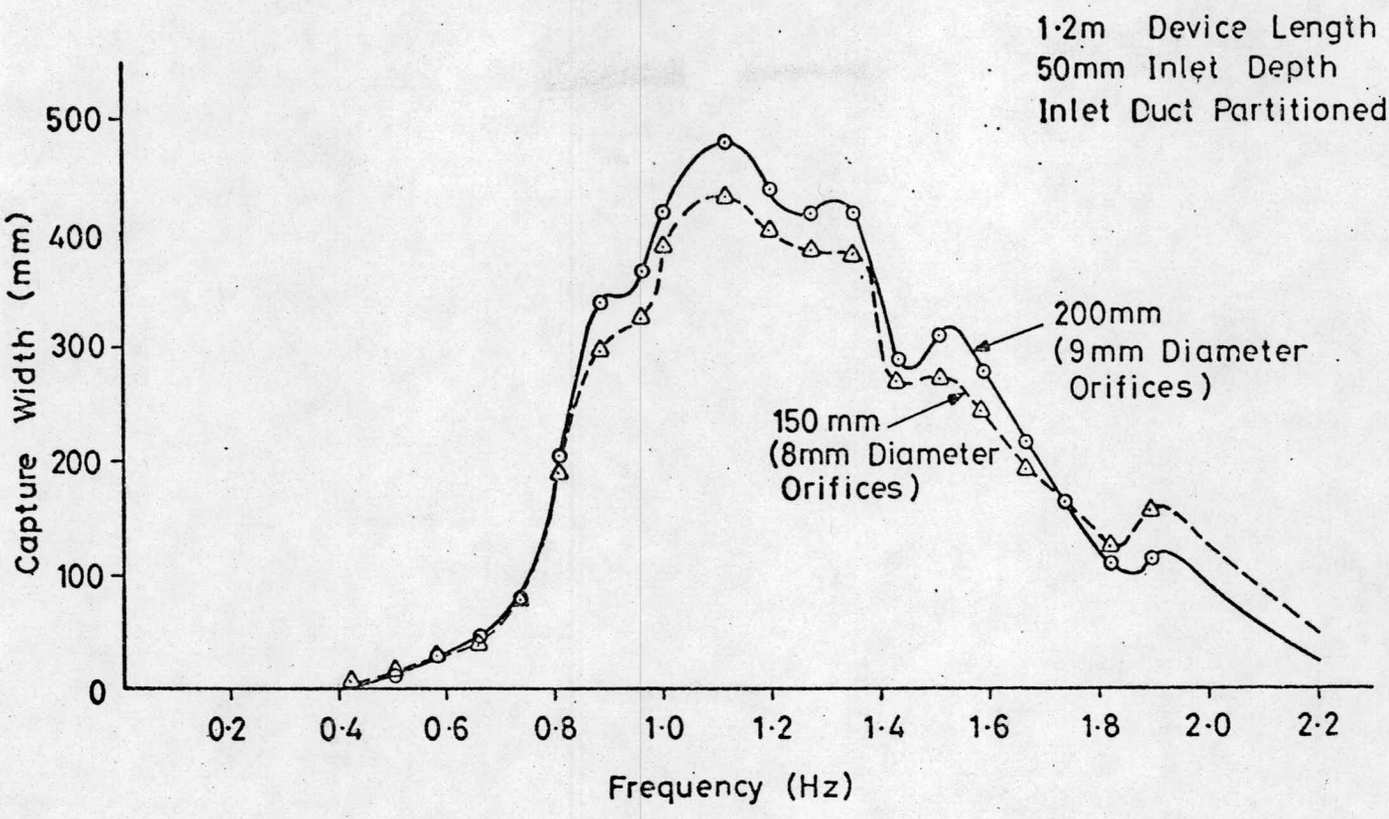

(b)

Submerged Wave Chamber. Effect of Cell Length on Capture Width in Mixed Seas.

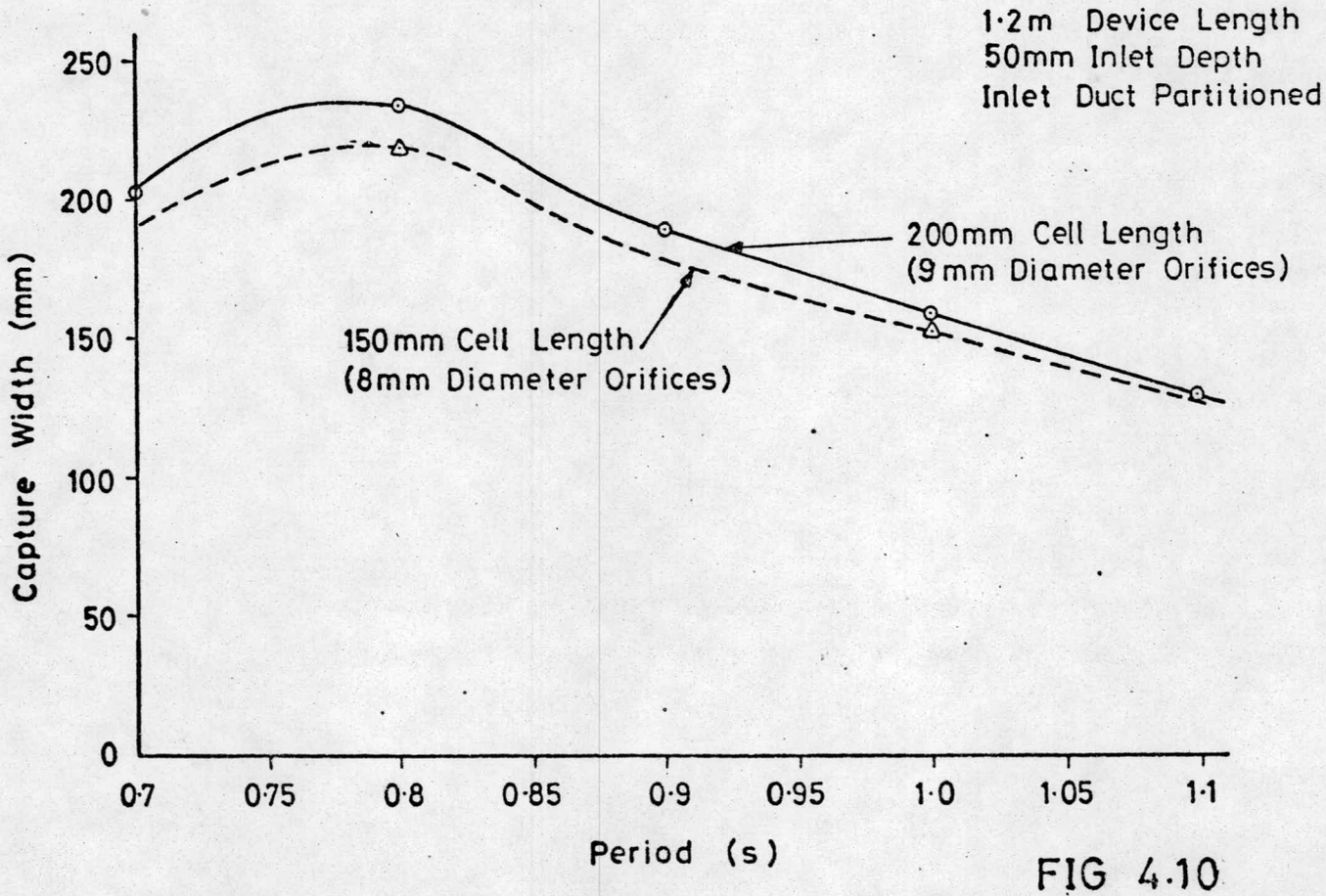

FIG 4.10

(a) Submerged Wave Chamber. Effect of Device Length on Frequency Response.

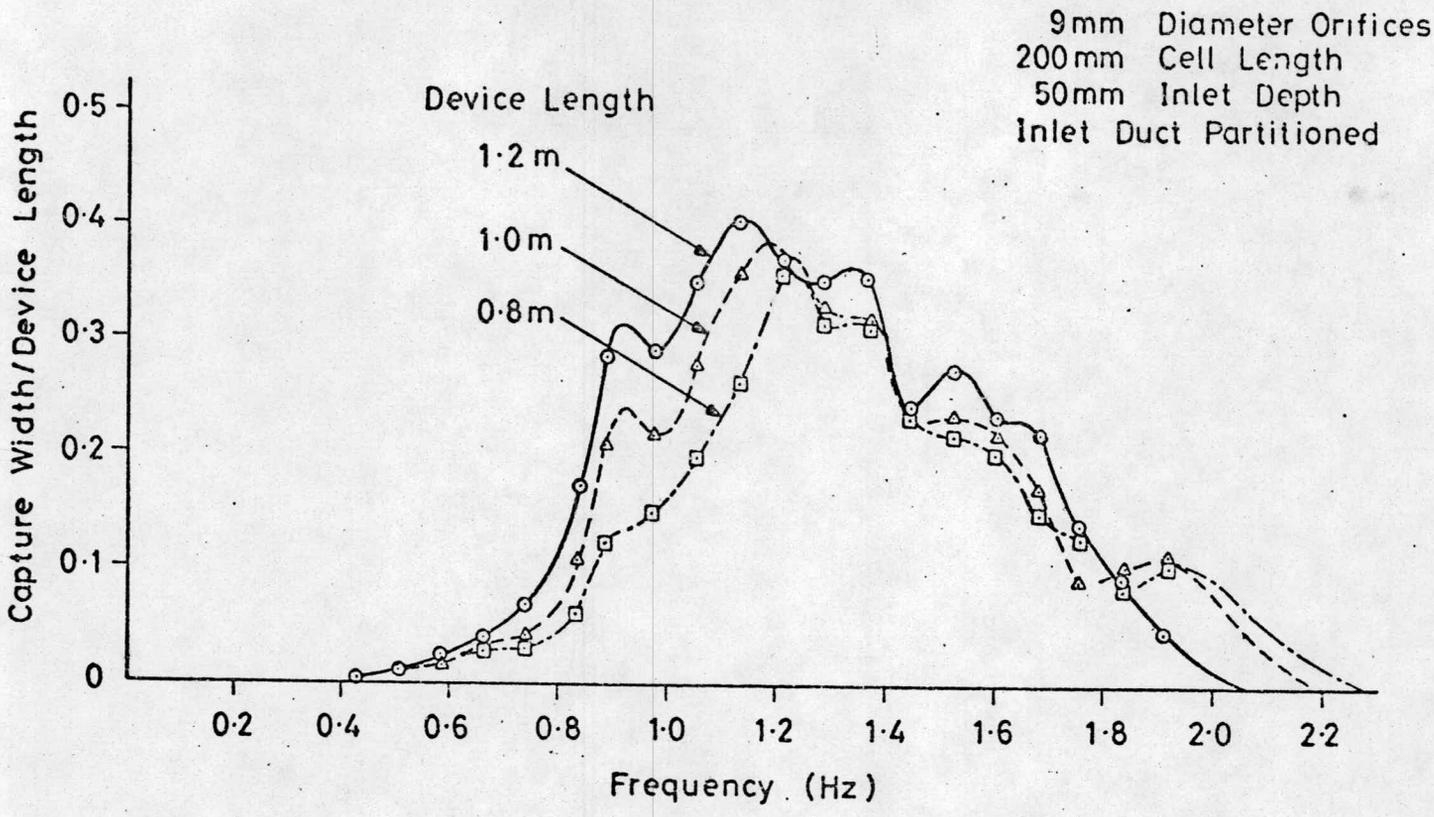

(b)

Submerged Wave Chamber. Effect of Device Length on Capture Width in Mixed Seas.

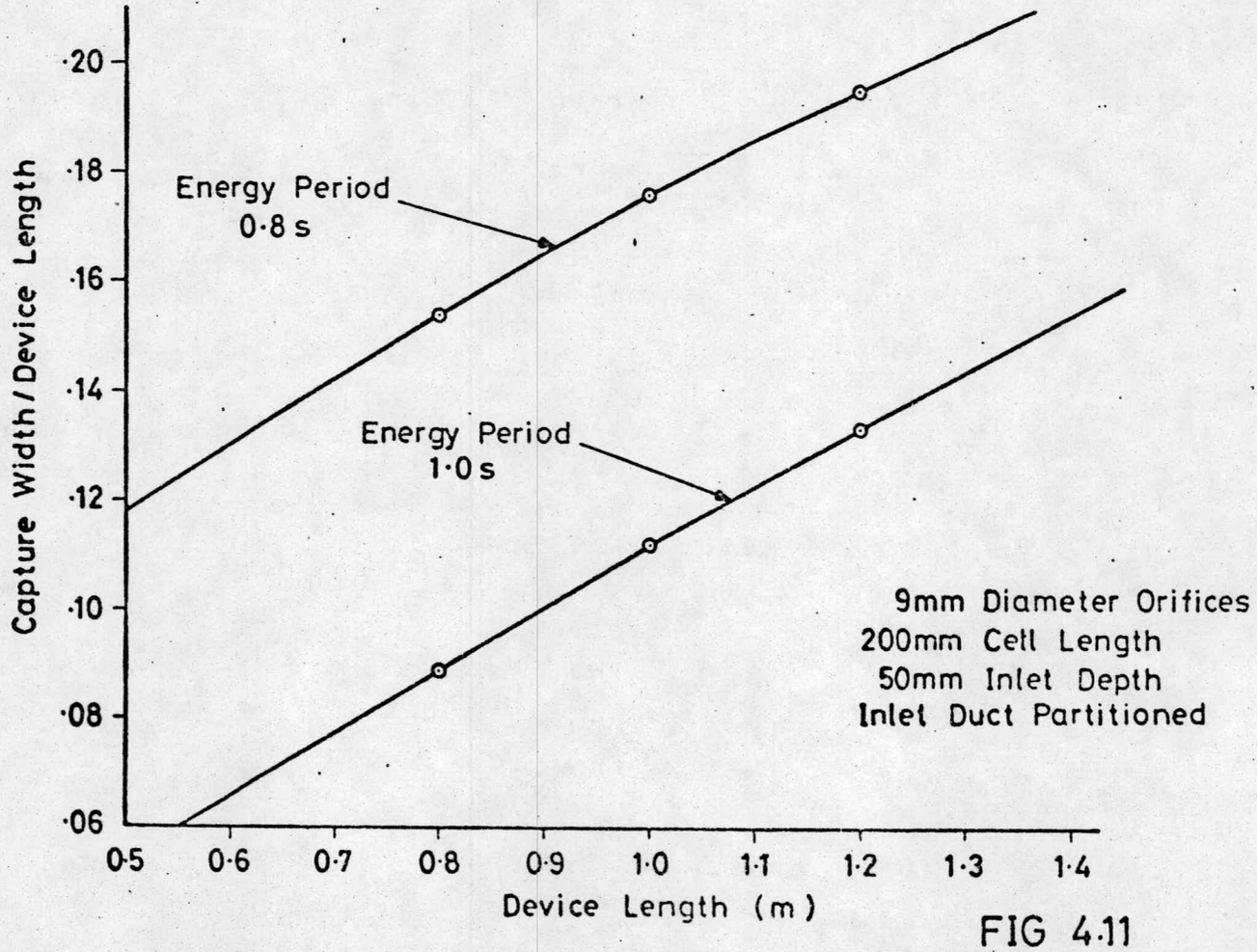

FIG 4.11

Submerged Wave Chamber. Effect of an Enclosed Air Space

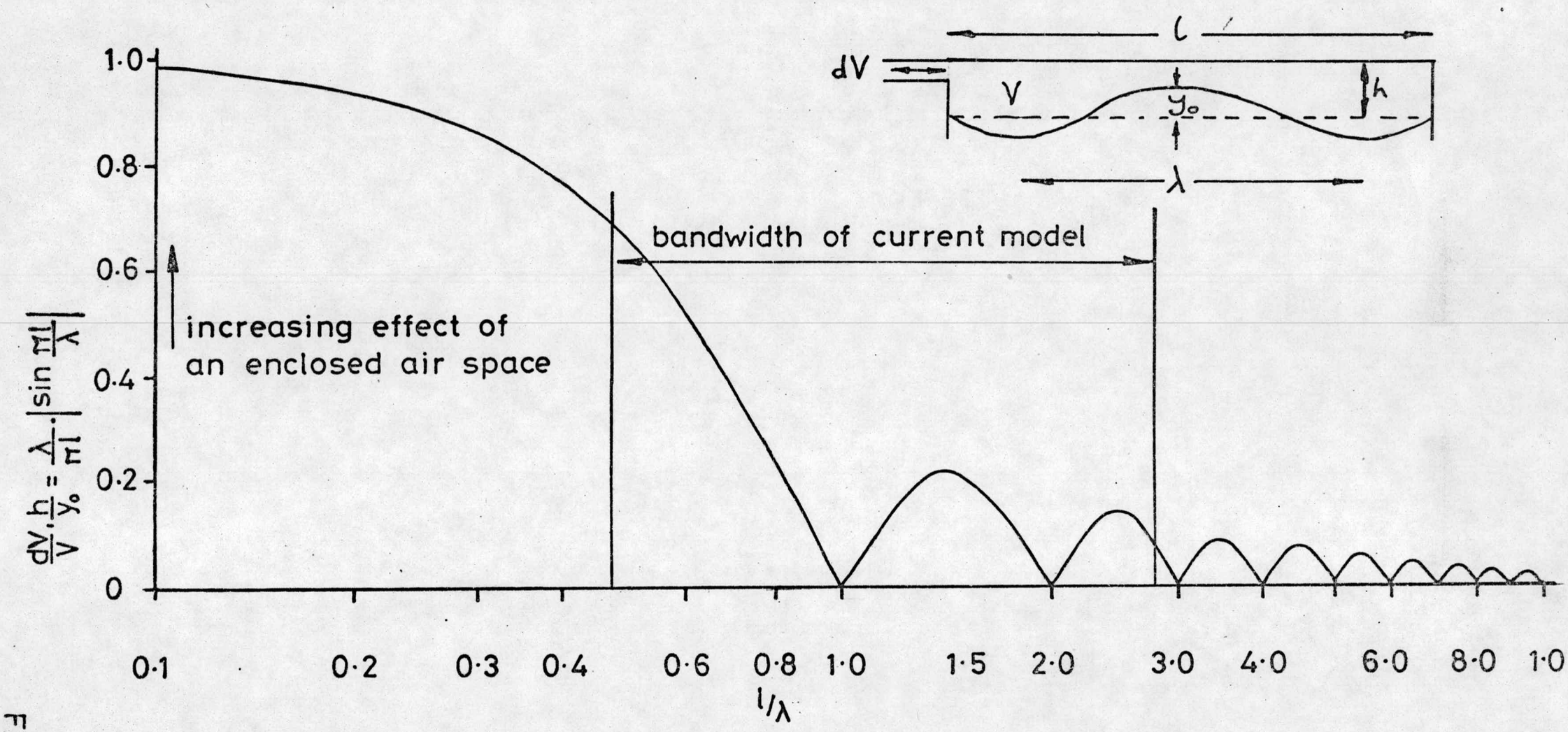

FIG 4.12

(a) Submerged Wave Chamber. Effect of Inlet Depth on Frequency Response.

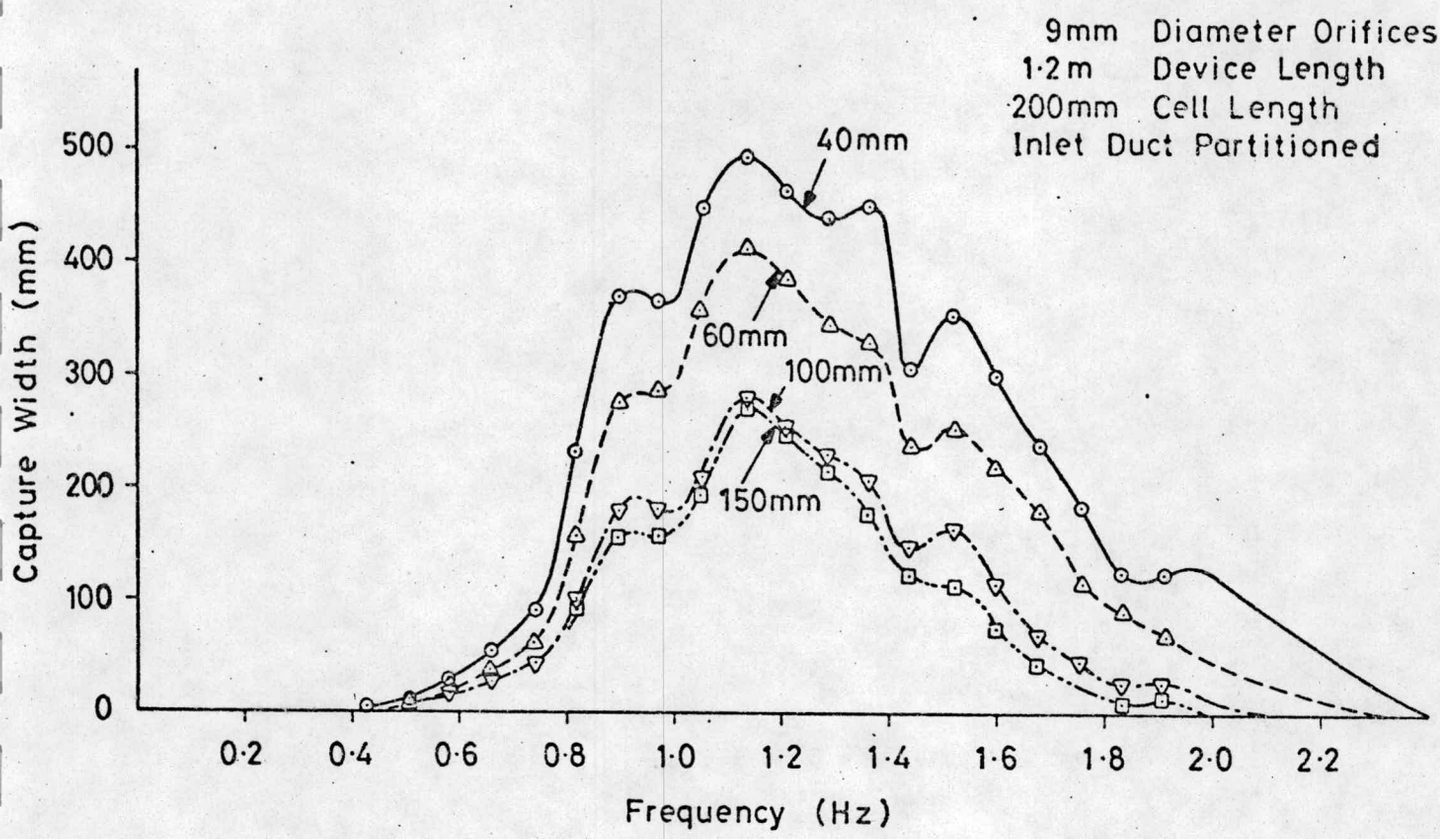

(b) Submerged Wave Chamber. Effect of Inlet Depth on Capture Width in Mixed Seas.

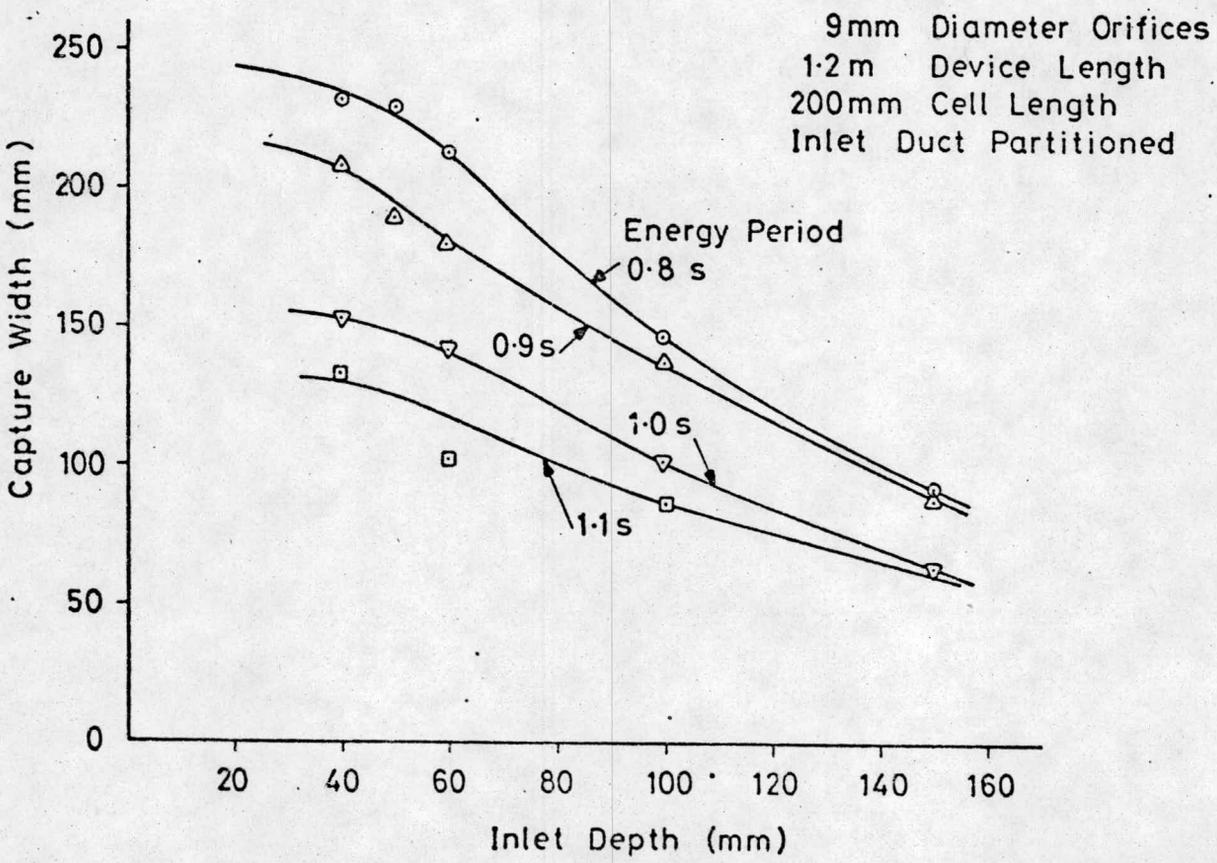

FIG 4.13

Submerged Wave Chamber. Variation in Performance at Depth With Frequency 150 mm Relative to 40 mm Depth.

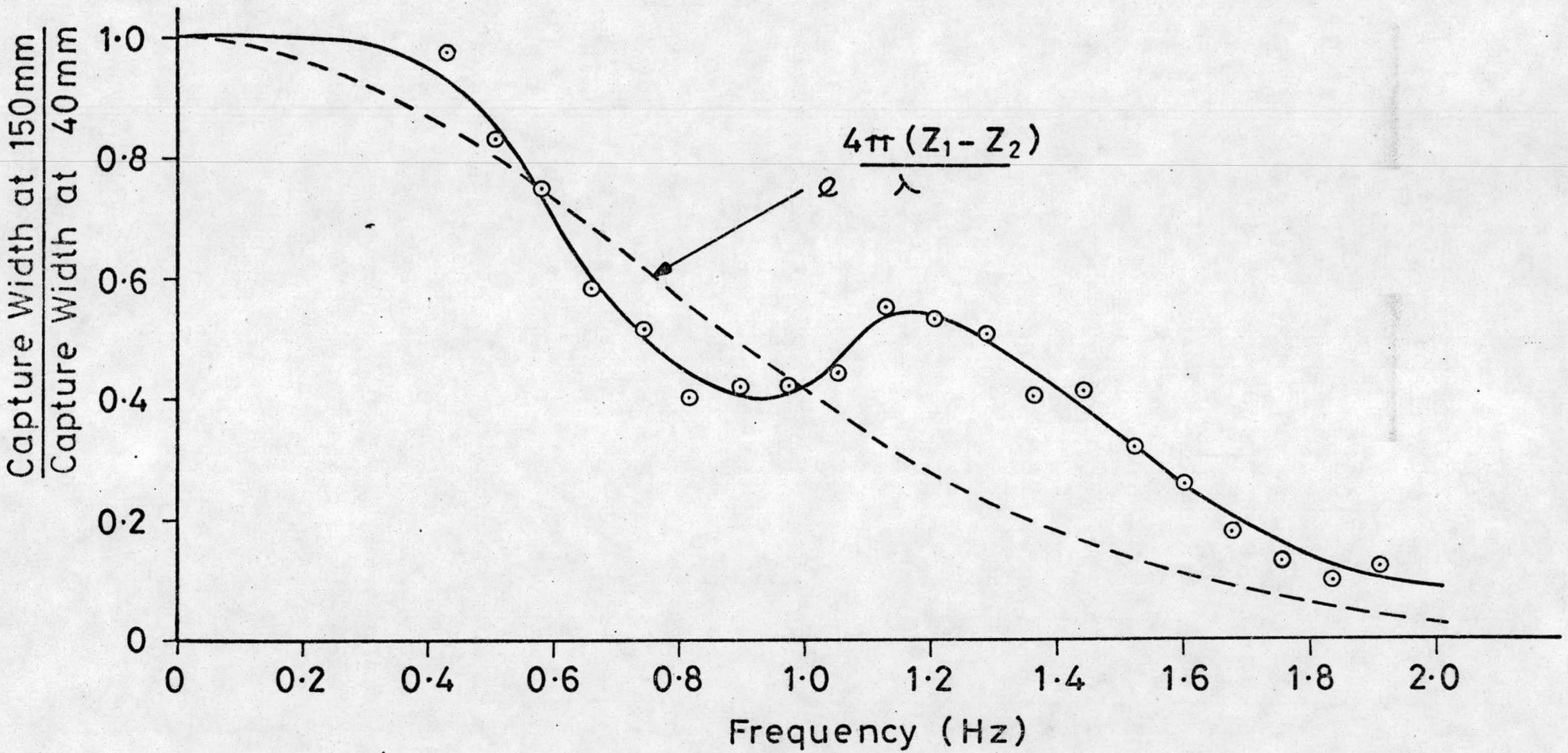

FIG 4.14

Submerged Wave Chamber. Effect of Wave Height on Capture Width in Mixed Seas.

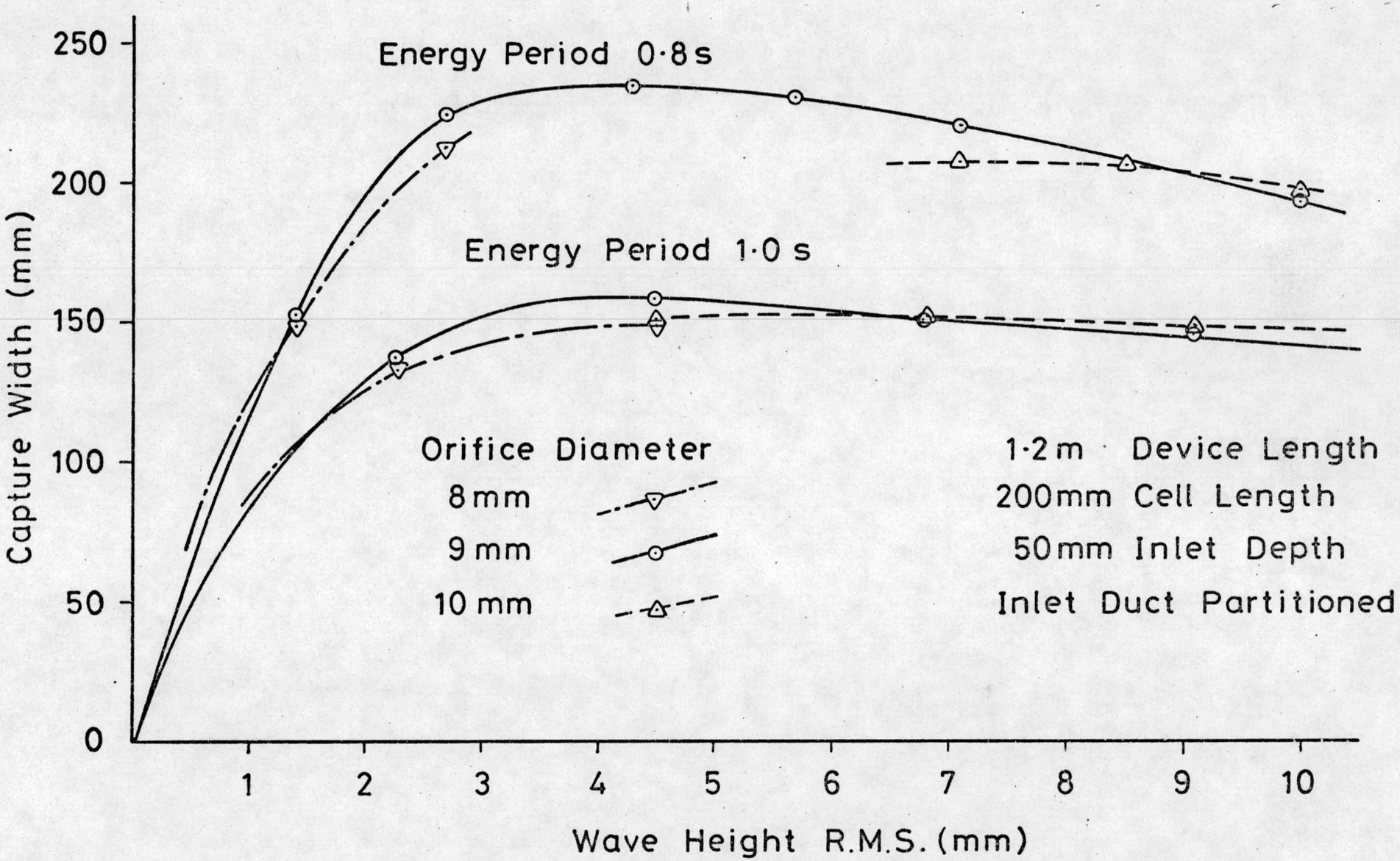

FIG 4.15

(a) Submerged Wave Chamber. Effect of Duct Taper on Frequency Response.

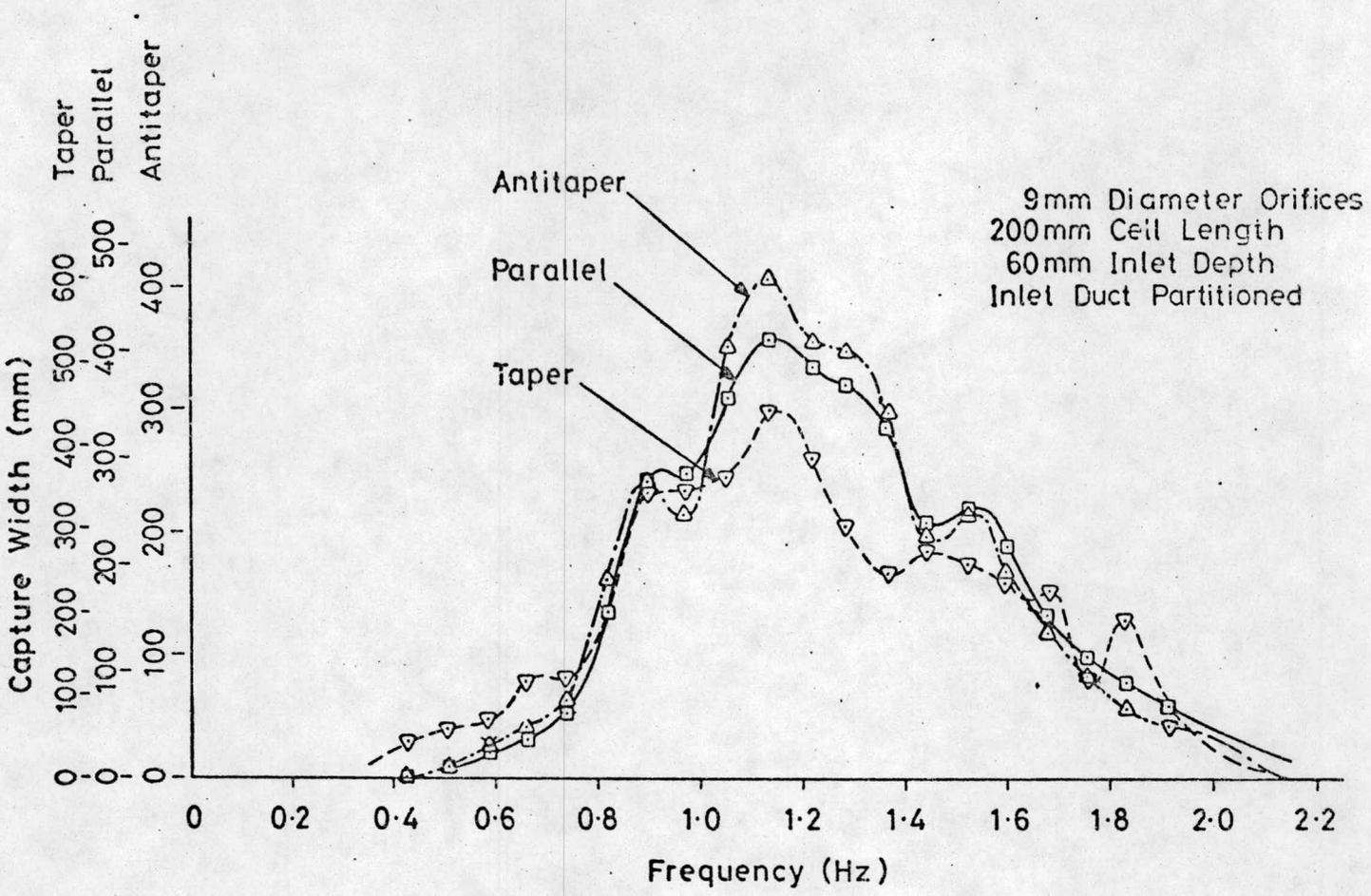

(b) Submerged Wave Chamber.
Effect of Duct Taper on Capture Width in Mixed Seas.

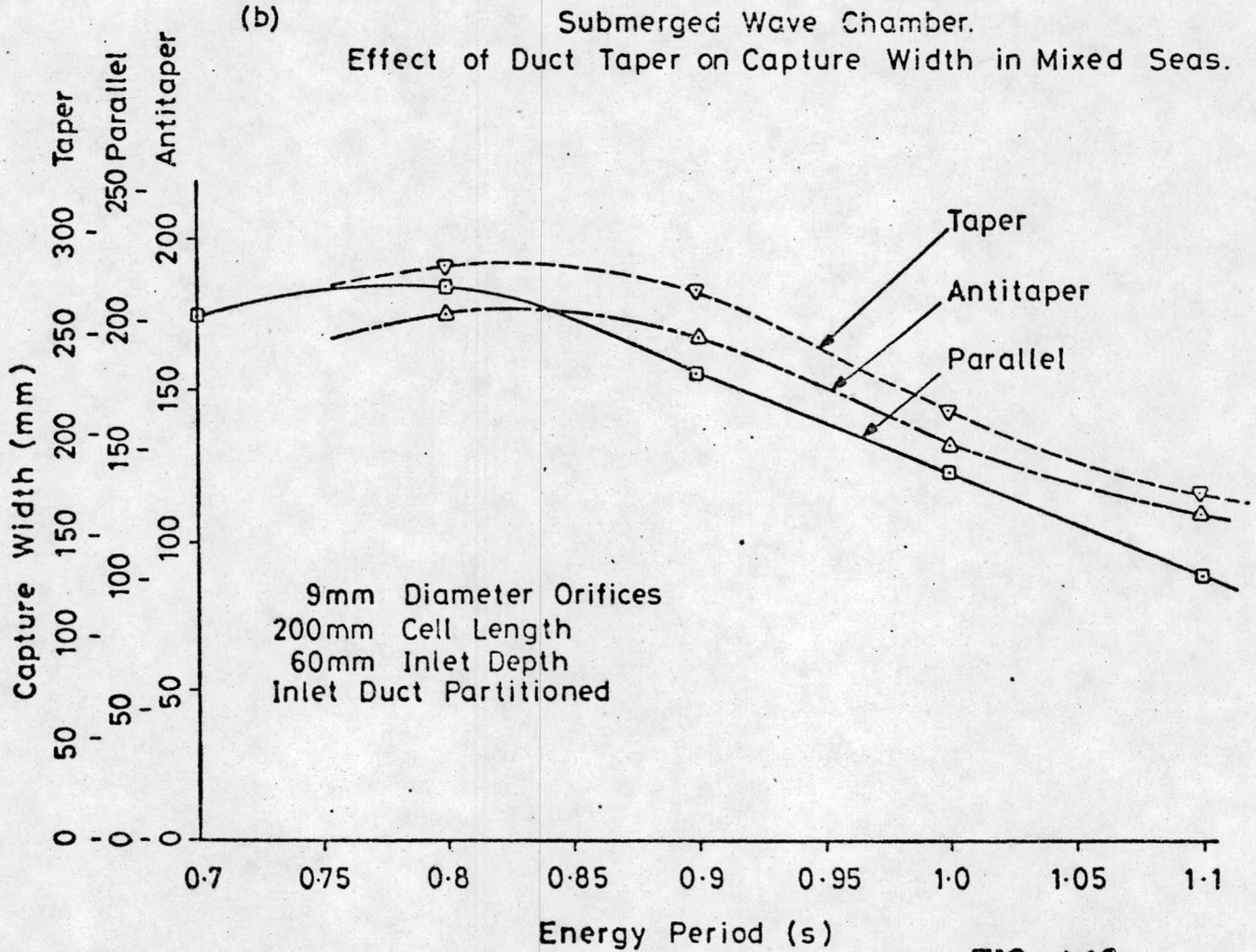

FIG 4.16

Submerged Wave Chamber. Distribution of Capture Width Between Cells.

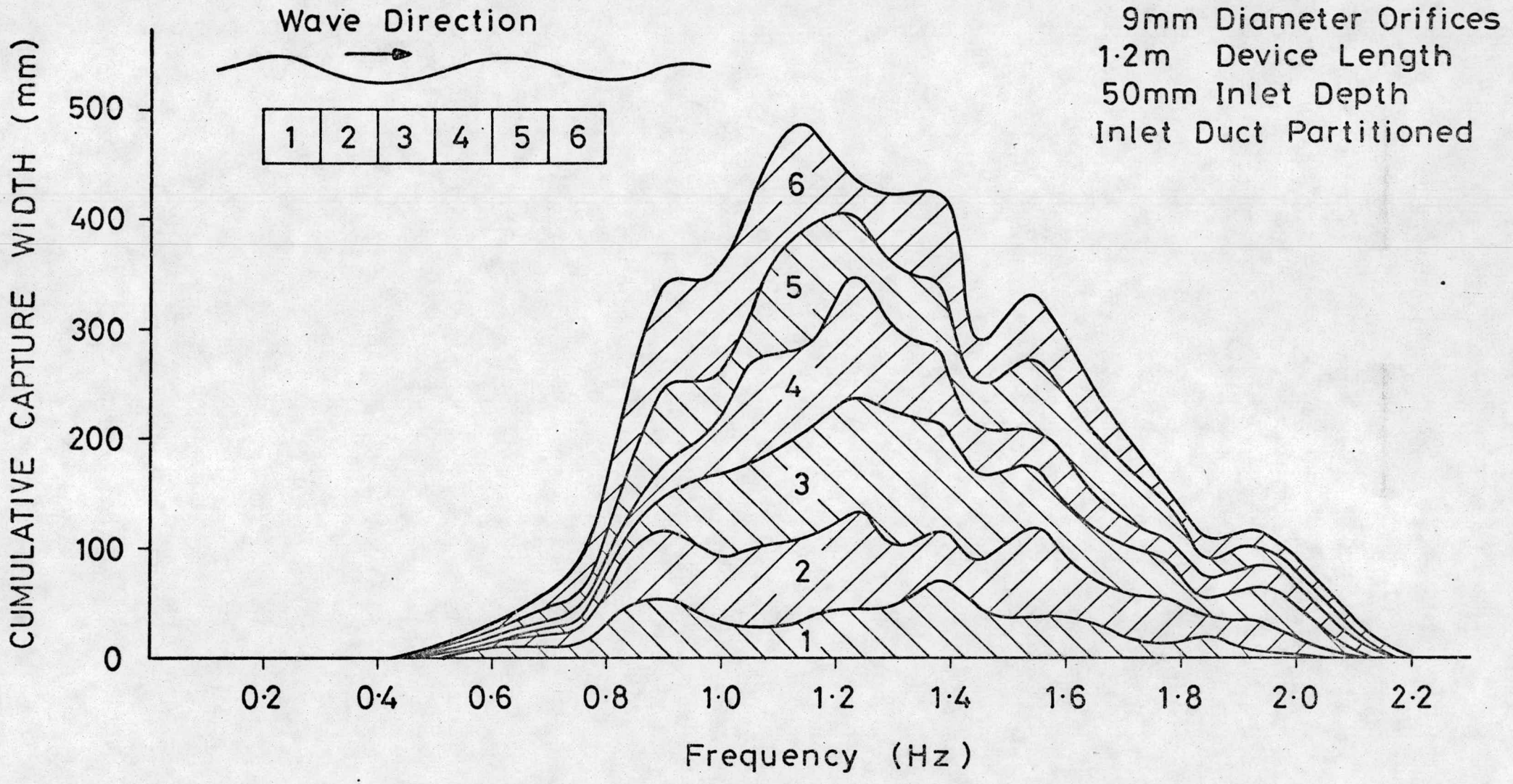

FIG 4.17

Submerged Wave Chamber.
Variation of Orifice Pressure
Drop Between Cells - Mixed Seas.

9mm Diameter Orifices. 50mm Inlet Depth.
1·2m Device Length. Inlet Duct Partitioned.

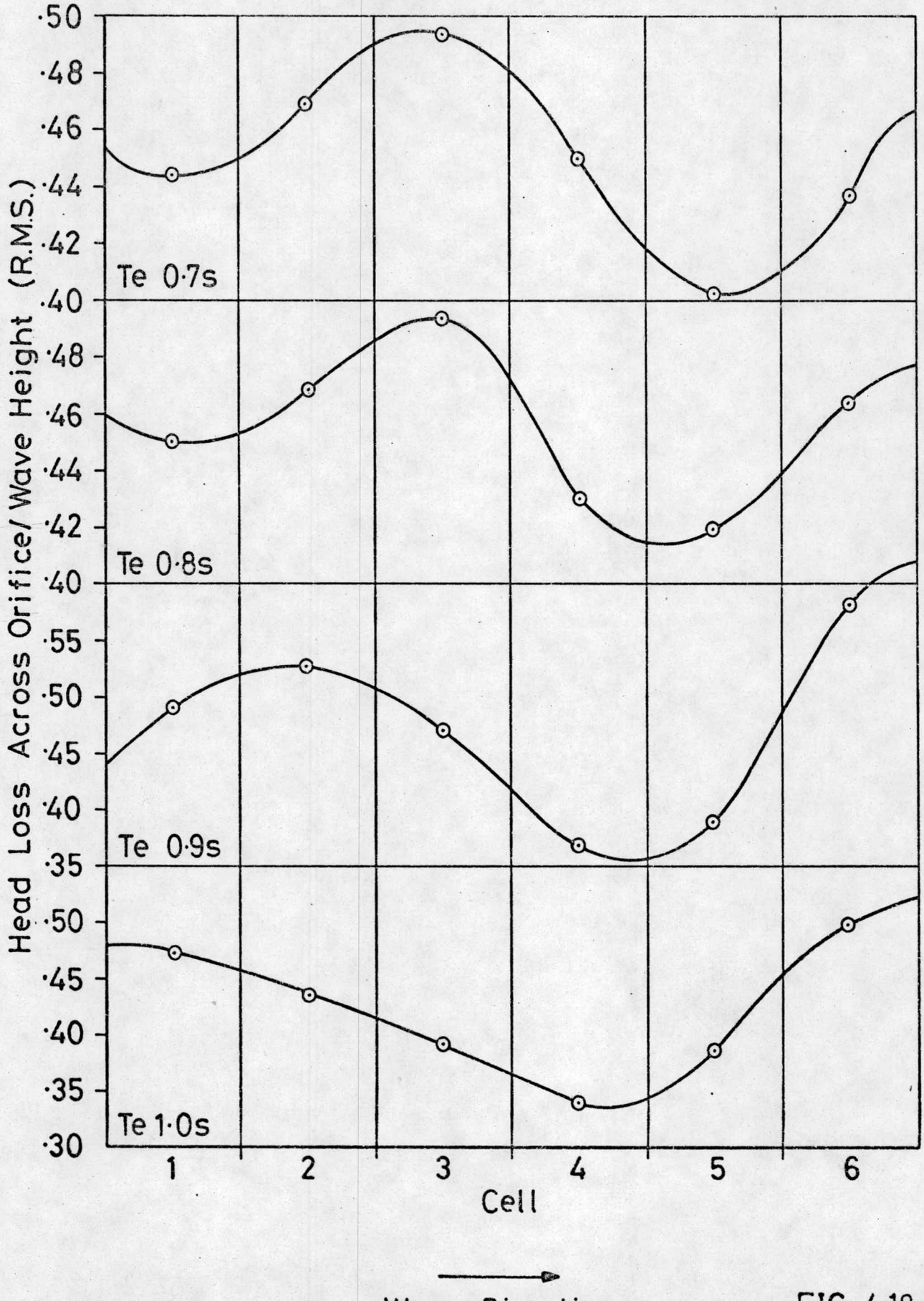

FIG 4·18

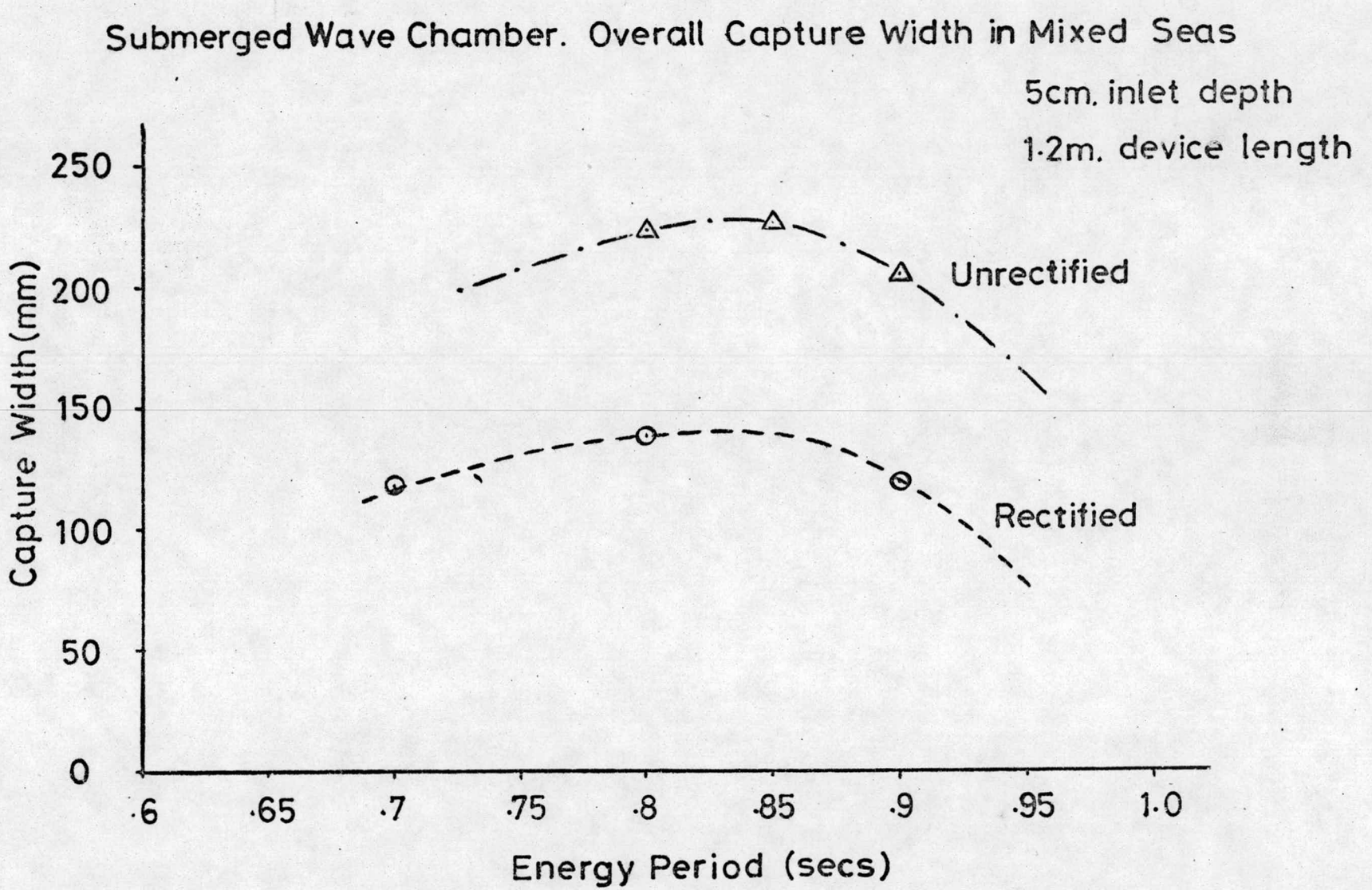
Submerged Wave Chamber. Overall Capture Width in Mixed Seas
5cm. inlet depth
1·2m. device length
Capture Width (mm)
250
200
150
100
50
0
Unrectified
Rectified
·6
·65
·7
·75
·8
·85
·9
·95
1·0
Energy Period (secs)

FIG 4·19

(a)

Submerged Wave Chamber.
Projected Frequency Response Curves of Devices 100, 120 & 150 x Model Scale
(Inlet Depth 6m) Compared With Typical Sea Spectra

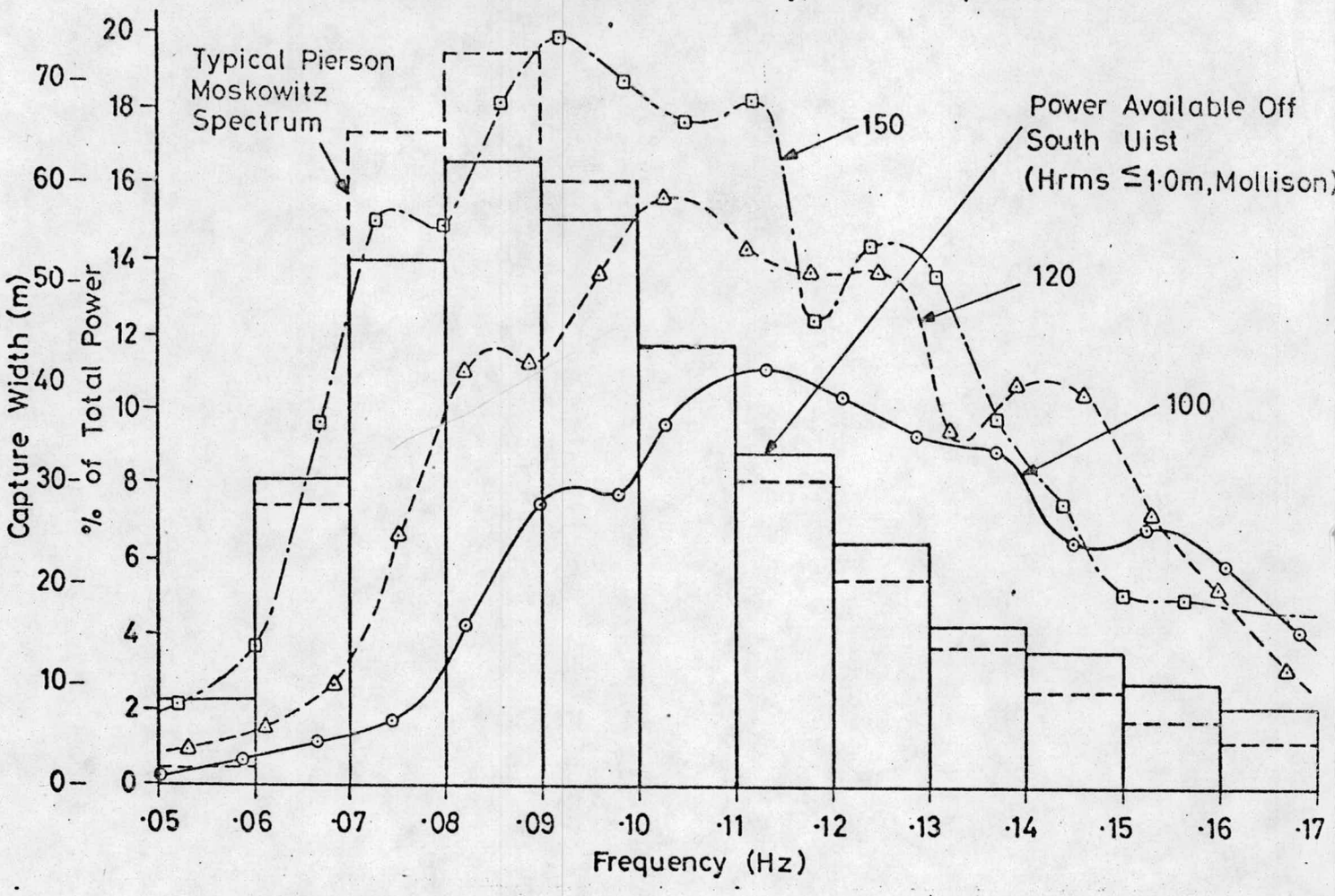

(b)

Product of Capture Width and Wave Power Distribution.

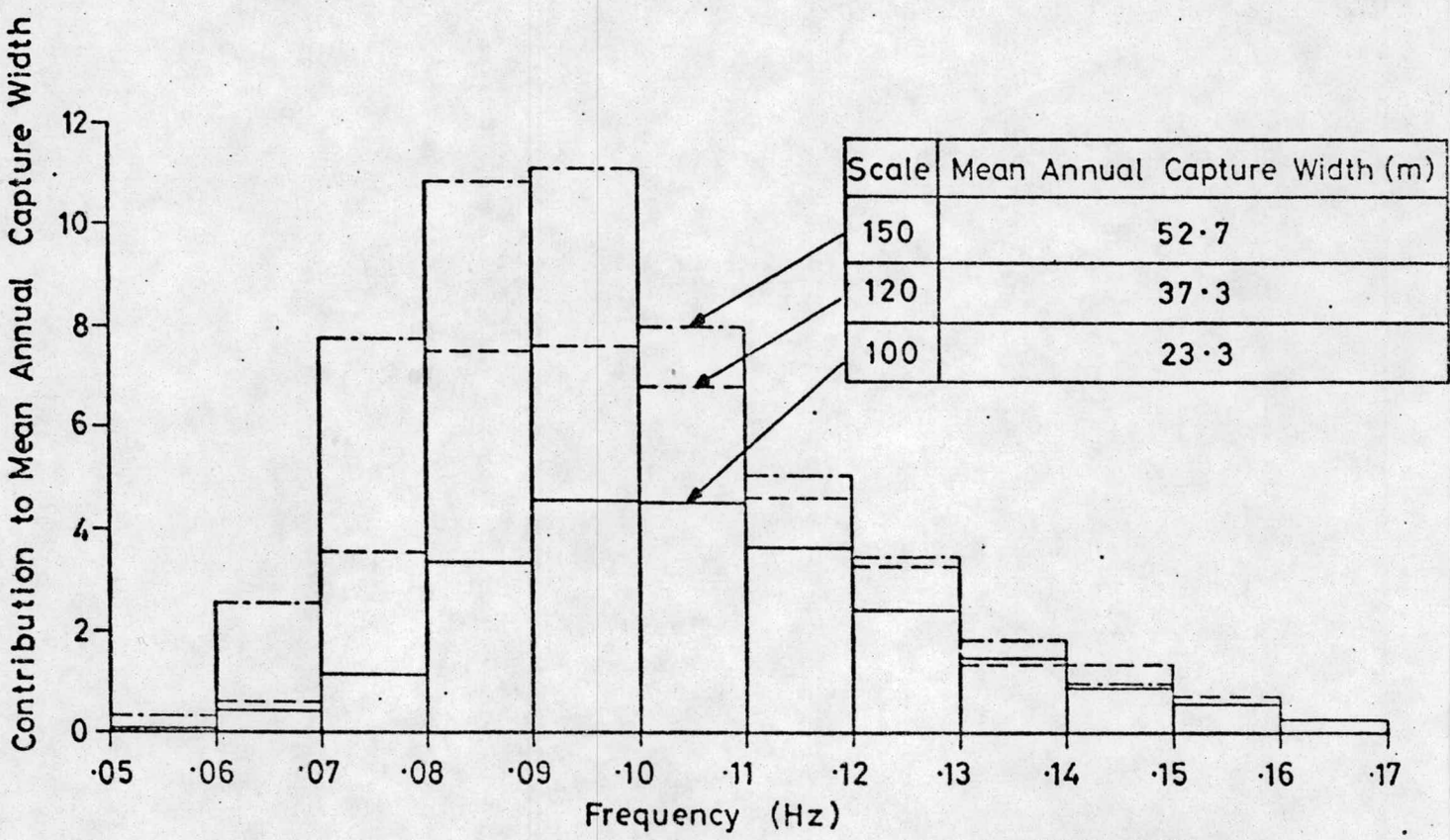

Scale	Mean Annual Capture Width (m)
150	52·7
120	37·3
100	23·3

FIG 4.20

Submerged Wave Chamber.
Effect of Device Scale on Mean Annual Capture Width and the Cost Implications.

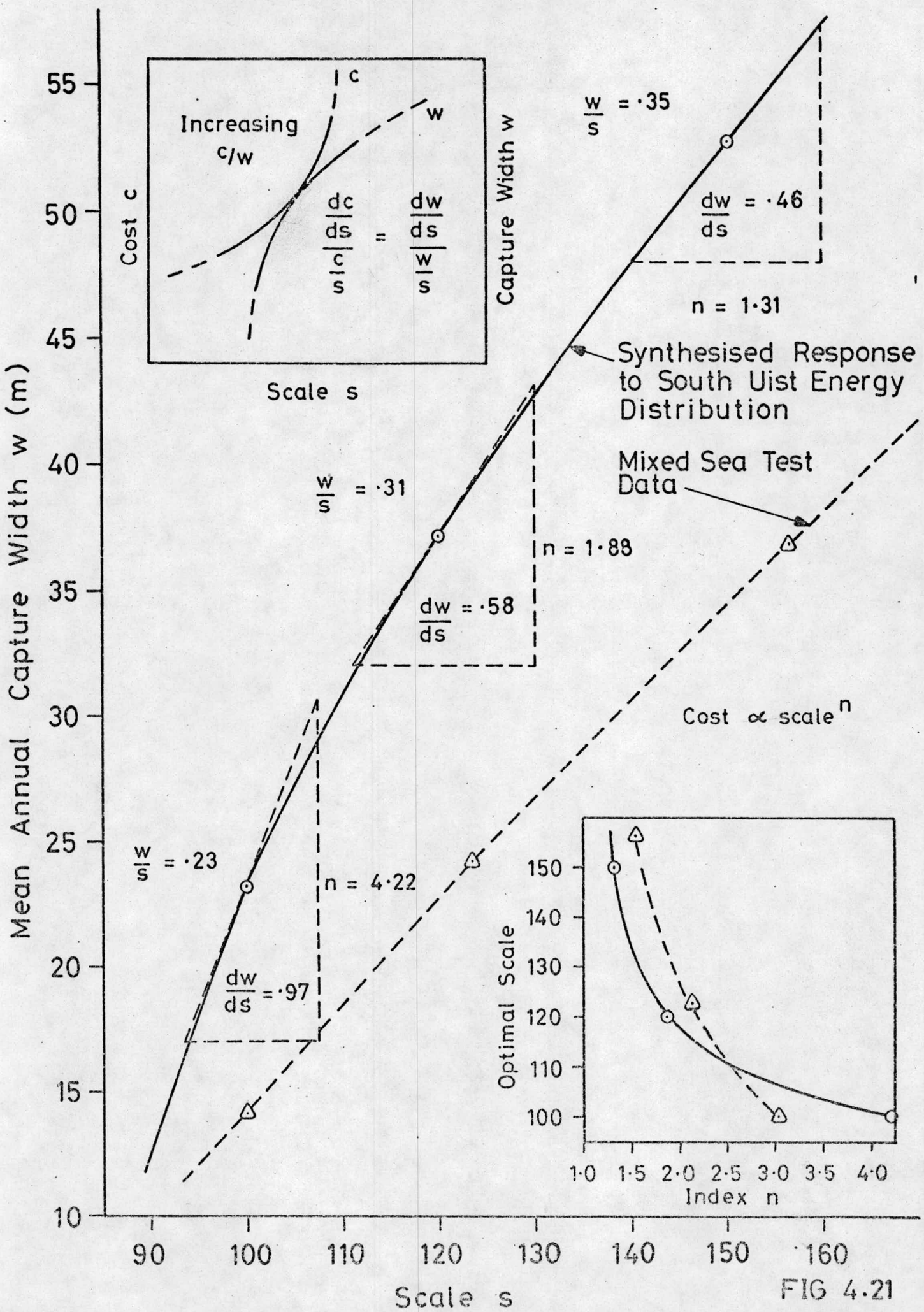

FIG 4.21

Effect of Device Capacity on Utilisable Energy Available.

(Based on Total Energy Available Off South Uist
March 1976 – February 1978, Miller & Hogben)

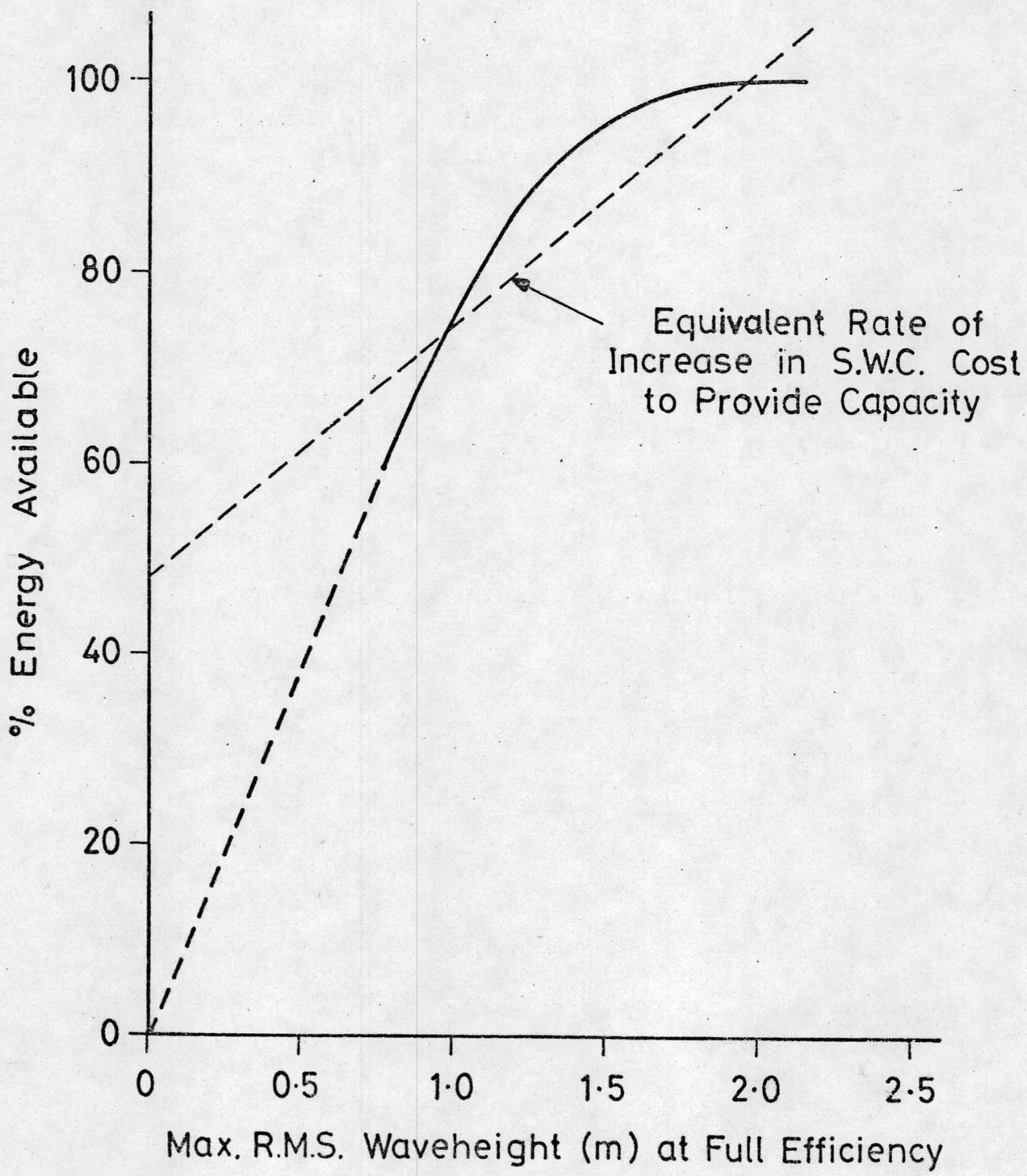

FIG 4.22

5.0 THEORETICAL ANALYSIS

In 1978 Sir James Lighthill [1] published an anlysis of a two-dimensional submerged resonant duct. The initial comparison with our 'point absorber' type device although predicting the general trends, did not give very good agreement with the depth experiments. However, with later tests with a 'terminator' type device the general agreement is better and this is also true for our 'attenuator' type device. The theoretical prediction of no change in the resonant frequency with depth is born out by the experimental data for these models. Further comparison with these devices is made in the experimental section.

For some time M. Simon [2] has been investigating theoretically a three-dimensional symmetrical oscillating water column, with an upward facing inlet duct. The main assumptions being infinite sea depth and monochromatic seas. Several important points have emerged to give guidelines for a symmetrical wave power device based on the oscillating water column concept.

From [2] defining the energy radiation in new waves as

$$Ew = \frac{1}{4} \rho \, wKDr|Q|^2$$

where

K = wave number = $2\pi/\lambda$
λ = wave length
w = wave frequency
Dr = radiation damping coefficient
Q = flow in the duct

5.0 THEORETICAL ANALYSIS (CONTINUED)

With a linear energy extraction system, the energy extraction rate can be written as

$$Ee = \frac{1}{4} \rho w K De|Q|^2$$

where

De = extraction damping coefficient.

Defining C_W as the capture width of the duct $KC_W = 1$ only at the resonant condition and when $E_W = Ee$. Then $C_W = \lambda/2\pi$ the theoretical maximum. Setting the aspect ratio h/r (where h = duct inlet depth, r = duct radius) and $\mu = 2\pi r/\lambda$, then

$$\frac{f(Z)}{\mu_o} - \frac{1}{r} \int_o^Z f(s)ds = l(\mu o)$$

where $\mu_o = \mu$ at resonance

$\hat{rl}\ (\mu_o)$ = the added length at $\mu = \mu_o$

f(s) = a function describing taper f(s) = A(o)/A(s)

A(o) = duct inlet area

A(s) = duct area at distance s from inlet

Z = the length of the water column

For the untapered case the above equation simply becomes

$$\hat{rl}\ (\mu_o) = \lambda/2\pi - Z$$

The energy extraction properties will only depend on A(o)/A(s) provided the taper is smooth, i.e. there is no abrupt change in area.

5.0 Theoretical Analysis (continued)

If the taper function f(z) is fixed then

$$K.Cw = \frac{Dr(\mu_o)\,Dr(\mu)}{1/4[Dr(\mu_o)+Dr(\mu)]^2+(f(z)/\mu_o-\hat{1}(\mu_o)+\hat{1}(\mu)-f(z)/\mu)^2/\pi^2\mu^2}$$

This assumes $De(\mu) = De(\mu_o)$

For the 'optimum' design, the second term in the denominator should be as small as possible over as wide a frequency band as possible. This implies that the modified length $f(z)/\mu - \hat{1}(\mu)$ should change as little as possible over the frequency range.

Figure 5.1 shows the modification to water column length as a function of μ for various inlet duct depths and with a fixed duct diameter. From this figure, it is clear that there is an optimum depth for the above condition and that above or below this depth the modified length varies more rapidly. The optimum occurs because the added length has a negative portion below a certain aspect ratio. This was also predicted with the two dimensional analysis. This optimum variation in modified length occurs at $h/r \triangleq 0.4$, and taking the middle of the range $\mu = 0.75$. For a tuned wavelength of $\lambda = 100$m this gives an inlet depth of 4.8m and for $\lambda = 120$m an inlet depth of 6m. It is very interesting that there seems to be a significant change in the added length (and therefore modified length) going from a two dimensional to a three dimensional analysis.

5.0 Theoretical Analysis (continued)

Figure 5.2 is a plot of modified length for a straight duct and for a duct with anti-taper where A(Z) = 1.25A(o). There is a further reduction in the change in modified length across the bandwidth, and this is reflected by a slight increase in bandwidth. For the scale model devices the anti-taper can be increased so that A(Z)≏2A(o), and this should give a significant improvement in bandwidth if the theoretical trend continues for larger area ratios.

Figure 5.3 shows how the theoretical bandwidth varies with inlet depth for $\mu_o = 0.8$ and indicates how the modified length affects the bandwidth. The implication is that it would be very difficult to design a device that has good bandwidth and also a large duct inlet depth without having a very large device.

Figure 5.4 is a comparison of the theoretical (half power) bandwidth ratio (the bandwidth at depth h/maximum bandwidth) with experimental values for the T.O.W.C.and the S.W.C. The main reason for the discrepancy is probably due to the non axi-symmetric nature of the devices, (they are somewhere between two dimensional and three dimensional in their behaviour). There will be a finite depth effect, and also the T.O.W.C. has a significant change in resonant frequency with depth.

As mentioned previously it has been assumed that De has some fixed value over the frequency range.

5.0 Theoretical Analysis (continued)

Examining the expression $\frac{(De + Dr)^2}{4DeDr}$

for De/Dr from 0.5 to 5 the expression only varies from 1.125 to 1.8 Simon [2] has shown that Dr only varies by approximately a factor of 2 over the range of interest. It thus depends mainly on how De varies for the chosen method of power extraction. We have chosen the Wells turbine and we have insufficient information to evaluate De at present. The two-dimensional analysis [1] gives similar values for the radiation damping coefficient Dr over the range of interest.

Effect of Depth on Modified Length

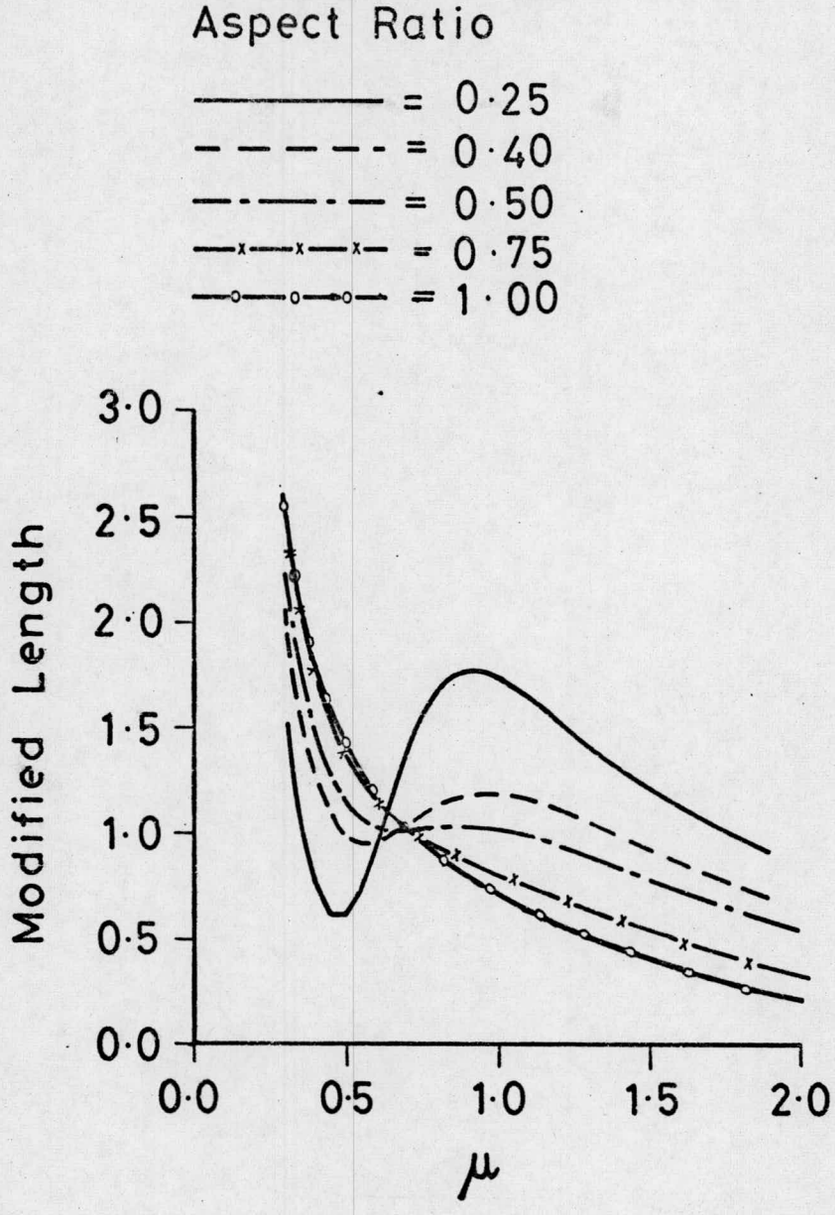

FIG. 5.1.

Effect of Taper on Modified Length

Aspect Ratio = 0·4

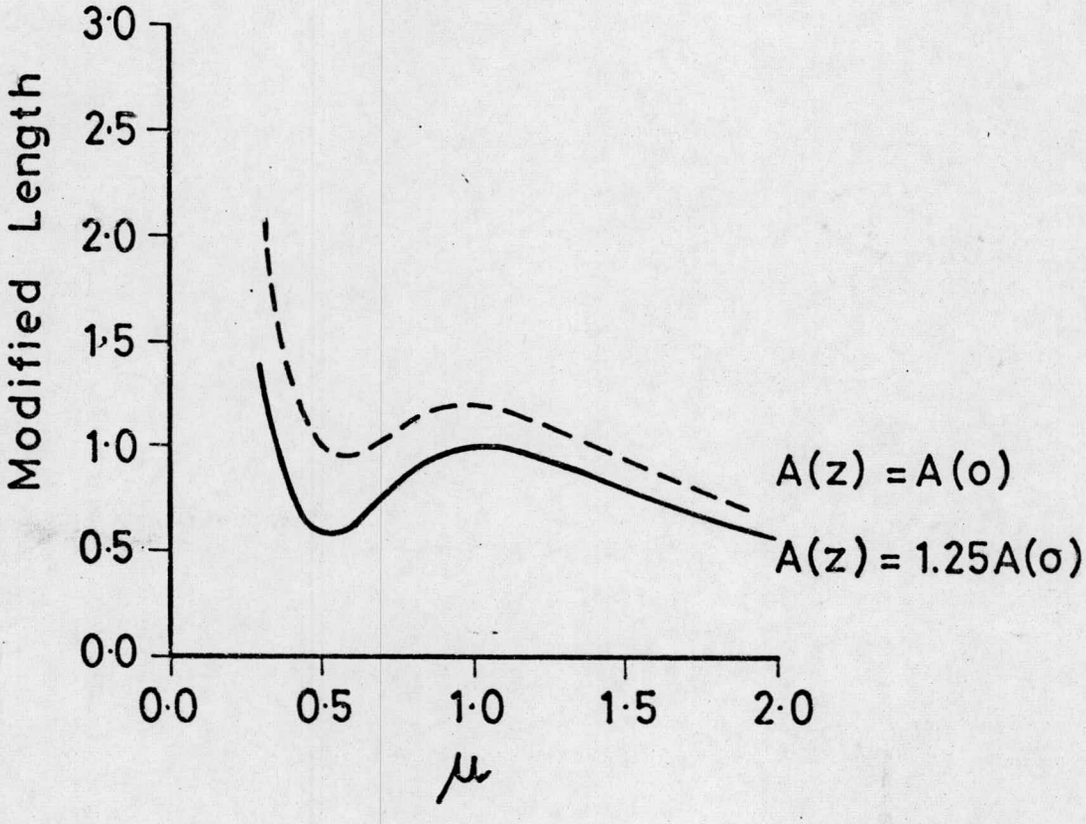

FIG. 5.2.

Effect of Depth on Band Width

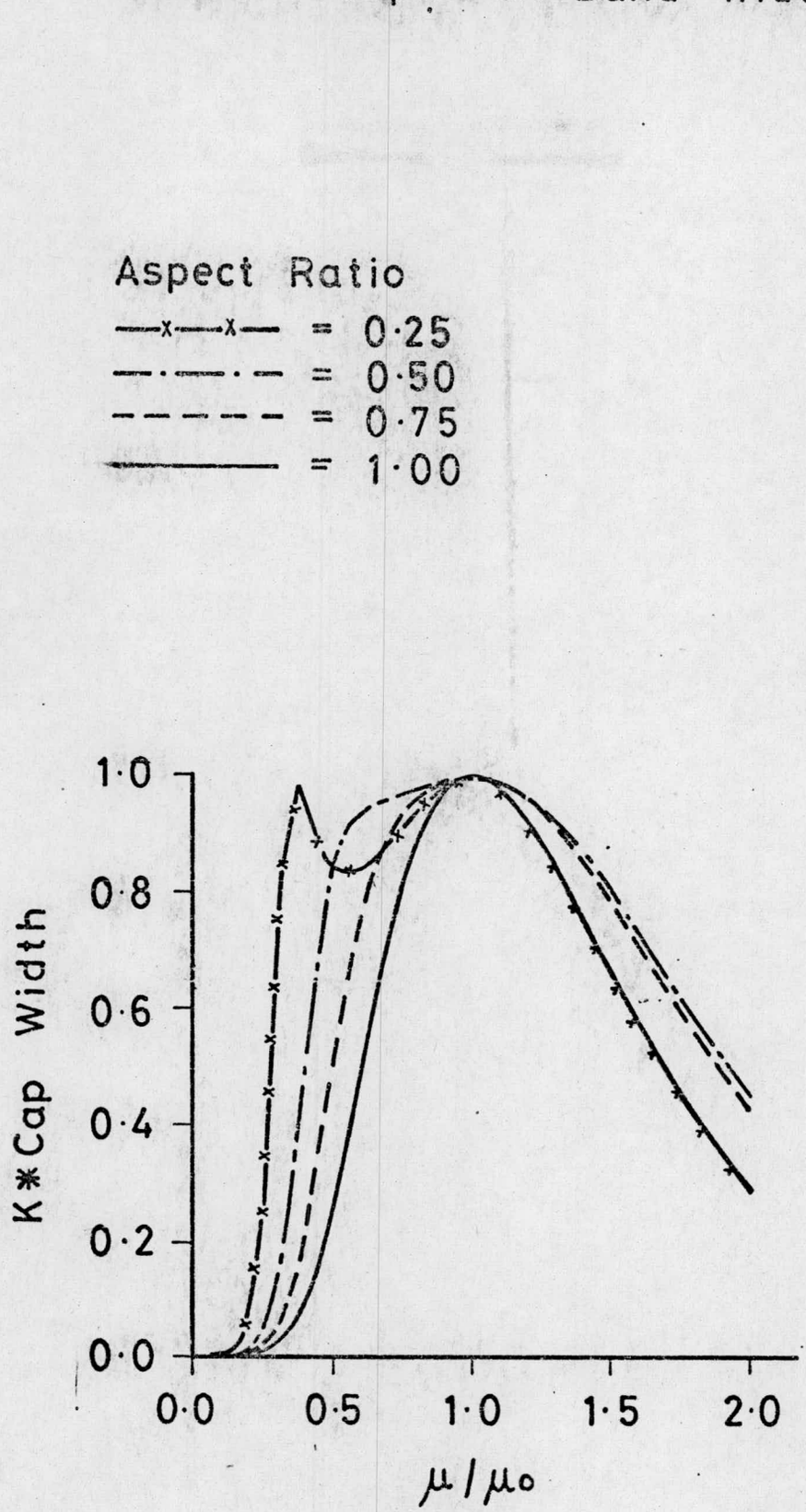

FIG. 5.3.

Band Width Ratio Versus Inlet Depth For Fixed Duct Dimensions

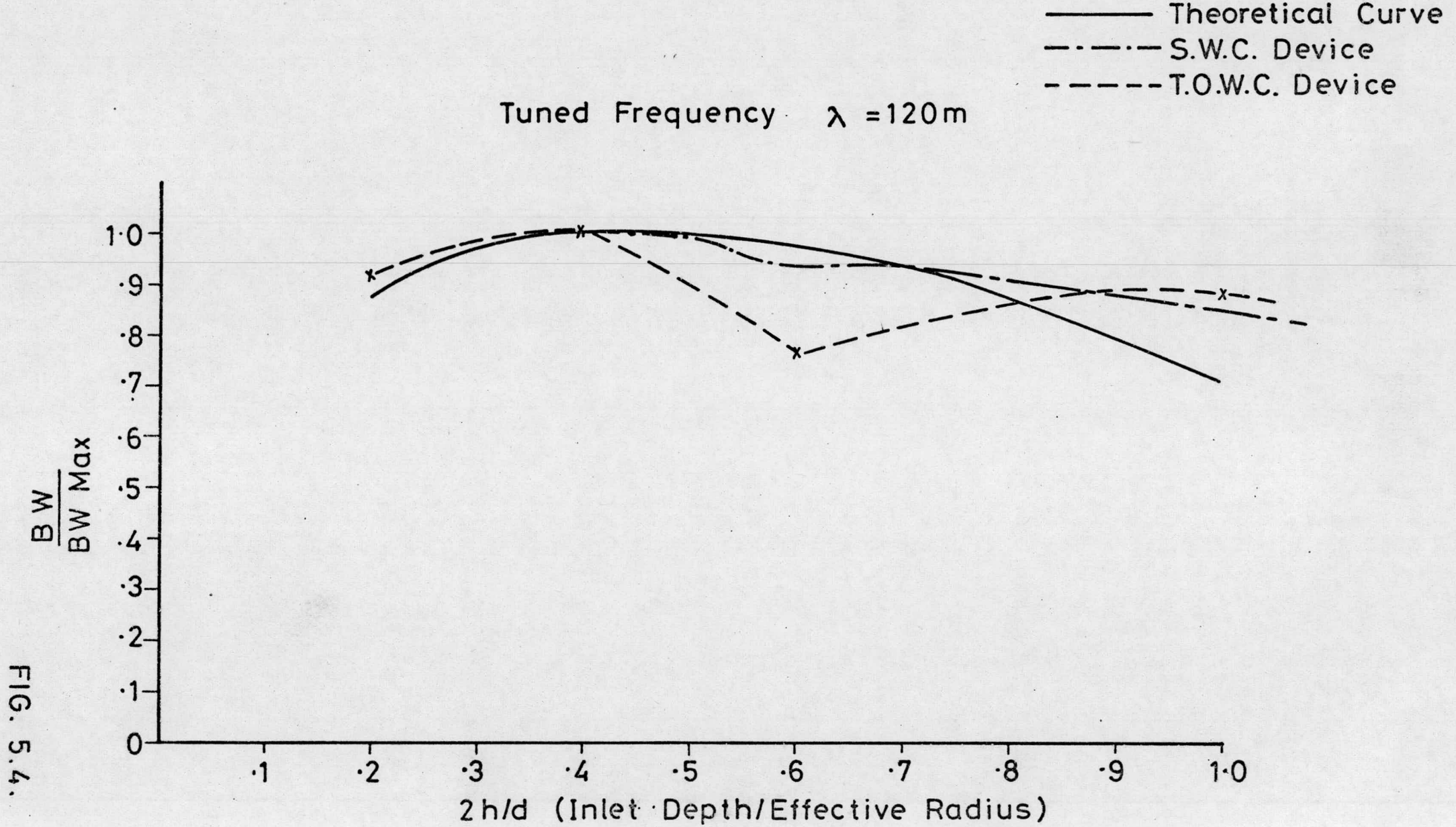

FIG. 5.4.

6. FORCES ON DEVICES

The forces on all the devices have been determined for the 100 year storm wave which has a period of 16 seconds and whose height is limited to the maximum unbreaking wave inshore or 32 metres offshore.

The forces acting on a submerged device, which give resultant horizontal and vertical forces are inertia, drag and buoyancy.

Once a device breaks the surface of the water additional forces due to slamming and surge are imposed.

The resultant vertical and horizontal components of the inertia and drag force were computed using Morrison Equations. The inertia is a function of the water particle acceleration and the drag force is dependent on the square of the particle velocity.

Both these terms are variable and dependent on the position of the wave crest relative to the point being considered and its vertical position from the sea bed.

When the dimension of the device perpendicular to the wave crest is less than 15% of the wave length, the pessimistic assumption was made that the water particle velocity and acceleration are constant across the device. When longer devices were being assessed, such variations were considered. In all cases the variation with respect to wave height was taken into account.

6 FORCES ON DEVICES (Continued)

The buoyancy force was taken as a fluxional force when the device breaks the surface of the water.

The slamming force was only considered when a rising water level passed an increasing horizontal cross-section.

The surge force was found to exist experimental when the top of the device approached the surface of the water.

6.1 ORIGINAL VICKERS DEVICE

A detailed investigation has been carried out on this device. The paper "Wave Pressure on Vertical Circular Cylindrical Obstacles" by D.D. Lappo and V.V. Kaplin[6] gives the horizontal pressure distribution around the device in four terms, T_1, T_2, T_3, and T_4.

These terms being positive for pressures acting towards the centre of the cylinder.

$T_1 = \gamma z$ and is the static pressure in still water

$$T_2 = \frac{\gamma h}{2} \frac{\cosh k(H-z)}{\cosh kH} \cos \sigma t$$

is the pressure due to the height of the wave.

$$T_3 = \gamma d k K_v \frac{h}{2} \frac{\cosh k(H-Z)}{\cosh kH} \sin \sigma t \cos \theta$$

and is the pressure due to the inertia forces.

$$T4 = -\frac{\gamma h^2 k K_v^2}{4} \frac{\cosh^2 k(H-Z}{\sinh 2kH} [3 \sin^2 \theta \cos \sigma t - \cos \theta | \cos \theta \cos \sigma t |] \cos \sigma t$$

and is the pressure due to the drag force.

6.1 ORIGINAL VICKERS DEVICE (Continued)

These terms were integrated around and over the height of the device to achieve the resultant horizontal forces.

Terms T_1 and T_2 give no resultant force.

Term T_3 gives a net horizontal force F_3^1 per unit length and a total force of F_3.

$$F_3^1 = -\frac{\gamma\pi d^2 k K_V h}{4} \frac{\cosh k(H-Z)}{\cosh kH} \sin\sigma t \text{ per unit length}$$

$$F_3 = -\frac{\gamma\pi d^2}{4} K_V h \frac{\sinh kb}{\cosh kH} \sin\sigma t$$ as the device sits on the sea bed.

This conforms with the inertia term in Morrisons Equation if K_V (velocity correction factor) is replaced by Cm/2.

Term T_4 gives a net horizontal force F_4^1 per unit height and a total force F_4.

$$F_4^1 = \frac{\gamma d h^2}{3} k K_V^2 \frac{\cosh^2 k(H-Z)}{\sinh 2kH} \cos\sigma t|\cos\sigma t| \text{ per unit height}$$

$$F_4 = \frac{\gamma d h^2}{12} K_V^2 \frac{(2kb + \sinh 2kb)}{\sinh 2kH} \cos\sigma t|\cos\sigma t|$$

This conforms with the drag term in Morrisons Equation if K_V^2 is replaced by $3 \times C_D/4$.

There is an air/water interface in the device. Where there is water on the inside of the shell, T_1 becomes zero. The air in the device will modify T_1 to $\gamma Z - P_A$, where P_A is the air pressure.

6.1 ORIGINAL VICKERS DEVICE (Continued)

Term T_1 is constant pressure load and will give a circumferential tension in the ring of P_1

$$P_1 = -(\gamma z - P_A)\frac{d}{2} \quad / \text{ unit length}$$

Term T_2 is constant pressure load around the device at a particular position of the wave and will give a circumferential tension P_2.

$$P_2 = -\gamma \frac{d\ h}{4} \frac{\cosh k\ (H-Z)}{\cosh k\ H} \cos \sigma t \ / \text{ unit length}$$

Term T_3 is a varying pressure load around the device and the horizontal force will be reacted by a circumferential shear load within the shell. The result will not cause any bending or radial shear load in the ring but a circumferential tension P_3.

$$P_3 = -\gamma K_V \frac{d^2}{4} h\ k \frac{\cosh k\ (H-Z)}{\cosh k\ H} \cos\theta \sin \sigma t / \text{unit length}$$

$$= + \frac{1}{\pi} F_3^1 \cos\theta \sin \sigma t / \text{ unit length}$$

Term T_4 is a varying pressure load around the device and the horizontal force will again be reacted by circumferential shear load within the shell. This will result in bending, radial shear and circumferential tension.

6.1 ORIGINAL VICKERS DEVICE (Continued)

Using Morrison's Equation the vertical inertia and drag forces are:

$$F_{3v} = - \frac{\gamma \pi d^2}{4} \frac{Cm}{2} h \frac{(\cosh kb - 1)}{\cosh kH} \cos \sigma t$$

$$F_{4v} = \frac{\gamma \pi d^2}{16} h^2 k C_D \frac{\sin^2 kb}{\sinh 2kH} \sin \sigma t |\sin \sigma t| \text{ per unit height.}$$

After investigating several variations of the submerged duct design, a device 16m high and 29m diameter was decided upon as the best compromise for the currently available information.

The operating sea depth of the device is 23m. The considered maximum wave has a period of 16 seconds and length of 225m from

$$\lambda = \frac{gT^2}{2\pi} \tanh\left(\frac{2\pi H}{\lambda}\right)$$

The maximum wave height of 18.1m, associated with the wave length was determined by

$$h = 0.142 \lambda \tanh\left(\frac{2\pi H}{\lambda}\right)$$

These were the criteria used for the design of the device.

6.1 ORIGINAL VICKERS DEVICE (Continued)

The loading in the vertical walls was computed for increments of wave position of 5^{o} and around the device of 5^{o} and the maximum and minimum tensile and compressive load in each wall together with maximum shear load between them, (all per unit length) were tabulated (See Appendix I) at 1 metre spacing down the device. Also in Appendix I is the maximum horizontal inertia and drag forces.

Each wall was considered to be pre-stressed during construction to take account of the tensile load. Both walls are 0.6m thick concrete.

To assess the quantity of circumferential pre-stressed steel the average tensile load was determined, in the outer ring 1.24MN/m, inner ring 1.48MN/m. Allowing the pre-stressing steel to be set up at 170MN/m, the average content in each wall is $0.0073m^2/m$ (1.22% by volume) in the outer wall and $0.0087m^2/m$ (1.45% by volume) in the inner wall.

Combining the compressive with the pre-stressing loading, the maximum compressive loading in the concrete is 2.14MN/m in the outer wall and 2.325MN/m in the inner wall, giving maximum compressive stresses in the concrete of $3.57MN/m^2$ and $3.88MN/m^2$ respectively.

The top surface will be subjected to a pressure difference of 16m of water ($0.157MN/m^2$). The area between the walls was considered to be a flat plate 0.6m thick, 28.4m O/D and 21.6m I/D with both ends supported and fixed. The maximum radial stress occurs at the inner edge and is equal to $1.63MN/m^2$.

6.1 ORIGINAL VICKERS DEVICE (Continued)

To remove the tensile stresses, the surface of the concrete will be pre-stressed to the above value, which will require 1.55% of steel by volume working at 170MN/m^2.

The curved top surface has a similar thickness of concrete as the flat section. As its shape and the smaller diameter will reduce the loading, only 1/3 of the concentration of pre-stressing steel will be required.

The total pressure loading on the top surface will be 70MN. The weight of the structure within the inner wall is 15MN. The combined horizontal cross-section of the two walls is 94.25m^2, which gives an average tensile stress in the concrete of 0.58MN/m^2, which would require vertical pre-stressing steel of 0.34% at the top, reducing to 0.17% at the bottom. By grading the pre-stressing steel down the device, the average will be 0.26%.

Combining the circumferential and vertical pre-stressing steel gives an average content for the two walls of 1.5% by volume (155 tonne). vol 1316 m^3

The flat top surface has a volume of 188m^3 of concrete and 2.9m^3 (22.9 tonne) of pre-stressing steel. The curved top surface is 135m^3 of concrete 0.7m^2 (5.5 tonne) of pre-stressing steel.

6.1 ORIGINAL VICKERS DEVICE (Continued)

Total pre-stressing steel in vertical walls and top surfaces is 184 tonne. The remaining 46 tonne is an allowance made for use in the anchor attachment area.

The remaining concrete, 3300m^3, including attachment area, has not been the subject of detail analysis, but is generally considered to be lightly loaded, so an allowance of 1% reinforcing steel has been taken (260 tonne).

The power modules will be fabricated from steel. The generator and control equipment compartment of the modules will be pressurised to apprcximately 17 metres of water, before the device is placed on site, to ensure minimal loading during operation. They have been designed to withstand this pressure while dry.

No investigations have been carried out into the effects of the discontinuity of the ring force caused by the power modules.

6.1 ORIGINAL VICKERS DEVICE (Continued)

APPENDIX I

VICKERS WAVE POWER DEVICE

Loading in vertical walls due to horizontal wave forces (Static and wave height pressure, internal pressure, inertia forces and drag forces).

Water level in device from base		7.0 metres
Diameter of device		29.0 metres
Height of Device		16.0 metres
Boom separation		3.5 metres
Velocity correction		1
Wave period		16.0 seconds
Depth of water		23.0 metres
Wave length		225.8 metres
Wave height		18.1 metres
Maximum vertical inertia force	=	9.75MN
Maximum vertical drag force	=	2.51MN
Maximum horizontal inertia force	=	44.52MN
Maximum horizontal drag force	=	8.91MN

6.1 ORIGINAL VICKERS DEVICE (Continued)

DISTANCE FROM TOP OF DEVICE = 0 METRES

OVER WHOLE WAVE CYCLE

Max Tens. Load in Outer Ring	=	1.5001MN/m
Max Comp. Load in Outer Ring	=	0.3988MN/m
Max Tens. Load in Inner Ring	=	1.8638MN/m
Max Comp. Load in Inner Ring	=	0.3236MN/m
Max Shear Load in Whole Ring	=	0.2480MN/m

DISTANCE FROM TOP OF DEVICE = 1 METRE

OVER WHOLE WAVE CYCLE

Max Tens. Load in Outer Ring	=	1.5429MN/m
Max Comp. Load in Outer Ring	=	0.4546MN/m
Max Tens. Load in Inner Ring	=	1.8933MN/m
Max Comp. Load in Inner Ring	=	0.3797MN/m
Max Shear Load in Whole Ring	=	0.2424MN/m

DISTANCE FROM TOP OF DEVICE = 2 METRES

OVER WHOLE WAVE CYCLE

Max Tens. Load in Outer Ring	=	1.6303MN/m
Max Comp. Load in Outer Ring	=	0.5115MN/m
Max Tens. Load in Inner Ring	=	1.8887MN/m
Max Comp. Load in Inner Ring	=	0.4369MN/m
Max Shear Load in Whole Ring	=	0.2373MN/m

ORDER FORM

TO:
Publications Sales Office
Building Research Establishment
Garston
Watford, WD2 7JR

Please send . . . . . copy/copies of the *BRE Microcomputer Package: Assessment of condensation risk in the envelope of a building* at £75 plus VAT.

Quote Reference AP15

Please note that this package is for a Hewlett Packard HP85, although it could be easily transferred to other machines.

I enclose payment of . . . . . (cheques payable to the Department of the Environment)

Name . . . . . .

Address . . . . . .

. . . . . .

. . . . . .

. . . . . .

. . . . . .

BUILDING RESEARCH ESTABLISHMENT
Department of the Environment

Microcomputer package for assessing condensation risk

BRE-CON

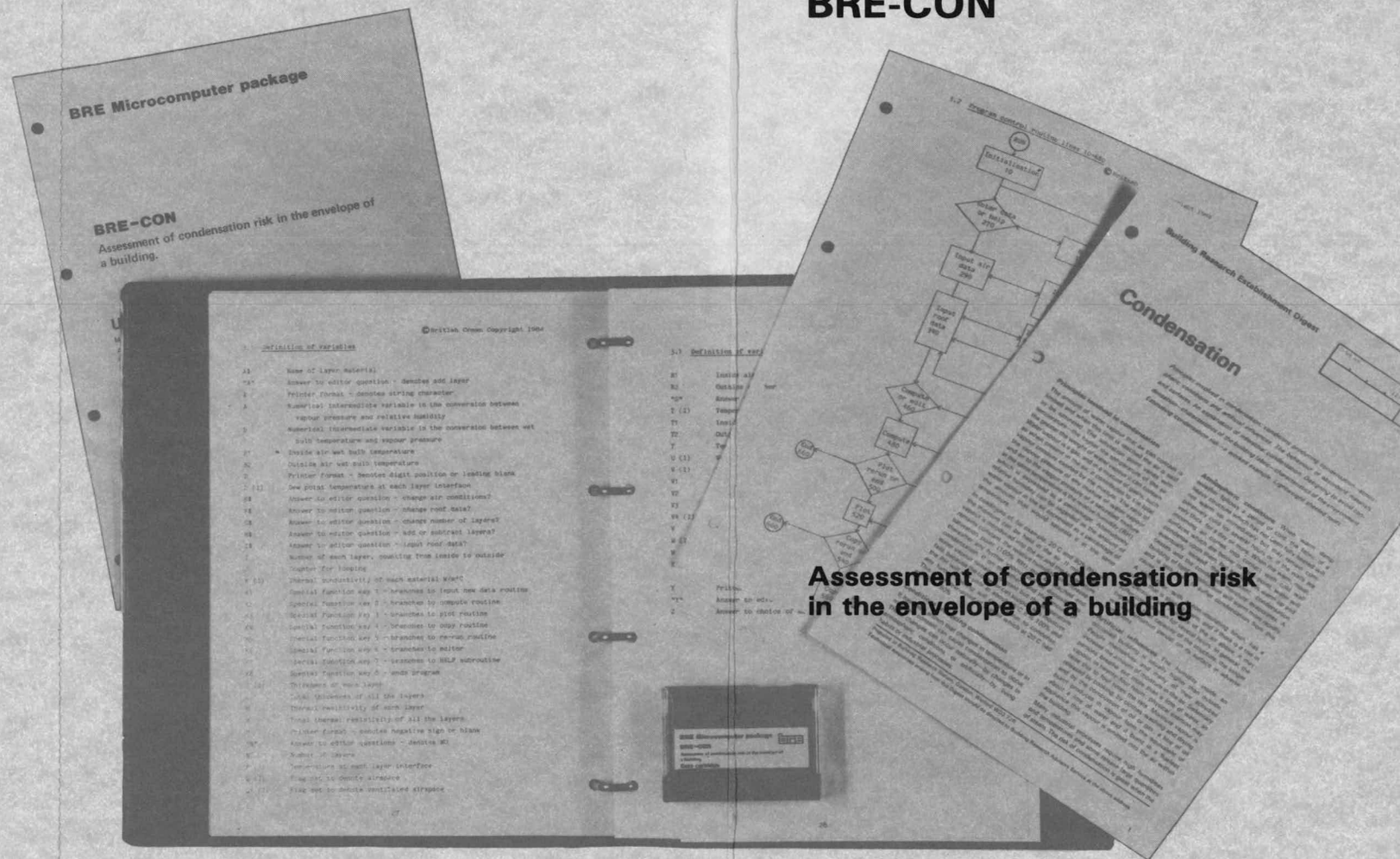

Assessment of condensation risk in the envelope of a building

BUILDING RESEARCH ESTABLISHMENT
Department of the Environment

The consideration of the risk of condensation occurring should form an early part of the building design procedure.

This BRE package is designed for architects, specifiers, builders and others concerned with the thermal performance of buildings, and can be applied to walls as well as flat roofs. The program allows the user to calculate:

(1) the U-value of the structure

(2) the temperature profile through the structure

(3) the vapour pressure profile through the structure

(4) the dew point profile through the structure and hence the risk of condensation at each point in the structure

This package includes

A user's guide making clear the assumptions and limitations of the program and presenting worked examples

A programmer's guide containing a description of the variables used, flow charts, and program listings, which is intended to aid the transfer of the program to other computers

A theory paper on the subject of condensation (Digest 110)

A programmed DC 100A tape

A data bank of thermal and vapour resistivities accessible by appropriate keywords published in the user's guide

Worked example No 2 from 'BRE—CON'

Example 2

Example 2

Thermal upgrading of cold plywood deck roof with leaking, but physically sound built-up roofing.

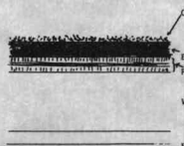

Scrape off chippings, add polyurethane insulation, built-up roofing and chippings, seal off air vents.

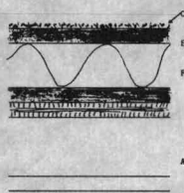

Then the calculations show that it may be necessary to control air humidity inside the building to reduce risk of condensation.

Worked example No 2

WORKED EXAMPLE No 2

USER ACTION		PRINT OUT
Keyboard	Reason	
Press RUN		ASSESSING THE RISK OF CONDENSATION IN A ROOF BY THE DEW POINT METHOD
Press CONT		
Press K1	Newdata	INPUT DATA
Type 2	Air temp + $ rh	TEMP V P R H
Type 20	Inside air temp	Tin = 20.0 Vin =15.3 RH =65.0%
Type 65	Inside air $ rh	Tout= 1.0 Vout= 5.9 RH =90.0%
Type 1	Outside air temp	
Type 90	Outside air $ rh	NO OF LAYERS = 5
Type 5	No of layers	
Type PLASTBRD	Layer 1 material	LAYER MATERIAL K V L
Type 13	Layer 1 thickness	1 PLASTBRD .159 45 13
Type AIRVENT	Layer 2 material	2 AIRVENT 5.556 0 250
Type 1	Air exchange rate	3 DOUGLPLY .143 2000 25
Type 250	Layer 2 thickness	4 BUR .189 60000 12
Type DOUGLPLY	Layer 3 material	5 CHIPPINS .500 20 10
Type 25	Layer 3 thickness	
Type BUR	Layer 4 material	AIRVENT EXCHANGE RATE = 1 per hour
Type 12	Layer 4 thickness	
Type CHIPPINS	Layer 5 material	SURFACE VAPOUR TEMP DEW POINT
Type 10	Layer 5 thickness	0 15.27 19.35 13.64
		1 15.26 18.86 13.63
Press K2	Compute	2 14.26 2.00 12.62 *
		3 13.72 1.49 12.04 *
		4 5.92 1.38 -.49
		5 5.92 1.24 -.50
		* = CONDENSATION LIKELY
		U-VALUE = .312382856429
		WARNING - U-VALUE NOT CORRECT VALUE AFFECTED BY AIRVENT LAYER

USER ACTION		PRINT OUT
Keyboard	Reason	
Press K3	Plot	
Press K4	Copy	

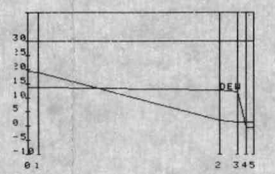

Worked example No 2 (continued)

WORKED EXAMPLE No 2 (Continued)

USER ACTION		PRINT OUT
Keyboard	Reason	
Press K5	Re-run	ROOM HAS NOW BEEN MADE FOR NEW LAYER 5
Press K6	Edit	N CHANGED TO 6
Type N	Not edit air data	ROOM HAS NOW BEEN MADE FOR NEW LAYER 6
Type Y	Edit roof data	N CHANGED TO 7
Type Y	Change No of layers	LAYER MATERIAL K V L
Type A	Add layer	2 AIR 5.556 0 250
Type 5	New layer 5 (Chippins becomes 6)	5 FOMPOLYU .020 150 25 6 BUR .189 60000 12
Type Y	Change No of layers	
Type A	Add layer	SURFACE VAPOUR TEMP DEW POINT
Type 6	New layer 6 (Chippins becomes 7)	0 15.27 18.95 13.64 1 15.27 18.16 13.63 2 15.27 16.44 13.63 3 14.95 14.76 13.32 4 10.44 14.15 7.96 5 10.41 2.18 7.93 * 6 5.90 1.57 -.55 7 5.90 1.38 -.55
Type N	Enough layers	
Type Y	Input data	* = CONDENSATION LIKELY
Type 2	Input layer 2	
Type AIR	Layer 2 material	U-VALUE = .504006854493
Type 250	Layer 2 thickness	
Type Y	Another layer	
Type 5	Input layer 5	
Type FOMPOLYU	Layer 5 material	
Type 25	Layer 5 thickness	
Type Y	Another layer	
Type 6	Input layer 6	TEMP V P R H Tin = 20.0 Vin = 9.4 RH =48.0% Tout= 1.0 Vout= 5.9 RH =90.0%
Type BUR	Layer 6 material	
Type 12	Layer 6 thickness	
Type N	Not another layer	SURFACE VAPOUR TEMP DEW POINT 0 9.40 18.95 6.39 1 9.39 18.16 6.39 2 9.39 16.44 6.39 3 9.28 14.76 6.21 4 7.59 14.15 3.22 5 7.58 2.18 3.20 * 6 5.90 1.57 -.55 7 5.90 1.38 -.55
Press K2	Compute	
Press K5	Re-run	* = CONDENSATION LIKELY
Press K6	Edit	
Type Y	Edit air data	U-VALUE = .504006854493
Type 2	Air temp + $ rh	
Type 20	Inside air temp	
Type 40	Inside air$ rh	
Type 1	Outside air temp	
Type 90	Outside air $ rh	
Type N	Not edit roof data	
Press K2	Compute	
Press K8	End	

The program has been implemented on a low-cost microcomputer (an HP85) and is written in BASIC; it should be transferable to other computers reasonably easily. The program is interactive, prompting the user to input each piece of relevant information. As part of this philosophy, the program has been developed to allow data input and subsequent editing.

£75 + VAT

ORDER FORM OVERLEAF

6.1 ORIGINAL VICKERS DEVICE (Continued)

DISTANCE FROM TOP OF DEVICE = 3 METRES

OVER WHOLE WAVE CYCLE

Max Tens. Load in Outer Ring	=	1.5640MN/m
Max Comp. Load in Outer Ring	=	0.5695MN/m
Max Tens. Load in Inner Ring	=	1.7967MN/m
Max Comp. Load in Inner Ring	=	0.4951MN/m
Max Shear Load in Whole Ring	=	0.2326MN/m

DISTANCE FROM TOP OF DEVICE = 4 METRES

OVER WHOLE WAVE CYCLE

Max Tens. Load in Outer Ring	=	1.4771MN/m
Max Comp. Load in Outer Ring	=	0.6286MN/m
Max Tens. Load in Inner Ring	=	1.7064MN/m
Max Comp. Load in Inner Ring	=	0.5544MN/m
Max Shear Load in Whole Ring	=	0.2284MN/m

DISTANCE FROM TOP OF DEVICE = 5 METRES

OVER WHOLE WAVE CYCLE

Max Tens. Load in Outer Ring	=	1.3916MN/m
Max Comp. Load in Outer Ring	=	0.6887MN/m
Max Tens. Load in Inner Ring	=	1.6179MN/m
Max Comp. Load in Inner Ring	=	0.6148MN/m
Max Shear Load in Whole Ring	=	0.2245MN/m

6.1 ORIGINAL VICKERS DEVICE (Continued)

DISTANCE FROM TOP OF DEVICE = 6 METRES

OVER WHOLE WAVE CYCLE

Max Tens. Load in Outer Ring	=	1.3075MN/m
Max Comp. Load in Outer Ring	=	0.7498MN/m
Max Tens. Load in Inner Ring	=	1.5309MN/m
Max Comp. Load in Inner Ring	=	0.6762MN/m
Max Shear Load in Whole Ring	=	0.2209MN/m

DISTANCE FROM TOP OF DEVICE = 7 METRES

OVER WHOLE WAVE CYCLE

Max Tens. Load in Outer Ring	=	1.2247MN/m
Max Comp. Load in Outer Ring	=	0.8120MN/m
Max Tens. Load in Inner Ring	=	1.4456MN/m
Max Comp. Load in Inner Ring	=	0.7385MN/m
Max Shear Load in Whole Ring	=	0.2178MN/m

DISTANCE FROM TOP OF DEVICE = 8 METRES

OVER WHOLE WAVE CYCLE

Max Tens. Load in Outer Ring	=	1.1431MN/m
Max Comp. Load in Outer Ring	=	0.8751MN/m
Max Tens. Load in Inner Ring	=	1.3619MN/m
Max Comp. Load in Inner Ring	=	0.8018MN/m
Max Shear Load in Whole Ring	=	0.2150MN/m

6.1 ORIGINAL VICKERS DEVICE (Continued)

DISTANCE FROM TOP OF DEVICE = 9 METRES

OVER WHOLE WAVE CYCLE

Max Tens. Load in Outer Ring	=	1.0629MN/m
Max Comp. Load in Outer Ring	=	0.9392MN/m
Max Tens. Load in Inner Ring	=	1.2797MN/m
Max Comp. Load in Inner Ring	=	0.8661MN/m
Max Shear Load in Whole Ring	=	0.2125MN/m

DISTANCE FROM TOP OF DEVICE = 10 METRES

OVER WHOLE WAVE CYCLE

Max Tens. Load in Outer Ring	=	1.0551MN/m
Max Comp. Load in Outer Ring	=	0.9332MN/m
Max Tens. Load in Inner Ring	=	1.2701MN/m
Max Comp. Load in Inner Ring	=	0.8602MN/m
Max Shear Load in Whole Ring	=	0.2104MN/m

DISTANCE FROM TOP OF DEVICE = 11 METRES

OVER WHOLE WAVE CYCLE

Max Tens. Load in Outer Ring	=	1.0484MN/m
Max Comp. Load in Outer Ring	=	0.9281MN/m
Max Tens. Load in Inner Ring	=	1.2621MN/m
Max Comp. Load in Inner Ring	=	0.8552MN/m
Max Shear Load in Whole Ring	=	0.2087MN/m

6.1 ORIGINAL VICKERS DEVICE (Continued)

DISTANCE FROM TOP OF DEVICE = 12 METRES

OVER WHOLE WAVE CYCLE

Max Tens. Load in Outer Ring	=	1.0430MN/m
Max Comp. Load in Outer Ring	=	0.9239MN/m
Max Tens. Load in Inner Ring	=	1.2556MN/m
Max Comp. Load in Inner Ring	=	0.8512MN/m
Max Shear Load in Whole Ring	=	0.2072MN/m

DISTANCE FROM TOP OF DEVICE = 13 METRES

OVER WHOLE WAVE CYCLE

Max Tens. Load in Outer Ring	=	1.0389MN/m
Max Comp. Load in Outer Ring	=	0.9207MN/m
Max Tens. Load in Inner Ring	=	1.2505MN/m
Max Comp. Load in Inner Ring	=	0.8480MN/m
Max Shear Load in Whole Ring	=	0.2061MN/m

DISTANCE FROM TOP OF DEVICE = 14 METRES

OVER WHOLE WAVE CYCLE

Max Tens. Load in Outer Ring	=	1.0359MN/m
Max Comp. Load in Outer Ring	=	0.9184MN/m
Max Tens. Load in Inner Ring	=	1.2469MN/m
Max Comp. Load in Inner Ring	=	0.8458MN/m
Max Shear Load in Whole Ring	=	0.2053MN/m

6.1 ORIGINAL VICKERS DEVICE (Continued)

DISTANCE FROM TOP OF DEVICE = 15 METRES

OVER WHOLE WAVE CYCLE

Max Tens. Load in Outer Ring	=	1.0341MN/m
Max Comp. Load in Outer Ring	=	0.9170MN/m
Max Tens. Load in Inner Ring	=	1.2447MN/m
Max Comp. Load in Inner Ring	=	0.8444MN/m
Max Shear Load in Whole Ring	=	0.2048MN/m

DISTANCE FROM TOP OF DEVICE = 16 METRES

OVER WHOLE WAVE CYCLE

Max Tens. Load in Outer Ring	=	1.0335MN/m
Max Comp. Load in Outer Ring	=	0.9165MN/m
Max Tens. Load in Inner Ring	=	1.2440MN/m
Max Comp. Load in Inner Ring	=	0.8440MN/m
Max Shear Load in Whole Ring	=	0.2047MN/m

6.2 TWIN OSCILLATING WATER COLUMN TERMINATOR

This device will be sited in 26 metres of water and is positioned such that the top of the device is 5 metres below the mean water surface.

The main body of the device is 17.25 metres high, 22 metres wide and 32 metres long.

With a wave length of 80 metres, period 7.3 seconds, the maximum unbreaking wave is 10.7 metres peak to trough. This wave will uncover the device.

The net forces on the device were calculated for wave periods up to 16 seconds, 240 metres length and 17.7 metres peak to trough. The mass and drag coeficients were taken as 2 and 1.33 for both vertical and horizontal conditions.

The maximum combination of horizontal inertia and drag forces was 52.2MN and occurs at a wave length of 160 metres. The experimental work on the model of this device, suggests that the surge force which occurs once the top of the device approaches the trough of the wave has a significant effect on the maximum horizontal forces. To date, no theoretical assessment of these loads has been found and there is insufficient experimental data to make a comprehensive assessment of the surge force with various sea state conditions. The limited available experimental data measured the R.M.S. value of the horizontal wave forces and these exceed the R.M.S. value of the calculated forces by up to 50% when the device top is uncovered.

6.2 TWIN OSCILLATING WATER COLUMN TERMINATOR (CONTINUED)

In the design of the full scale device the maximum calculated combined inertia and drag forces were increased by 50% to allow for the surge force. This is a pessimistic assumption since the surge force may be found to be out of phase with the inertia force.

The vertical force was assessed assuming that the weight of the device equalled the weight of water it displaced. The slamming forces were not considered since the wave with the maximum height only exposes 25% of the device.

The maximum lift on the device is 30MN and the maximum down load 36MN.

No theoretical assessment has been carried out on the pressure distribution around the device during the wave cycle. The assumptions made in the detail of the full scale device were:

(1) that pressure varies as per water particle acceleration in respect of depth,

and

(2) that pressure varies as a half sine wave along the device's horizontal plane.

6.3 SUBMERGED WAVE CHAMBER

The device will be sited in 60 metres of water and is 120 metres long, 11 metres high and 10 metres wide. Its weight was taken as 0.75 of that of the water it displaces.

The loading on the device was calculated for the device being either 5 metres or 20 metres below the surface for wave periods from 5 to 16 seconds, and wave lengths from 40 to 340 metres. These loads were assessed taking into consideration the variation in water particle acceleration and velocity along the device.

With the device 5 metres below the mean surface, the resultant vertical force always provides lift until the wave length reaches 160 metres, but the moment caused by these loadings results in some of the supports taking compressive loads when the wave length reaches 130 metres. Under storm wave conditions, 340 metres wave length, 32 metres peak to trough, 16 second period, the total vertical loading will vary from 71MN lift to 67MN down thrust over a wave cycle.

With the device 20 metres below the surface, the resultant vertical force always provides lift, it is a maximum at 260 metres when the lift is 60MN

As with the Twin Oscillating Water Column terminator, there is no information on the pressure distribution around and along the device, so only a very approximate analysis has been carried out on the full scale design of this device.

6.3 SUBMERGED WAVE CHAMBER (Continued)

The bending moments arising within the device have not been analysed fully since they depend on the frequency and relative stiffness of the tethers. The case of a wave of wavelength equal to the device length, 120 m, on an unrestrained neutrally buoyant device does however give some idea of the bending moments involved, since in this condition the net vertical force applied is zero, and the assumptions of restraint are less critical.

The maximum bending moment due to such a wave, of 17 m height, on a device just fully submerged is 340 MNm. This compares with a value of 1000MNm for a similar device free floating 25% above the still water line, which provides a powerful case for submerged beam type devices.

If however, the device is restrained by comparatively stiff tethers, the bending moments applied to the device are further reduced. This enables the length of the device to be increased considerably, so that the net forces applied to it are eliminated completely.

6.4 TWIN OSCILLATING WATER COLUMN POINT ABSORBER

The device is 24 metres diameter and 14.5 metres high and is bottom mounted in 19 metres of water.

This device is similar in construction to the original Submerged Water Column with the exception of the lower inlet.

The loading in this device is generally 70% of that in the original device and the surface area is also 70% less. These two conditions would lead to a 50% reduction in the material content of the device relative to the original Submerged Water Column, but because of the discontinuity in the outer shell due to the lower duct only 40% has been allowed for.

7.0 CONSTRUCTION - PRELIMINARY CONSIDERATIONS

7.1 Point Absorbers

The original device was designed in concrete to avoid the necessity of on-site ballasting for a light structure.

The high mass was used to relieve the anchoring requirement.

For the same reasons the Twin Oscillating Water Column Point Absorber was designed in concrete.

Method of Construction

The concrete base and shell of the device will be constructed on a platform, enabling the device to be moved to successive adjacent work stations on the production line and to be launched down a slipway on completion of the construction, fitting-out and curing stages. Conventional concrete moulding and slip forming techniques would be employed, using a steel shuttering to obtain the required surface curvatures, with epoxy surface finish on those internal working surfaces where marine fouling and friction is to be minimised. Steel seatings for the removable power modules are moulded into the shell structure to ensure accurate location of the modules.

The removable power modules, each weighing some 45 tonnes complete, will be assembled on a production line basis in a purpose-built factory and delivered to the device construction site. The power modules would normally be fitted to the device prior to launch, although post-launch fitting can be easily achieved, if required.

Method of Construction (Continued)

After curing and fitting-out, the device will be launched on its platform down a slipway into sufficient depth of water for the special emplacement vessel to position itself around the device and raise the device into position for transportation. The platform will be recovered and moved back to the first production station.

The special emplacement vessel (SEV) comprises two identical half-vessels, each half being autonomous and fitted with hydraulic, pneumatic and electric power supplies, 12 lifting winches, a dynamic positioning system, normal salvage and domestic systems and crane. Each half vessel is also provided with a control bridge enabling full control of the winch and dynamic positioning systems of either the half-vessel or both half-vessels when they are engaged together as one SEV.

The two half-vessels will be positively located and locked together as an SEV after enclosing the wave power device, and the device will then be raised by the 24 "synchrolift" type winches until the wave power device is positively located within the circular well. The loaded SEV would then be towed out to the prepared sea bed by two medium tugs.

The device is lowered into position by the SEV using the dynamic positioning system and synchronised winches to ensure precise emplacement. Pumping necessary to establish the correct air volume will be provided by the SEV at this stage.

Method of Construction (Continued)

The SEV will then be towed back to the production site by the tugs. Cable connections will be made before lowering the device or, if necessary, by divers operating from a smaller support vessel.

The SEV would be capable of recovering or repositioning a complete device, should this ever be required for operational or damage reasons.

Time for Construction

Construction of the device base and shell will be accomplished within 28 days, with a further period of 28 days required for curing. Final fitting-out of the device including installation of the power modules, will be completed during the curing period. The maximum production rate required is four devices per week, on a seven-day shiftwork basis, to achieve an average annual output in excess of 300 devices.

The required device production rate could be achieved from two 8-stage production lines, either co-located or at separate sites. One slipway could handle four device launches per week.

In the event of sustained bad weather delaying emplacement operations, production output could be temporarily stored either on land or in the sea, using the SEV. Sea storage in a convenient area with water depths of 7 metres or greater offers an attractively low-cost means of temporarily absorbing over-production.

7.2 Attenuator and Terminator

The initial design of the terminator has been carried out in steel but it does lend itself also to a concrete structure, in which case its method of construction follows that of the Point Absorbers. In this case, however, the device will be slipformed vertically in a dry dock followed by loading and flotation techniques to bring the device horizontal.

The attenuator, being tethered on mooring lines, required high buoyancy loads. This requirement led to the choice of a steel device.

Method of Construction

The steel construction of the attenuator and terminator, by virtue of their size and shape lend themselves to conventional ship building technique. They could be built on slipways, launched and towed to a storage area before deployment.

The devices could be constructed in sections and joined while in the storage area, this applies particularly to the S.W.C. attenuator.

Facts on structural softwood

STRENGTH CLASSES

This new BRE wallchart for designers and suppliers of structural timber presents the basic facts on the strength class system of grading structural timber given in BS 5268: Part 2.

Anyone specifying or marketing structural timber, or checking material on site, will find the wallchart an easy-to-use reference document for the office, sawmill or timber stockyard. The wallchart also presents – for easy reference – a table of the softwoods graded to BS 4978 which can be supplied for each strength class, and another giving the strength classes for the stress grades of hem-fir and spruce-pine-fir from North America.

In conjunction with the new wallchart, BRE has updated and re-issued an earlier one, 'Facts on structural softwood – stress grades', which gives information on the stress grades in BS 4978 in a similar simple, easy-to-refer-to, form.

XYZ TIMBER CO. LTD

SC3 LIC. NO. **1000 BS4978**

To: **Publications Sales Office**
Building Research Establishment
Garston
Watford
WD2 7JR

Please send me:

. . . . copy/copies of the wallchart **'Facts on structural softwood – strength classes'** at £1.00 each (including postage in the UK)

. . . . copy/copies of the wallchart **'Facts on structural softwood – stress grades'** at £1.00 each (including postage in the UK)

Please note, there is a minimum order charge of £2.00 to cover handling costs

I enclose payment of £. . . . . payable to the Department of the Environment

Name: . . . . . .

Address: . . . . . .

. . . . . .

. . . . . .

. . . . . .

. . . . . .

BUILDING RESEARCH ESTABLISHMENT
Department of the Environment

8.0 MOORINGS AND ANCHORAGE

8.1 Vickers Original Device

Three methods have been considered:

1. Semi-burying the device
2. Piling
3. Anchoring

For case 1 a large cutter suction dredger capable of operating to depths of 30 metres has been assumed. Currently no such dredger is thought to exist although it would be possible to convert an existing dredger to cope.

Once the hole has been dredged the device would be sunk into it. Substantial temporary works in the form of guides would be needed to avoid the device oscillating as it sank.

For case 2 a bed must be first prepared and the unit sunk onto it as for case 1. Piles would then be driven to secure the device. The costing of this piling is very speculative as there is no readily available data.

For case 3 almost the same problems apply as for the piles in that currently the equipment does not exist to put these anchors down. Here, however, the equipment manufacturers expressed greater optimism in their ability to overcome the problems, and this method has been selected as the most feasible for this device.

The device chosen for the reference design is for a 'hard' sea bed and includes provision for 24 x 340 tonne anchors to resist the maximum side force.

8.1 Moorings and Anchorage (Continued)

For a 'soft' sea bed, the base of the device in the reference design would be altered to give a skirt and anti-scour ring. This will be sufficient to withstand the side forces and additional moorings would not be necessary. There is sufficient excess material in the base, so that the skirt and anti-scour ring could be constructed without any additional material.

As designed the device will have excess net weight when in operation. The number and size of anchors will depend on bed friction and also the directional variability of the wave forces.

Recent experimental data has indicated that the horizontal force can be increased by up to 50% if the device breaks the water line, and this has been allowed for in the size of the anchors.

8.2 Twin Oscillating Water Column

Again, because it appears to be the most feasible system, rock anchors have been selected for this device. The theoretical calculations give a maximum horizontal force on the point absorber version of ±26MN. Allowing 50% for the device breaking water in storm waves, gives a force of 39MN.

The device will only be anchored on each side to allow unimpeded flow to the lower duct. Allowing 8 x 500 tonne anchors/side gives sufficient margin to cover the bending moment introduced by having the device mounted above the supports.

With a suitable seabed as indicated off South Uist, piling offers an obvious alternative, but we have insufficient information to evaluate this method with any confidence.

8.3 Submerged Wave Chamber

It is envisaged that this device will be sited in deeper water than the Twin Oscillating Water Column devices (about 60m sea depth) to take advantage of the greater resource of power available, so that anchoring as a tethered unit may well be preferable to supporting on a fixed structure. This method has been found to be unattractive for use with surface breaking platforms in depths of water under 100m, but the economics of a submerged structure, which by nature of its function' has excess buoyancy, may well differ considerably. One complication introduced by mooring the device however is that a more flexible power cable is required.

8.3 Submerged Wave Chamber (Continued)

Particular attention must be paid to the dynamics of a tethered buoyant structure, in particular to ensure that its natural period of oscillation lies outside the wave spectrum. A preliminary analysis indicates that this can be achieved.

Assuming vertical tethers for minimum stiffness (Figure 8.1), for small displacements:-

$$\frac{dF}{g(Mw-M)} = \frac{dx}{l_t}$$

$$\text{Stiffness } K = \frac{dF}{dx} = g\,\frac{(Mw-M)}{l_t}$$

$$\therefore \text{ Natural frequency } w = \sqrt{\frac{K}{M}} \quad \sqrt{\frac{g(Mw-M)}{l_t M}}$$

$$\text{Natural period of oscillation } T = 2 \quad \sqrt{\frac{l_t}{g(Mw/M-1)}}$$

Assuming that the length of tethers l_t = 55m, and the mass of the structure is 75% of its displacement

$$T = 2\pi \quad \sqrt{\frac{55}{9.81\ (1/.75-1)}}$$

$$= 25.8 \text{ seconds}$$

This exceeds the longest period expected in the wave spectrum by 60%.

8.3 Submerged Wave Chamber (Continued)

The maximum horizontal loads are of similar magnitude to those of the original device, but there are significant vertical loads that have to be considered. If the device is allowed to break water and reduce the buoyancy force, then the tethers have to be designed to take the snatch loads that could occur. It is hoped that with further investigation into the mooring system, that the mean wave forces, reported by Longuet-Higgins[5], can be used to push the device deeper into the water and thus avoid breaking the water line.

Catenary moorings will also need to be investigated to see if they can offer an alternative solution. There is also the possibility of using rigid struts articulated at each end, so that a certain amount of compression can be tolerated without introducing snatch loads.

Vickers are already involved in an ongoing investigation into the design of a seabed anchoring system for the North Sea Oil Industry from which valuable experience can be drawn.

Dynamics of a Tethered Buoyant Structure

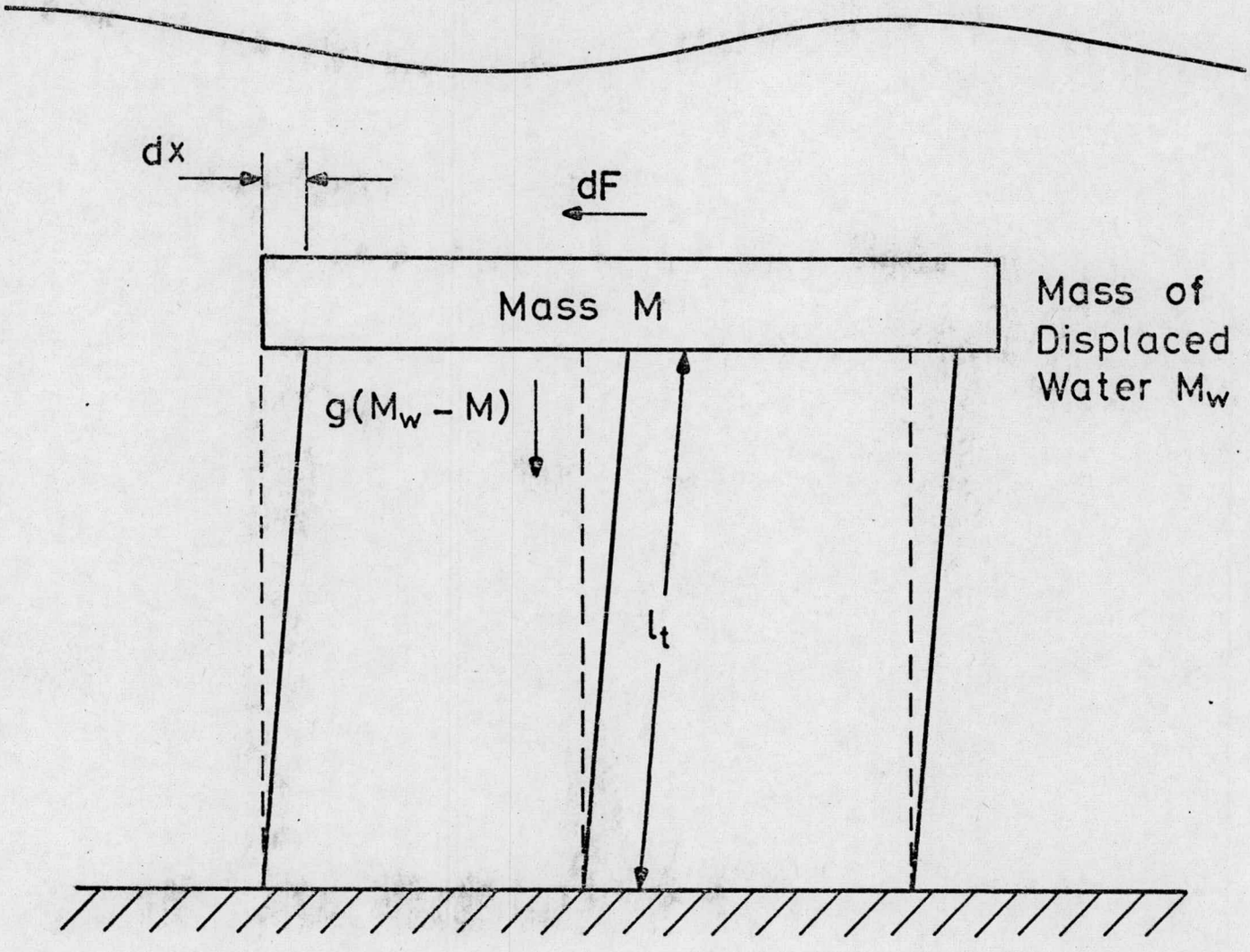

$$\text{Natural Period of Oscillation} = 2\pi \sqrt{\frac{l_t}{g\left(\frac{M_w}{M} - 1\right)}}$$

FIG 8.1

9.0 REFERENCES

1) Lighthill J., "Two-dimensional analyses related to wave energy extraction by submerged resonant ducts" J.Fluid Mech., Vol.91, Part 2.pp253-317,1979

2) Simon M., Private communication.

3) Mollison D., "Distribution of power at South Uist with Frequency" Tag 2 paper DA92,WESC(79).1979.

4) Miller B.L. and Hogben N., "Synthesis of directional wave climate from station Fitzroy" N.M.I., project number 302011. Sept.1979.

5) Longuet-Higgins, M.S., "The mean forces exerted by waves on floating or submerged bodies with applications to sand bars and wave power machines". Proc. Royal Society, London. A352, pp463-480, 1977.

6) Lappo and D.D. Kaplin V.V. "Wave Pressure on Vertical Circular Cylindrical Obstacles". Oceanology, Vol.7, No.3 1967.